2050
Heat Roadmap Europe
A low-carbon heating and cooling strategy

Methodologies and assumptions used in the mapping

Deliverable 2.3: A final report outlining the methodology and assumptions used in the mapping

Project Number:	695989
Project acronym:	HRE
Project title:	Heat Roadmap Europe (HRE): Building the knowledge, skills, and capacity required to enable new policies and encourage new investments in the heating and cooling sector
Contract type:	H2020-EE-2015-3-MarketUptake

This project has received funding from the European Union's Horizon 2020 research and innovation programme under grant agreement No. 695989.

Deliverable number:	**D2.3**
Deliverable title:	**A final report outlining the methodology and assumptions used in the mapping**
Work package:	WP2
Due date of deliverable:	31 August 2017
Actual submission date:	M18 - 31/08/2017 (Revised version 28/09/2018)
Start date of project:	01/03/2016
Duration:	36 months
Author/editor:	Urban Persson (HU), Bernd Möller (EUF), Eva Wiechers (EUF)
Reviewer(s):	Brian Vad Mathiesen (AAU), Lars Grundahl (AAU)
Project Coordinator	Brian Vad Mathiesen, Aalborg University

Dissemination Level of this Deliverable:	**PU**
Public	*PU*
Confidential, only for members of the consortium (including the Commission Services)	***C0***

Contact: Urban Persson, Work Package 2 leader
Email: urban.persson@hh.se
School of Business, Engineering and Science
Halmstad University
Box 823
SE-301 18 Halmstad
Sweden

E-mail: info@heatroadmap.eu
Heat Roadmap Europe website: www.heatroadmap.eu

Deliverable No. D2.3: Public Report

This project has received funding from the European Union's Horizon 2020 research and innovation programme under grant agreement No. 695989. The sole responsibility for the content of this document lies with the authors. It does not necessarily reflect the opinion of the funding authorities. The funding authorities are not responsible for any use that may be made of the information contained therein.

This project has received funding from the European Union's Horizon 2020 research and innovation programme under grant agreement No. 695989.

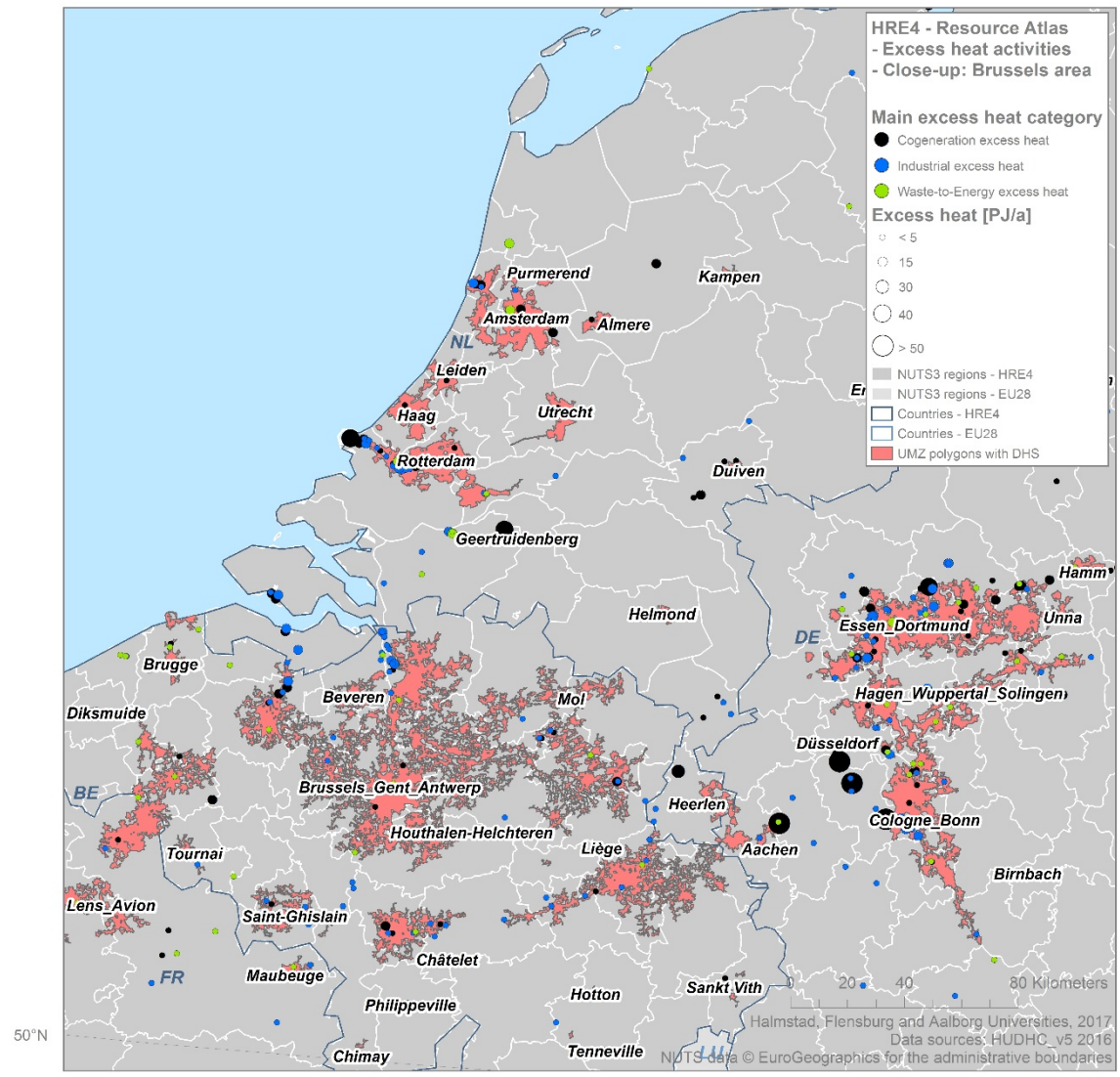

Figure 0.1. Mapping of coherent district heating areas (UMZ_DH) and their spatial connectivity to large-scale energy and industry sector excess heat facilities. Snapshot overview of Belgium, northern France, the Ruhr, and the Netherlands areas of western central Europe

Table of Contents

Abstract

This report is the main account for the methodologies, assumptions, data, and tools used in the WP2 mapping of the fourth Heat Roadmap Europe (HRE) project during its first reporting period (March 2016 to August 2017). During this period, the work with the major tasks assigned to WP2 in the project, including e.g. highly resolved spatial demand and resource atlases for the 14 MS´s of the EU under study, has resulted in a wide array of intermediate, complementary, and final outputs. Mentionable among these are for example hectare level projections of demand densities (residential and service sector heating and cooling demands) and investment costs for district heating and cooling systems, as well as feature polygon representations of current district heating cities in these countries. However, since the core focus here is to describe the methodological approaches and data sets used in the work, and not explicitly to present the results of the application of these, only a limited representative selection of study results are included in this report. For more exhaustive output presentations of the WP2 productions (apart from deliverables D2.1 and D2.2), all final output datasets generated are made available as operational layers in the online web map application Peta4 (the fourth Pan-European Thermal Atlas).

List of acronyms

Table 0.1. List of acronyms

Acronym	Meaning
BBR	Bygnings- og Boligregistret (Danish National Building Register)
DC	District cooling
DH	District heating
DHC	District heating and cooling
CDD	Cold demand density/Cooling degree days
CHP	Combined heat and power
CPC	Chemical and petrochemical
EC	European Commission
ECI	European Cooling Index
EE	Energy efficiency
EEA	European Environment Agency
EHI	European Heating Index
ES	Eurostat
ESM	European Settlement Map
EU	European Union
FSR	Fuel supply and refineries
FT	Food and tobacco
GDP	Gross Domestic Product
GHSL	Global Human Settlement Layer
HDD	Heat demand density/Heating degree days
HRE	Heat Roadmap Europe
HRE4	Heat Roadmap Europe 4 (H2020 project)
GIS	Geographical Information System
IEA	International Energy Agency
IND	Industrial sector
IS	Iron and steel
JRC	Joint Research Centre
MFH	Multi-Family Housing
MQ	Mining and quarrying
N-FM	Non-ferrous metals
N-MM	Non-metallic minerals
OSM	Open Streetmap
PPP	Paper, pulp and printing
RES	Residential sector
SER	Service sector
SFH	Single-Family Housing
SQL	Structured Query Language
TP-AP	Thermal Power Generation – Auto Producer
TP-MA	Thermal Power Generation – Main Activity
TP-WTE	Thermal Power Generation – Waste-to-Energy
UNEP	United Nations Environmental Programme
WTE	Waste-to-Energy

Acknowledgements

The present report draws on the results of several previous and parallel EU-projects, some of which have kindly allowed HRE4 to use the data prepared in them. First, the good cooperation with the GeoDH project, co-funded by the Intelligent Energy Europe Programme (Dumas and Bartosik, 2014, Nádor et al., 2013, GeoDH, 2014, GeoDH, 2017), which was already established during the EU Stratego-Project (HRE3), has been extended to include all resulting geodata for geothermal heat potentials. We thank in particular the Geological and Geophysical Institute of Hungary for their assistance in making available their data to HRE4.

Second, the BioBoost project (Contract No 282873 within the Seventh Framework Programme by the European Commission) has generously made available and shared their data on biomass potentials across Europe at high geographical resolution (Pudelko et al., 2013). We would in particular like to thank Karlsruhe Institute of Technology and IUNG (Instytut Uprawy Nawozenia I Gleboznawstwa, Panstwowy Instytut Badawczy) for allowing us to use the results of the project as input to the biomass resources mapping in HRE4.

Third, by collaboration with Task 52 of the International Energy Agency Solar Heating & Cooling Programme (IEA-SHC, 2017, IEA-SHC-T52, 2017), the original 2016 data on large-scale European solar thermal installation from the Intelligent Energy Europe project Solar District Heating (SDH-dataset, 2016), was kindly made available to the project. We would like to thank especially our Danish HRE4 partner PlanEnergi for sharing this data and for fruitful cooperation in developing a conceptual and spatial methodological approach to assess the theoretical and economical potential for large-scale solar thermal installations in current district heating towns and cities in Europe.

Without the large amount of geographical data collected at institutions like the Joint Research Centre (JRC) of the European Commission and the European Environmental Agency EEA), not to speak of Eurostat (ES), the modelling of local conditions at the achieved resolution would not have been possible. Since local conditions, e.g. heating and cooling demands, excess heat availabilities etc., constitute the core elements of the demand and resource atlases conceived in this project, a great acknowledgment is in place here for all the staff at the mentioned organisations who has brought forward the development of highly innovative data and assisted with technical advice. References are made to the individual data sets where appropriate.

1 Introduction

In Europe, there is a clear long-term objective to decarbonise the energy system, but it remains largely unclear how this could be achieved in the heating and cooling sector. The Heat Roadmap Europe (HRE) project will enable new policies and prepare the ground for new investments by creating more certainty regarding the changes that are required. Heat Roadmap Europe is co-funded by the European Union, brings together 24 academic, industrial, governmental and civil society partners, and runs from 2016 to 2019.

The overall objective of the HRE project is to provide new capacity and skills for lead users in heating and cooling sectors, including policymakers, industry, and researchers at local, national, and EU levels, by developing data, tools, and methodologies necessary to quantify the impact of implementing more energy efficiency measures on both the demand and supply sides of the sector. The HRE project has developed from its start with two pre-studies in 2012 and 2013 (Connolly et al., 2012, Connolly et al., 2013), through a third, the 2014 to 2016 IEE Stratego project (Connolly et al., 2014a), into this current and fourth project, why the frequent annotation “HRE4” has become customary when referring to this project.

The HRE4 project consists of seven work packages, where the second (WP2 – GIS mapping of heating and cooling within the 14 MS´s in the EU) is designated to the work of gathering, analysing, generating, and preparing quantitative data for spatial distribution in Geographical Information Systems (GIS), in other words, mapping of heating and cooling demands and resources. This WP2 report aims to describe and account for data, methodological approaches, assumptions, tools, and some of the outputs used and produced in the pursuit of WP2 objectives during the first reporting period of the project (from March 2016 to August 2017).

For this end, the report is structured – with reference to data management, methodology developments, theory, application of tools etc. – in accordance with the five tasks[1] specified in Annex 1 (Part A) of the grant agreement, and – with reference to results and produced outputs – essentially in accordance with the first two (out of four) deliverables[2] detailed in the same annex. The first section of the report begins with an account of the general objectives of WP2 and continues with a brief description of the general background of combining spatial mapping and energy system modelling, a central theme of the HRE project series since the start in 2012, as well as mentioning some limitations in the current work.

Section 2 constitutes the backbone and core content of the report, addressing in sequence and in multiple subsections the work on demand atlases (see section 2.1),

[1] Task 2.1: Demand Atlases, Task 2.2: Mapping the Renewable Heat Resources, Task 2.3: Heat Synergy Regions (hot spots), Task 2.4: Connect heat and cooling densities with district heating and cooling network costs, and Task 2.5: Quantifying the potential mix of rural heating solutions.

[2] D.2.1: Demand and Resource Atlases for all 14 MSs, D.2.2: Map of the heat synergy regions and the cost to expand district heating and cooling in all 14 MSs, D.2.3: A final report outlining the methodology and assumptions used in the mapping, and D.2.4: Maps manual for lead users.

resource atlases (section 2.2), heat synergy regions (section 2.3), district heating and cooling investment costs (section 2.4), and the potential mix of rural heating technologies (section 2.5).

In section 3, a summary of the main results and outputs from the mapping exercises is presented, including some general properties of the heat and cold demand density rasters of towns, cities, urban, rural, and countryside areas generated for the 14 EU Member States (MS´s) which constitute the study population in the HRE4 project[3]. This results summary, which is to be regarded as a complement to the main results dissemination format of the Peta4 web map application, also highlights some of the renewable resource output layers, the annual excess heat volumes assessed, the heat synergy regions, as well as the aggregated MS totals with respect to district heating and cooling investment costs per hectare grid cells.

In the remaining section 4, the complete effort of WP2 under the first reporting period is condensed to a set of conclusive remarks which are briefly discussed. This includes some reflections on the main achievements and shortcomings of the performed work and some thoughts on study areas suitable for continued research and development.

1.1 General objectives

The main objective of WP2, as specified in Annex 1 (Part A) of the grant agreement, is to update and use the Pan-European Thermal Atlas to quantify and map the spatial distribution of significant elements that constitute the European heat and cold market. Most pronounced among these elements are the heating and cooling demands in European buildings and industrial activities, the excess and renewable heat resources that potentially could be used to meet these demands, the investment cost levels for installing district heating and cooling systems, and the identification of key regions suitable for district heating and cooling technologies. In extension to this, the general objective is to develop methodological frameworks to build and maintain spatial databases for sustainable energy systems, i.e. demand and resource atlases.

1.1.1 Update the Pan-European Thermal Atlas

In more specific terms, these objectives represent in several aspects considerable improvements and advances compared to the attempts of producing geographically specific images of thermal demands and assets in previous HRE studies, as well as in relation to many other contemporary European mapping projects (Planheat, 2017, Thermos, 2017). Most significantly, heat and cold demands used in the demand atlases are here based on more refined input data than previous HRE studies[4]. Partly, this refinement consist in the use of energy demand input data from the FORECAST model

[3] These countries are the 14 MS´s with the largest heat demands in contemporary EU28: Austria, Belgium, Czech Republic, Finland, France, Germany, Hungary, Italy, Netherlands, Poland, Romania, Spain, Sweden, and United Kingdom.
[4] HRE1-3 relied on much more coarse energy demand input data, based principally on international energy statistics onto which EU average default conversion efficiencies for different technologies were applied to produce generic assessments of delivered energy demands at national levels.

of WP3 (see e.g. (Fleiter et al., 2017)). Additionally, the development and application of improved geo-statistical modelling of the built environment in European cities, towns, and rural areas has increased the accuracy of anticipating the spatial distribution of these heating and cooling demands in different user sectors.

The main improvements in this respect refers essentially to the introduction of more advanced models with a greater variety of independent variables[5] or inputs to geo-statistical, quantitative models of building intensity; by a more rigorous approach of variable testing and by coefficient adjustments to arrive at most significant and fitting outputs. The spatial resolution itself, by which these more appropriately conceived and geographically distributed demands appear in the project output formats, i.e. as static maps (images) and as dynamic maps (online web map application layers), is moreover increased here from square kilometre to hectares, i.e. rasterization at hectare grid cell resolution of residential and service sector heat demands as continuous data[6].

In terms of these raster representations, further, apart from including cooling demands as well, this enhancement refers also to the delineation of prospective, coherent supply areas, thus extending into highly resolved mapping of district heating and cooling (DHC) investment costs and several layers contextual to these (e.g. plot ratio, effective width, linear heat and cold densities etc. (see also section 2.4 below)). By combining information on demands by their density and location with that of corresponding investment costs, the spatially explicit model results allow resource economic analyses to be made, which generally means that technical and economic district heating potentials can be derived in the project.

With respect to the resource atlases, the Pan-European Thermal Atlas has been updated by the full incorporation of geothermal and biomass data from other contemporary EU projects like GeoDH and BioBoost. Complemented also with an assessment of solar district heating potentials (the result of a collaboration with Task 52 of the International Energy Agency Solar Heating & Cooling Programme (see further section 2.2.3)) and an extensive mapping of large-scale excess heat activities, the HRE4 project has produced a more coherent resource atlas compared to previous HRE studies.

At the time of writing, the mapping of future (2050) baseline and HRE4 scenarios remains to be completed since they are scheduled for the second reporting period of the project. According to the project plan, a feedback loop from the WP6 modelling of future district heating levels recommended for each of the 14 MS´s is thought to result in maps that represent these output levels. In addition, this will eventually also include the finalisation of task 2.5 (Quantifying the potential mix of rural heating solutions) since this task is largely dependent on future baseline scenario input data as well (see also further comments under task 2.5 below).

[5] For example residential and service sector floor areas, shares of residential building heat demands in single-family housing (SFH) vs. multi-family housing (MFH), level of soil sealing, degree of built-up areas, degree of settlement, regional GDP etc.

[6] This represents a major achievement in this project. In all previous HRE projects, with the exception of some local project sites in STRATEGO (HRE3), all rasterization was performed by square kilometer resolution.

1.1.2 Online web map application

The Pan-European Thermal Atlas of this HRE4 project is referred to as Peta4, since it constitute an update and development of Peta 3, the corresponding mapping output of the 2014 to 2016 IEE Stratego project[7] (Stratego, 2014). As a convention, each major update of the Peta4 is indicated by a version number, why the first version, available in the form of an online, interactive web map application since March 2017, was labelled Peta4.1. The welcome screen of Peta4.1 is shown in Figure 1.1.

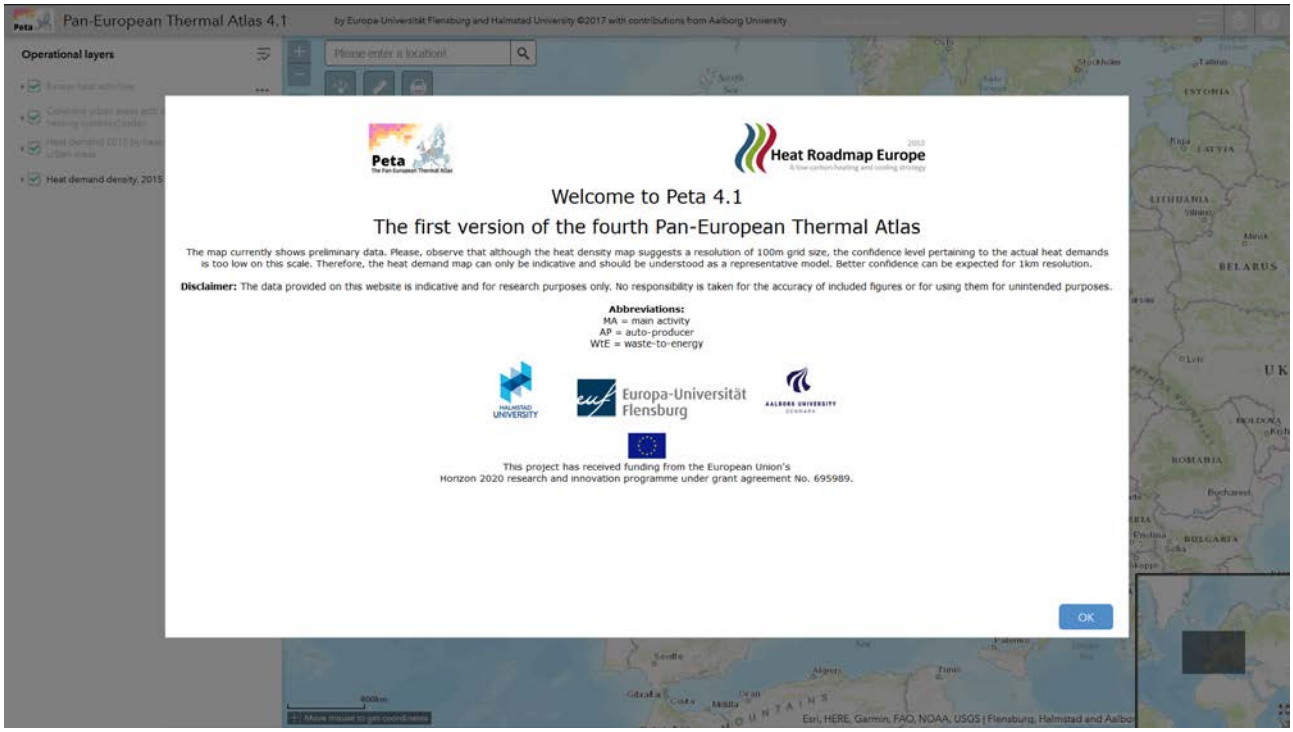

Figure 1.1. Welcome screen at the HRE4 WP2 ArcGIS Online web map application Peta4.1 (Pan-European Thermal Atlas 4, version 1), hosted by Flensburg University in Germany. Source: (Peta4, 2017).

The Peta4 web map application (Peta4, 2017) represents and serves as the main dissemination channel for the results and output layers generated and produced in WP2 of this project. Although some outputs have been published as static map images in previous project deliverables (Persson et al., 2016, Persson et al., 2017b), it is by their availability as "dynamic" images, that is as interactive, transparent, and user-friendly operational layers, that the full characteristics and properties of these highly resolved outputs best can be comprehended and utilised. A separate user guide for the navigation of the Peta4 web map application has been prepared in (Persson et al., 2017a).

[7] The terminology Pan-European Thermal Atlas (abbreviated Peta) was first used in the second HRE pre-study in 2013. The latest version of Peta, referred to here as subject for an update, is the third version developed in the IEE project Stratego (HRE3) during 2014 to 2016.

1.2 Background

As briefly mentioned in the introduction above, the Heat Roadmap Europe concept was first conceived in 2010 and 2011 during internal discussions among a group of Scandinavian based researchers within the field of energy system modelling, energy planning, district heating and cooling technology, and geographical information systems[8]. In essence, since heat cannot be transported transnationally as electricity or gas, the concept centred on the key idea of combining energy system modelling of high temporal resolution with that of high-resolution spatial mapping, to obtain the best possible representation of local conditions, assets, and possibilities on the European heat market.

The first (HRE1, 2012) and second (HRE2, 2013) Heat Roadmap Europe projects were both pre-studies co-financed by Euroheat & Power (Connolly et al., 2012, Connolly et al., 2013). In these, the general concept was tested and tried by the development of a series of suitable approaches and methods. Eventually, the growing consortia had at its disposal a considerable toolbox which came to the test as the third study, the 2014 to 2016 Intelligent Energy Europe Stratego project (Connolly et al., 2014a), set out to develop enhanced heating and cooling strategies for five EU MS (Croatia, Czech Republic, Italy, Romania and the United Kingdom).

In continuation, this fourth Heat Roadmap Europe study, now with an extended geographical scope including 14 EU MS´s, aims straight-out to create the scientific evidence required to support the decarbonisation of the heating and cooling sector in Europe, as well as to support in the anticipated redesign of this sector. In analogy to the original HRE concept, this is to be achieved e.g. by combining the increasing knowledge of local thermal conditions, of the potential savings in buildings, of the energy system analyses etc., and, last but not least, by the further improvement of the methodologies and approaches in the project mapping toolbox.

1.3 Limitations

Regarding demand and resource mapping, there are currently no general accounts for the spatial distribution of thermal demands and resources available for individual EU member states. Most probably, further, there will never (or at least not in a foreseeable future) be a system in place to record geographical distributions of individual demands, delivered energy volumes etc., which makes transparent the vast development potentials for monitoring practices within this sector. For this reason, which is essential, any – and hence all – attempts of describing and mapping heating and cooling demands and possible supplies have therefore to be based on models.

The demand and resource maps prepared in this project are hence models: more or less likely imaginations of how thermal demands and possible sources to meet them are

[8] At the time, these researchers were affiliated either to Aalborg University in Denmark (Professor H. Lund) or to Halmstad University in Sweden (Professor S. Werner).

distributed across cities, towns and rural areas in Europe. The models concerning thermal demands are based on statistical analyses of the correlation of variables that describe the built environment with an actual account of building floor areas in Denmark, where a national building register with address-level accuracy exists. The regression coefficients derived are being applied to other European countries, assuming a similar correlation. Subsequent adjustment to macro-level data has been carried out, resulting in confidence levels that decrease with increasing detail.

A major limitation is that specific heat demands are assumed equal for each sub-sector (single- and multi-family housing, service sector buildings) and within each country. We believe that rural buildings are different from urban buildings, and newer buildings show a better energy performance compared to older buildings, but we found no feasible way of incorporating these specifications into our current models.

It needs therefore to be stressed that the presented data cannot be used for feasibility studies of actual installations, and that the authors refuse any liability for the results of using the results of the present project for subsequent analyses. The present work has the nature of research, and any subsequent improvement of methods is highly welcomed.

Regarding the interactive map (the Pan-European Thermal Atlas); it has been prepared based on the different models and databases used in WP2. However, due to restrictions in uploading and hosting the extensive grid data, heating and cooling demands are available in density classes only, or aggregated by prospective heat supply areas. The interactive map, further, does not facilitate the public download of operational layer datasets, neither as portions nor in their entirety. This is a deliberate choice of the project team since the data itself is considered immaterial property of the HRE consortia.

Regarding scope, the spatial mapping of heating and cooling demands is limited to residential and service sectors, hence not including the thermal demands of the industrial sector. While the former sectors very well may be geographically represented by continuous raster data, the latter constitute spatially dispersed facilities – why the original ambition was to represent these industrial thermal demands as feature point sources. However, partly due to time restrictions, partly due to lack of appropriate data, this approach could not be completed in the context of the first reporting period.

Another area of partially limited scope refers to that of identified heat synergy regions. This report considers the excess heat of these regions, however not quantitatively so renewable heat resources. This is a consequence of the general stand point of WP2 not to enter into the field of “potential assessments” regarding renewable heat resources. Instead, the HRE4 resolve is Peta4, i.e. the online web map application, where the regional presence and spatial connectivity of these resources relative demand centres, heat infrastructures etc., may be observed and evaluated by any user. Finally, in terms of temporality, the work presented in this report is limited to the 2015 baseline scenario only. Hereby, all presented datasets are based either on real 2015 input data or on corresponding input data prepared to resemble 2015 conditions.

2 Methodologies and assumption used in the mapping

According to the order and structure of the five subsequent tasks of WP2, conceived in the grant agreement and depicted in Figure 2.1, this section will present and account for the methodologies and assumptions, as well as a wide array of additional input and generated data, of calculations, regressions, and analyses, used and performed to produce the work package outputs.

Hereby, the section begins with an account of how the final WP2 demand atlases (Task 2.1), i.e. the heat and cold demand density raster datasets for residential and service sector buildings were conceived, modelled and prepared. For this, the input data used, the geo-statistical modelling of the built-up environment, the floor area regressions models, as well as the subsequent heat and cold demand density models themselves are described.

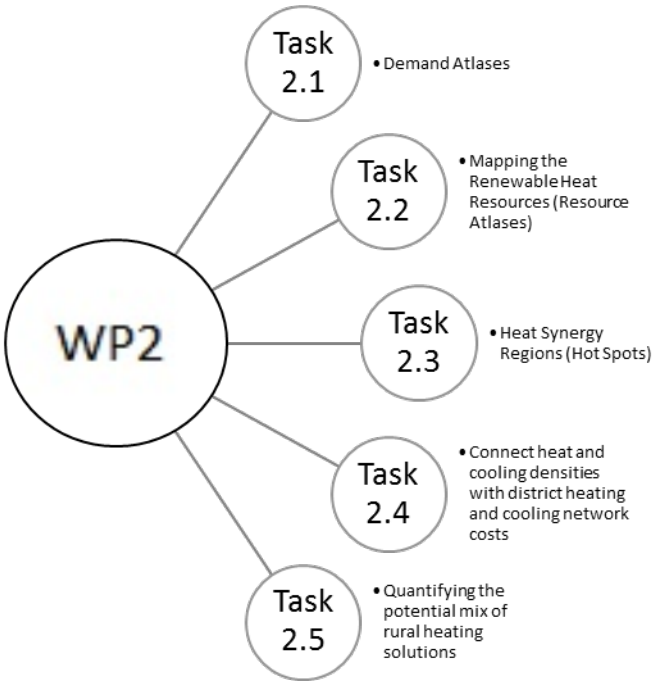

Figure 2.1. WP2 structure and tasks.

Next, the section continues with a thorough presentation of the approaches and data associated with the mapping of excess heat and renewable heat resources (the resource atlases, Task 2.2). This includes e.g. the assessments of large-scale energy sector and industry sector excess heat, of heating and cooling infrastructures, the data provided on regional availabilities of biomass and geothermal heat resources, as well as an account of the land availability investigation for future large-scale solar district heating systems in the 14 MS´s of the EU. Subsequently, the remaining tasks 2.3, 2.4, and 2.5 are addressed orderly with exhaustive presentations of key methodologies, approaches, and theoretical concepts by which the results were produced and obtained.

2.1 Task 2.1: Demand atlases

Knowledge on the distribution of heating and cooling demand densities at the highest possible geographical resolution are required for analyses of heat and cold supply strategies, as the costs and availability of technologies such as district heating highly depend on quantitative information on how demands are distributed within urban areas, towns and neighbourhoods. However, nowhere in Europe today can anyone access continental wide geographical heat and cold demand density data at as high a level of spatial resolution as that of 100 by 100 meters, i.e. by hectares. Apart from a few previous EU projects (Connolly et al., 2014b, Gils, 2012), that managed to assess and produce continuous heat demand densities by square kilometer resolution, the hectare level – or even lower – has so far been available only for a few geographical national settings, e.g. (Scottish-Government, 2017, Scottish-Government, 2014), and some local city projects (for example (Cornelis et al., 2016)).

It is one of the main and most important achievements of this project to have created methods and means by which to arrive at such highly resolved heat and cold demand density models for the 2015 baseline in the 14 MS´s of the EU. Even more so, since this has allowed several important outputs to be assessed and mapped at the same level of spatial resolution, perhaps most notably; specific investment costs for district heating and cooling systems. In addition, existing public geospatial data from institutions like the European Commission's Joint Research Centre and the European Environment Agency of the European Union have been used to the widest possible extent to establish a common denominator for spatial modelling of the European built environment and its heat supply.

However, it should be understood that these demand density rasters are models of real world circumstances, and should consequently not be interpreted as instant images of actual conditions. With this caveat kept in mind, the WP2 map outputs should most appropriately be perceived as representing qualified assumptions of the spatial distribution and extent of the heat and cold demands in the 14 MS´s. These assumptions, as opposed to the many sources of raw in-data used, may be viewed as the relationships between dependent and independent variables in the set of regression models used to anticipate the geographical properties of these demands.

In the following subsections, these assumption, data sources, and models will be accounted for in more detail. It should further be noted that the demand atlases developed and elaborated during the first reporting period refers mainly to the low temperature heat and cold demands in residential and serviced sector buildings for space heating and hot water preparation.

The HRE4 project has also assessed the magnitudes, temperature levels, and sub-sectoral distribution of heat demands in the industrial sector, as presented in the heating and cooling profiles provided by WP3 (Developing a baseline for the Heating and Cooling Systems within the 14 MS´s of the EU). The spatial distribution of these

industrial heat demands, however, are, for reasons further explained in sections 1.3, not part of the current demand atlases.

2.1.1 Residential and service sector thermal demand data

One of the most significant areas of methodological improvements in this fourth Heat Roadmap Europe project compared to its earlier forerunners is the level of detail and quality obtained in the heating and cooling demand data for the 14 MS´s of the EU. Although the core input data here, that is the data of the Eurostat energy balances (used in WP3 to produce MS heating and cooling profiles (Fleiter et al., 2017)), essentially correspond to the input data used in these previous studies[9], in none of these was it ever prepared and distinguished by such a high level of detail. This enhanced level of detail refers mainly to the determination of sectoral, sub-sectoral, technological, and thermal characteristics of the demand data, for which the FORECAST model was used.

For this reason, it is fair to say that the assessed 2730 TWh (~9.83 EJ) of annual heat demands during 2015 for space heating and hot water preparation in the residential (1942 TWh (~6.99 EJ)) and service sectors (788 TWh (~2.84 EJ)) of the 14 MS´s at hand, very likely represents the best estimate currently available. The full detail of this input data on MS level is presented in Table 2.1. Note, that for residential sector heat demands, a distinction is made between those demands originating in single-family housing (SFH) and multi-family housing (MFH).

Table 2.1. Heat demand input data from the HRE4 WP3 heating and cooling profiles for residential and service sectors in the 14 MS´s of the EU, by total volumes (Q_{tot}), by residential sectors (Q_{res}), divided by single-family housing (SFH) and multi-family housing (MFH), and by service sectors (Q_{ser}). Population (P) data from Eurostat. Sources: (Fleiter et al., 2017, ES, 2016)

MS	P [Mn]	Q_{tot} [TWh/a]	Q_{res} [TWh/a]	$Q_{res,SFH}$ [TWh/a]	$Q_{res,MFH}$ [TWh/a]	Q_{ser} [TWh/a]
AT	8.6	64.5	44.2	*32.2*	*12.0*	20.4
BE	11.3	90.1	62.0	*48.1*	*13.9*	28.1
CZ	10.5	65.9	47.3	*27.1*	*20.2*	18.6
DE	81.2	670.4	443.8	*284.5*	*159.3*	226.6
ES	46.4	130.8	92.5	*35.1*	*57.4*	38.2
FI	5.5	62.9	43.2	*32.0*	*11.2*	19.7
FR	66.4	420.6	306.5	*231.3*	*75.2*	114.1
HU	9.9	58.3	40.4	*39.1*	*1.3*	17.9
IT	60.8	354.7	270.4	*93.3*	*177.1*	84.3
NL	16.9	118.1	80.0	*65.3*	*14.6*	38.2
PL	38.0	182.7	138.6	*89.9*	*48.7*	44.1
RO	19.9	50.8	38.5	*26.6*	*11.9*	12.3
SE	9.7	82.3	54.4	*32.0*	*22.3*	27.9
UK	64.9	377.8	280.2	*261.6*	*18.7*	97.6
HRE4	**450.0**	**2730.0**	**1942.0**	***1298.3***	***643.7***	**788.0**

The corresponding cooling demand input data used in this report, as also prepared by WP3 partners and reported in (Dittmann et al., 2017), was estimated at 181 TWh (0.65

[9] That is the international energy statistics published as regular and extended energy balances by the International Energy Agency (IEA).

EJ) in total for the 14 MS´s, distributed by residential sectors at 52 TWh (0.19 EJ) and service sector at 129 TWh (0.46 EJ) respectively, as shown in Table 2.2.

For the production of the output heat and cold demand density rasters of the WP2 demands atlases, this received national level input data on heating and cooling demands needed further preparation and management. Depending on category (heat or cold demand data), these preparatory steps differed quite significantly. As will be presented in the following subsection 2.1.1.1, the heat demand data was distributed to regional levels (NUTS3 region) and adjusted for local climate conditions at this level. The cooling demand data, on the other hand, was used in combination with other complementary cooling sector specific information categories, for example share of cooled area (see subsections 2.1.4.3 and 2.1.4.4 below), in which adjustment for local climate conditions was an integral part (see also subsection 2.1.1.2).

Table 2.2. Cooling demand input data from the HRE4 WP3 heating and cooling profiles for residential and service sectors in the 14 MS´s of the EU, by total volumes (Q_{tot}), by residential sectors (Q_{res}), and by service sectors (Q_{ser}). Sources: (Dittmann et al., 2017)

MS	Q_{tot} [TWh/a]	Q_{res} [TWh/a]	Q_{ser} [TWh/a]
AT	1.43	0.15	1.28
BE	2.22	0.04	2.18
CZ	0.90	0.07	0.82
DE	8.80	0.24	8.56
ES	53.17	15.88	37.28
FI	0.60	0.01	0.59
FR	21.37	4.70	16.67
HU	1.67	0.30	1.37
IT	72.93	29.02	43.91
NL	2.05	0.02	2.03
PL	5.38	0.10	5.28
RO	3.32	0.94	2.38
SE	1.69	0.02	1.67
UK	5.56	0.08	5.47
HRE4	**181.08**	**51.58**	**129.50**

2.1.1.1 Conversion to NUTS3 region level

For the conversion of national level heat demand data to regional levels (NUTS3 region), the input data on total and sectoral heat demand volumes were first divided by total national population counts (as specified in Table 2.1) to produce general average per-capita values, as presented in Table 2.3. For further information on European NUTS3 regions, see also the map in Figure 6.1 of the Appendix in section 6.1, and Table 3.2 and Table 3.3.

Secondly, the corresponding NUTS3 regional heat demands were primarily assessed as the product of the derived specific demands and NUTS3 region population counts, P_{N3R} (ES, 2016), as totals ($Q_{tot,N3R}$) as well as by residential ($Q_{res,N3R}$) and service sectors ($Q_{ser;N3R}$). By this step, the national heat demand data was distributed equally among the NUTS3 regions of each country, as if the specific heat demands of these regions were identical within each country. Now, previous HRE studies have recognised that, especially for countries with far North-to-South stretches, as well as those with high altitude gradients, a correction factor that compensates for differences in local climate

conditions within single MS is needed in this context. Here, it was recognised that a correction mechanism for regional population distributions was motivated as well.

Table 2.3. Specific heat demands calculated based on HRE4 WP3 heating and cooling profiles input data for residential and service sectors and Eurostat population data for the 14 MS´s of the EU, by specific total volumes (q_{tot}), by residential sectors (q_{res}), and by service sectors (q_{ser}). Sources: (Fleiter et al., 2017, ES, 2016)

	[GJ/na]			[MWh/na]		
MS	q_{tot}	q_{res}	q_{ser}	q_{tot}	q_{res}	q_{ser}
AT	27.1	18.5	8.6	7.5	5.2	2.4
BE	28.8	19.8	9.0	8.0	5.5	2.5
CZ	22.5	16.2	6.3	6.3	4.5	1.8
DE	29.7	19.7	10.0	8.3	5.5	2.8
ES	10.1	7.2	3.0	2.8	2.0	0.8
FI	41.4	28.4	12.9	11.5	7.9	3.6
FR	22.8	16.6	6.2	6.3	4.6	1.7
HU	21.3	14.8	6.5	5.9	4.1	1.8
IT	21.0	16.0	5.0	5.8	4.4	1.4
NL	25.2	17.0	8.1	7.0	4.7	2.3
PL	17.3	13.1	4.2	4.8	3.6	1.2
RO	9.2	7.0	2.2	2.6	1.9	0.6
SE	30.4	20.1	10.3	8.4	5.6	2.9
UK	21.0	15.5	5.4	5.8	4.3	1.5
HRE4	**21.8**	**15.5**	**6.3**	**6.1**	**4.3**	**1.8**

2.1.1.2 Adjusting for local climate conditions and demography

As a final step in this preparation of demand data for spatial representation in map outputs, the European Heating Index (EHI) and the European Cooling Index (ECI), both documented previously inter alia in (Werner, 2006b, Werner, 2016, Werner, 2006a, Dalin et al., 2005), were used to compensate for variations in local versus national climate conditions.

The procedure, in brief, utilised original EHI and ECI data for 80 locations in Europe, as depicted with respect to EHI values in Figure 2.2 (and regarding ECI values in Figure 6.2 in section 6.2), to make contour lines (spatial interpolations of the respective index values) on which basis square kilometer raster layers, EHI_{1000m} and ECI_{1000m} respectively, could be made (grid cell values being here the geographical averages of the overlaid contour layers). Hereafter, two separate paths were followed, one for heat demands (dominated by residential sectors) and another for cold demands (dominated by service sectors).

With respect to heat demands, by superimposing a regular NUTS3 region layer with that of the EHI_{1000m} raster (by zonal statistics), the geographical average of all raster grid cell values within a NUTS3 region could be designated to it as its $EHI_{N3R,GM}$ value, i.e. the geographical mean EHI value per NUTS3 region. Hereafter, by nominating population as weight, these values were multiplied with the population of each respective NUTS3 region (P_{N3R}) and prolonged as national sum products, which then were divided by the total population counts of each corresponding country. Hereby, weighted average mean MS EHI values (labelled $EHI_{MS,WAM}$), were established.

The sought output, namely weighted arithmetic mean NUTS3 region indexes based on national average values, here labelled $NHI_{N3R,WAM}$, was finally arrived at by the quota:

$$NHI_{N3R,WAM} = \frac{EHI_{N3R,GM}}{EHI_{MS,WAM}} \quad [-] \qquad (1)$$

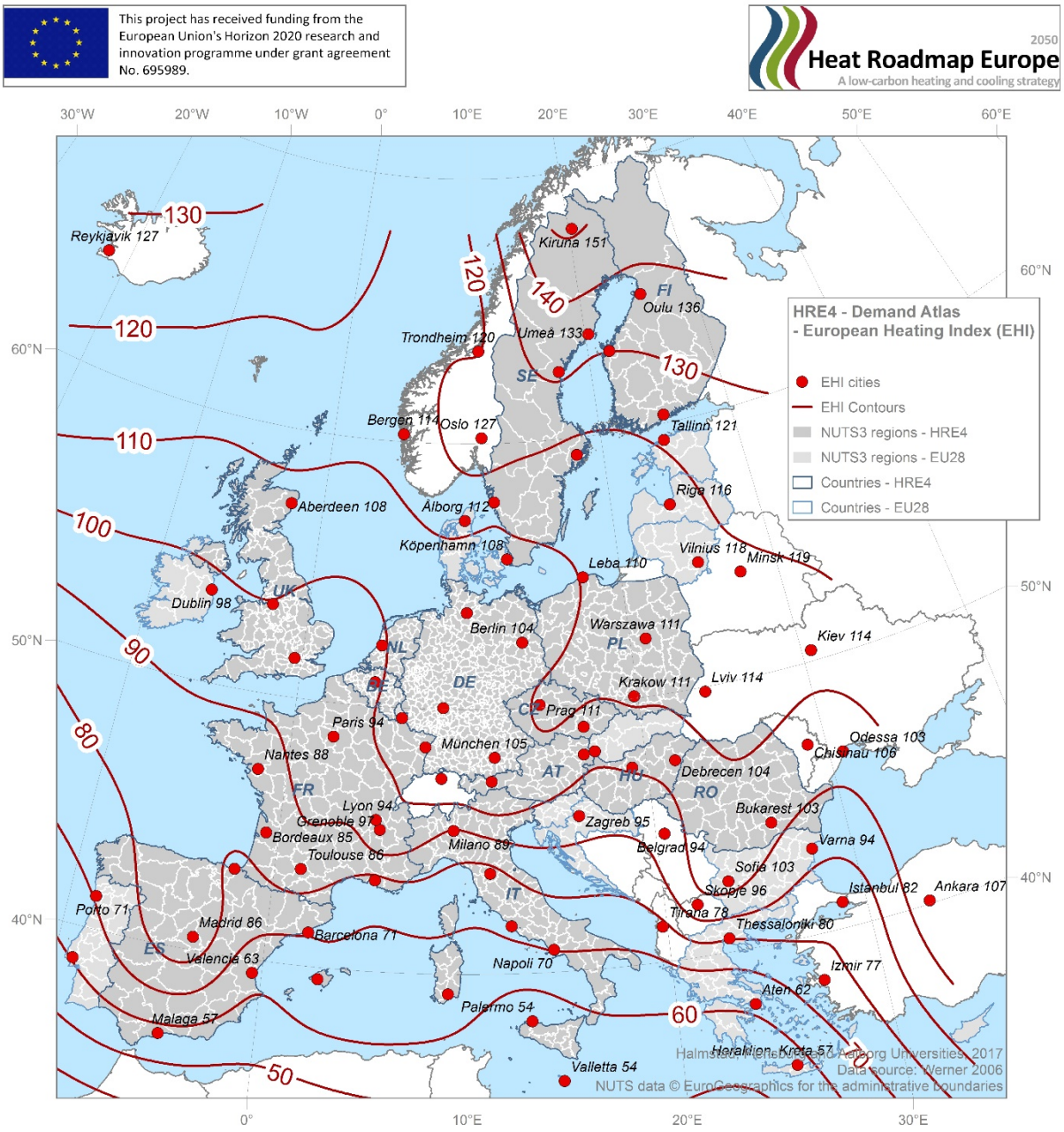

Figure 2.2. European Heating Index (EHI) values for 80 different locations in Europe and corresponding contour lines established by spatial interpolation. Sources: (Werner, 2006b, Werner, 2006a)

This value represents the climatic and demographic correction factor by which the derived heat demand in each NUTS3 region subsequently was multiplied to generate adjusted regional heat demands, as denoted for total demands in Equation (2):

$$Q_{tot,N3R} = q_{tot} \cdot P_{N3R} \cdot NHI_{N3R,WAM} \quad [J] \qquad (2)$$

For cooling demands, no demographic correction was performed mainly since population distributions does not reflect service sector demands such as those of residential sectors. Here, the corresponding square kilometer ECI raster (ECI_{1000m}) was instead used directly – by aggregation – to generate a geographical mean national MS ECI raster ($ECI_{MS,GM}$), which itself subsequently was used to establish a local national cooling index (NCI_{1000m}) specific for each raster cell (see also section 2.1.4.3), according to:

$$NCI_{1000m} = \frac{ECI_{1000m}}{ECI_{MS,GM}} \ [-] \qquad (3)$$

2.1.2 Geo-statistical modelling of the built environment

In absence of actual, recorded or accounted Pan-European heat and cooling demand density data at all desirable geographical levels, the geographical distribution of national heat and cooling demands from the FORECAST model in WP3 must be modelled using otherwise available spatial data which correlate with thermal demands, like for example population densities and built-up areas.

Heating and cooling demands are related to the floor area of residential and service-sector buildings by means of specific heat demands per floor area [kWh/m²], assuming similar building performance by sector. The floor area hence needs to be estimated for different types of buildings, across several types of settlements, and for each hectare. It is here assumed that variables like building area density, population density, land use category, the degree of soil sealing and other phenomena, which are subject to mapping the urban environment, the demographics, and other issues pertinent to European development, may be used to get an idea of the distribution of energy demands.

Multi-linear regression analyses were applied to identify independent variables and their correlation coefficients, which may be used to predict the residential floor area of single- and multi-family houses as well as the floor area of service-sector buildings. As the dependent variables (the known values) for these regressions, the Danish national building register (BBR) delivers floor areas by sector at the address point level (BBR, (n.d.)), which has been aggregated to the 100-metre grid.

In a series of exploratory regressions analyses using the ArcGIS 10 Spatial Statistics extension, independent variables like population densities, GPD densities, land use classes, share of built-up area and degree of soil sealing, as well as derived data, were tested against the dependent variables. The model selection was based on the coefficient of determination, called 'R^2', and the visual appearance (expert view) of the resulting raster data, compared with the recorded floor area data raster.

2.1.2.1 Regression techniques

Several phenomena, which map population and the built environment across Europe, have been analysed and tested by means of exploratory multilinear regression techniques. Regression analysis establishes whether there is a correlation between two

phenomena. Linear regression seeks to describe a proportionality between two phenomena, which can be expressed by a linear equation y = ax + b. Several independent variables x_i may be used in a multilinear regression analysis, where the dependent variable is correlated to several independent variables at the same time, and to a different degree.

Appreciating that the floor area density of buildings is not a function of just the population density, but also of the percentage of built-up area, of land use or GDP, a multilinear model may be better at representing the different types and intensities of the urban tissue. Especially since urban tissue, from low-density suburban dwelling districts, to central residential quarters, and further to areas intensively used by the service sector, all are characterised by different spatial properties.

The dependent, or known, variables for the regression analyses are derived from a 2012 extract of the Danish national building register, BBR (BBR, (n.d.)). BBR is a register of buildings by unit, building, or property, developed since 1979 and maintained daily by municipal administration. It is assumedly the best available national building register in Europe and has been used for the development of heat atlases for a long time (Möller, 2008). The present data set has been taken from the Danish heat atlas version 2.7, developed by Möller and Nielsen (2014) using a BBR extract on the building level dated January 4 2013, which is available as a point data layer.

Floor areas have been summarised for the categories Single Family Housing Residential (SFH), Multi-Family Housing Residential (MFH), Service, and Industry, on the 100-meter grid level using a Spatial Join in ArcGIS. In the following, the phenomena that have been considered or used as independent variables in the regression analyses are described.

2.1.2.2 Independent variables: Population per hectare

The GHSL (Global Human Settlement Layer) population grid (JRC, 2017c) provides the estimated population size for hectare cells in Europe. To quote the above source, it is “derived from Census datasets for 2011 (Eurostat), Corine Land Cover Refined 2006 (CLC06rV2) and European Settlement Map 2016 (ESM 2016)”. It is assumed here that the GHSL 100-metre population grid is the best available model of high-resolution demographics in Europe presently. Subsequent improvements of the data can be expected.

2.1.2.3 Independent variables: Soil sealing

The European Environment Agency (EEA, 2014) provides a 100-metre-by-100-metre raster showing the degree of soil sealing, i.e. the imperviousness of surface areas. Concrete and tarmac are highly sealed, whereas natural soil, agricultural area and forests are not sealed. The degree of soil sealing within one hectare has explanatory value for the presence of buildings, but also other urban functions such as transport

and parking. It is hence assumed that soil sealing is a measure or urban activity and structure.

2.1.2.4 Independent variables: Corine Land Cover

Corine Land Cover is a European database developed and maintained by the European Environment Agency since about 1990. The gridded version of Corine with 100-metre resolution comprises a discrete land use map, which may assist in the identification of urban areas. The numerical grid code of the different Corine Land Cover (EEA, 2017b) categories, with an approximately increasing value for decreasing "urbanity" was tested to be an indicator of urbanisation in the regression analyses. This approach was not convincing.

2.1.2.5 Independent variables: European Settlement Map

The European Settlement Map, (JRC, 2017a) provides information about the share of the area covered with buildings for 100-metre-by-100-metre (2014 and 2016) and 10-metre-by-10-metre (2016) large raster fields. It is partly based on the same source data as the soil sealing data; however, transport areas like roads, parking lots, harbour areas or airports have been edited out by means of a machine learning approach. The variable is henceforward called ESM.

2.1.2.6 Independent variables: UNEP Gross Domestic Product

UNEP/DEWA/GRID-Geneva (UNEP/DEWA/GRID, 2012) published an approximately 1km² raster of the GDP in 2010. Since it is believed that GDP, as a measure of economic activity, is correlated to floor area of especially the service sector, this distributed global GDP dataset has been considered as an independent variable. The metadata of the dataset explains that GDP was allocated to the proportional distribution of the population. Credit is given to GIS processing World Bank DECRG, Washington, DC, extrapolation UNEP/GRID-Geneva.

2.1.2.7 Derived data: Neighbour Mean and Neighbour Sum

Sometimes the presence of built-up areas or soil sealing in a single cell will give an indication of urban tissues quality and quantity not only for each given cell, but also within a defined neighbourhood. The underlying hypothesis is that the sum of all built-up areas around a cell will be high in areas with multi-family buildings. On the other hand, the average degree of built-up areas may be correlated to the floor area of single-family buildings, as these buildings are scattered, the mean value being a good measure for a negative correlation to floor areas.

Therefore, in order to consider the characteristics of the surrounding area of each considered 100-metre-by-100-metre raster cell, the parameters called "Neighbour Mean" (NbrMean) and "Neighbour Sum" (NbrSum) were introduced. These two

parameters have been derived using the ArcGIS Spatial Analyst toolbox with ESM built-up and EEA soil sealing data and are defined as follows:

- Neighbour Mean is the average built-up (or soil sealing resp.) of all cells lying in a three-cell radius around the cell (ignoring no data).
- Neighbour Sum is the sum of built-up (or soil sealing resp.) of all cells lying in a six-cell radius around the cell (ignoring no data).

The shape (circular), as well as the radius used, have been derived based on several test series: the square and the cube of ESM was included in order to account for the non-linearity between the degree of built-up and the floor areas, particularly in central urban areas. Here, ESM values range between 80 and 100%, which compares to ESM values of 40 – 60 % in low-density suburban areas. A linear correlation here would greatly underestimate the central urban areas, while giving too much weight on suburban low-density floor areas.

All the grid data used for raster-based analysis use the common European spatial reference system ETRS89 (EPSG:3035) by ISO19111, projected in the area-preserving Lambert Azimuthal Equal Area 5210 projection. Centre grid point is 52N 10E, false Easting: 4321000.0, and false Northing: 3210000.0.

Other data sets have also been considered, such as for example vector data from the Open Streetmap project (OSM, 2017). OSM is based on an open source (mapping) platform, resulting in large variations regarding coverage, quality, and content across Europe. An exploration of the use of building footprints for establishing a model for types of urban tissue, or the use of road length per hectare as an independent variable in the geo-statistical analysis, had to be given up partly because of data quality issues, partly because exploratory regression did not show any advantage of using OSM data.

2.1.3 Floor area regression models

Exploratory multilinear regression analyses were carried out to identify the best fit between different explanatory variables and the known variables. Criteria were high coefficients of determination (R^2), low residuals, statistical significance and a low level of collinearity. All derived models were tested against the actual distribution of floor areas in the Greater Copenhagen area using visual techniques.

As mentioned above, the demand density estimations are based on the assumption that floor areas for individual building categories (single-family housing, multi-family housing, service sector) are correlated to mapped and modelled phenomena such as demography, urban structure and economic performance. In the following, the regression models used to estimate the distribution of floor areas at 100-metre resolution are presented.

2.1.3.1 Estimation of residential floor areas: Single-family houses

The floor area density raster for single-family buildings, i.e. the spatial distribution of single-family house floor areas, is based on the relationship of variables ESM (%), representing the European Settlement Map data on built-up area coverage per hectare cell, the Neighbour Mean of soil sealing, $NbrMean_{Soilsealing}$ (-), and the square of ESM, as described in Table 2.4 and expressed in Equation 4:

$$A_{floor,ha,SFH} = -6.7 + 30.6 \cdot ESM + 6.8 \cdot NbrMean_{Soilsealing} - 0.48 \cdot ESM^2 \left[\frac{m^2}{ha}\right] \quad (4)$$

For all raster grid cells where the ESM grid cell value is not zero, and considering only results larger than zero square meters per hectare (whereby the floor area in non-built-up areas is kept at zero), the achieved R^2 is 0.27. Aggregated to a one square kilometre grid, the R^2 increases to 0.73.

Table 2.4. Variables used in the modelling of residential and service sector floor areas

Parameter	Unit	Description
$A_{floor,ha,SFH}$	[m²/ha]	Floor area of single-family houses per hectare cell
$A_{floor,ha,MFH}$	[m²/ha]	Floor area of multi-family houses per hectare cell
ESM	[%]	ESM built-up area coverage per hectare cell
$NbrMean_{Soilsealing}$	[-]	Neighbour Mean of seal sealing
$NbrSum_{ESM}$	[-]	Neighbour Sum of ESM built-up area
P_{ha}	[cap/ha], [n/ha]	Population per hectare cell

As presented in the three map images of Figure 2.3, the visual analysis of the single family floor area model shows that the model somewhat overestimates the real presence of single-family floor areas in central city areas, by generating higher densities in these areas, it must be noted that the heat demand models take these uncertainties into account by not relying on absolute values, but on the ratio between SFH and MFH areas. Even though the model predicts higher absolute densities in these areas, it is still believed to be the best of the available models.

2.1.3.2 Estimation of residential floor areas: Multi-family houses

Floor areas of multi-family residential buildings have been modelled using the variables ESM, Population per hectare (P_{ha}), the Neighbour Sum of ESM, and ESM raised to the power of three (as also described in Table 2.4), in accordance with Equation 5:

$$A_{floor,ha,MFH} = 7.4 - 18.1 \cdot ESM + 26.6 \cdot P_{ha} + 0.1 \cdot NbrSum_{ESM} + 0.003 \cdot ESM^3 \left[\frac{m^2}{ha}\right] \quad (5)$$

The modelling was performed for all cells where the ESM value is not zero and considering only results larger than 700 square meters MFH building area per hectare (7%) of all grid cells located within the EU MS boundaries. The resulting R^2 is 0.32, while aggregated to 1 km² resolution it increases to 0.94.

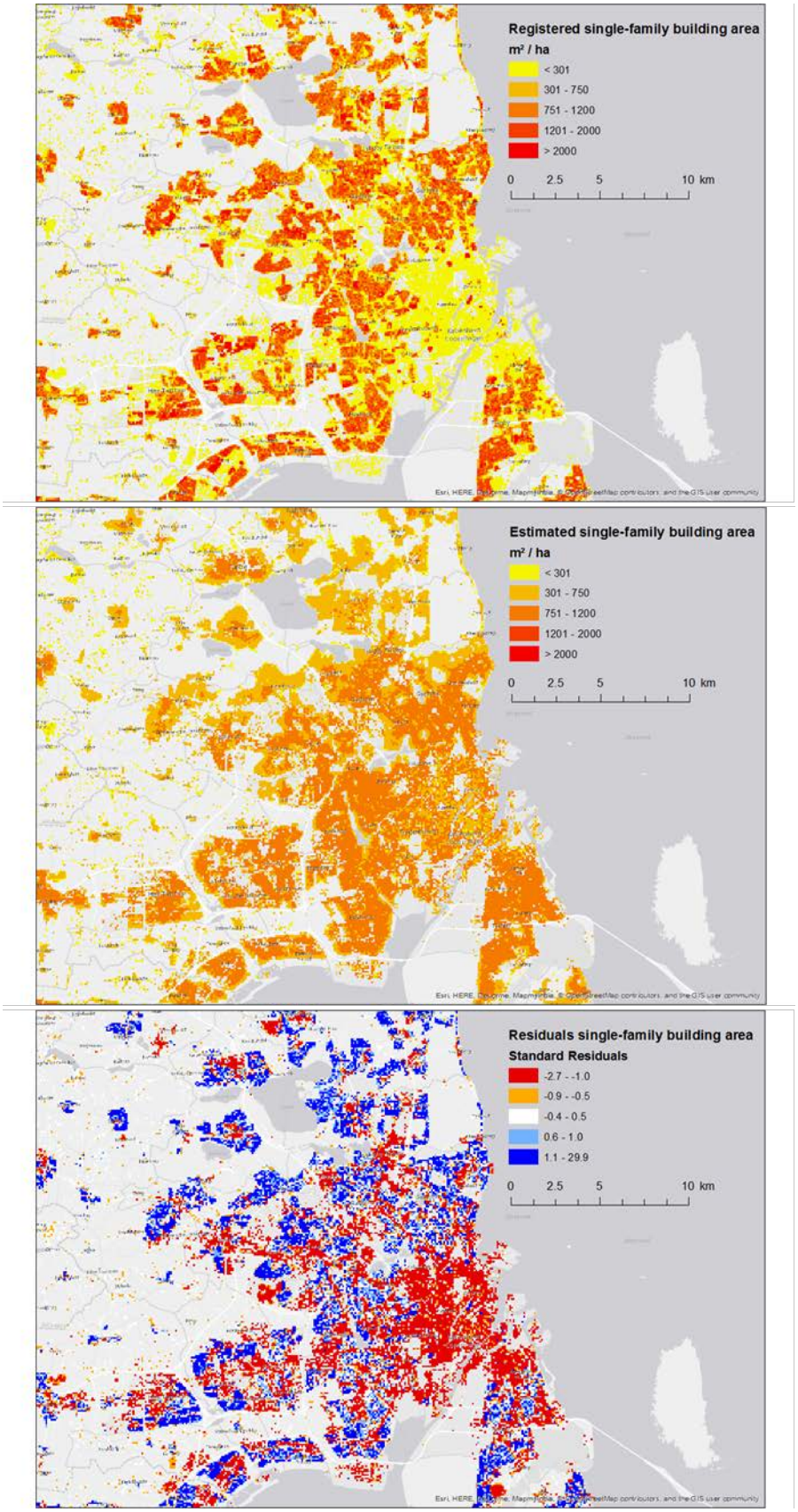

Figure 2.3. Estimation of residential sector floor areas – Single-family houses: Actual (top) and modelled (middle) floor area densities as well as their standard residuals (bottom) of single-family houses in the Copenhagen area.

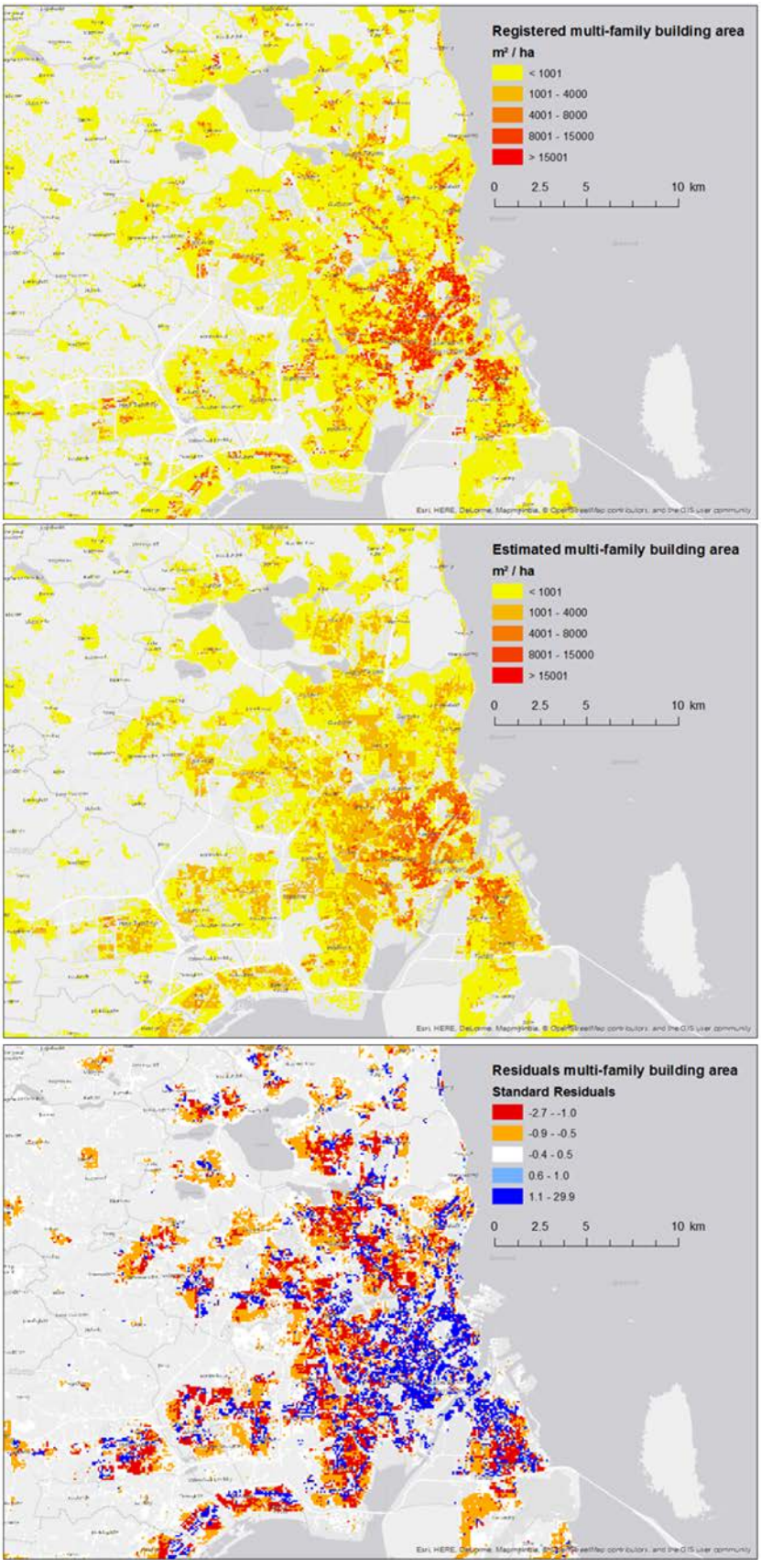

Figure 2.4. Estimation of residential sector floor areas – Multi-family houses: Actual (top) and modelled (middle) floor area densities as well as their standard residuals (bottom) of multi-family houses in the Copenhagen area.

Compared to single-family housing, this means that the modelling of multi-family housing shows higher coefficients of determination, probably because of higher homogeneity. A one square kilometre model based on aggregation would be very close to the recorded building mass in Denmark. Corresponding maps in Figure 2.4 show a clear concentration of estimated multi-family buildings in the same city centres where also the recorded multi-family buildings are located. This indicates that the model has a good fit and may be used to predict with high confidence the larger proportion of the built environment where district heating or cooling may be relevant.

The building floor areas calculated in this bottom-up manner are not used directly as absolute figures, but for the calculation of the ratio between single- and multifamily building floor areas, see section 2.1.4.1. Hence the distribution of floor areas rather than the actual floor area numbers are of relevance.

2.1.3.3 Estimation of service sector floor areas

The model for estimating service sector floor areas has been the most complicated and time-consuming one to prepare. The mapping of service sector buildings is most difficult because of two distinctively different agglomeration types for service sector floor areas: on one hand, shops and offices are concentrated in the city centres, while, on the other hand, retail centres and stores are located in the urban perimeter. Likewise, the public service buildings follow population centres, whereas the private sector buildings may be located in areas of high economic activity.

The estimation of the service sector floor areas using multiple regression analyses was based on hypotheses where population per hectare (P_{ha}), the Neighbour Sum of ESM ($NbrSum_{ESM}$), the Neighbour Sum of soil sealing ($NbrSum_{Soilsealing}$), Gross Domestic Product (GDP), and ESM, was evaluated as independent variables. Equation 6 accounts for the coefficients in the model output, Table 2.4 and Table 2.5 describe the variables in detail, and the three maps in Figure 2.5 illustrate the model fit to registered values for the case study of the Danish capital Copenhagen.

$$A_{floor,ha,ser} = -1188 - 6.3 \cdot P_{ha} - 0.7 \cdot NbrSum_{ESM} + 0.7 \cdot NbrSum_{Soilsealing} + 0.006 \cdot GDP + 0.011 \cdot ESM^3 \left[\frac{m^2}{ha}\right] \quad (6)$$

This model calculating the floor areas included only cells with an ESM built-up value larger than 50%; otherwise the floor area was set to zero. Further, only results larger than zero square metres per hectare were considered. The resulting R^2 for Denmark on 100 by 100-metre level of 0.09 is very low, but on one-by-one square kilometre level it is 0.55. It is concluded that the model for service sector floor areas has high uncertainties, which need to be addresses in subsequent work.

Table 2.5. Variables used in the modelling of service sector floor areas

Parameter	Unit	Description
$A_{floor,ha,ser}$	[m²/ha]	Floor area of service sector buildings per hectare cell
GDP	[USD/~km²][a]	UNEP Gross Domestic Product 2010

[a] Thousand of constant 2000 USD per 30 arc second (approximately 1km) grid cells.

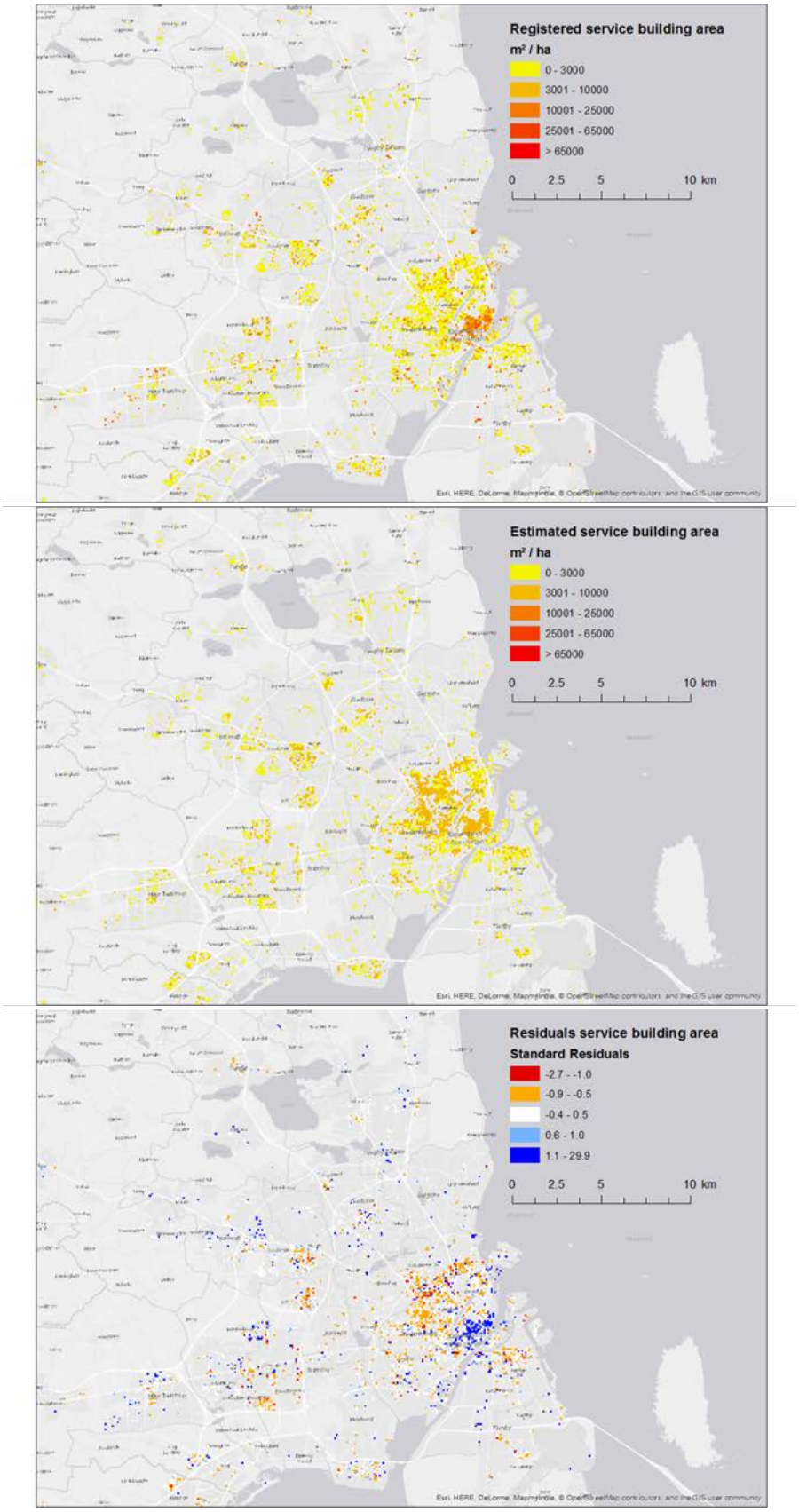

Figure 2.5. Estimation of service sector floor areas: Actual (top) and modelled (middle) floor area densities as well as their standard residuals (bottom) of service-sector buildings in the Copenhagen area.

The level at which R^2-values show a reasonably good fit depend on the context. The present model uses a very large number of observations because of the 100-metre grid representation of the building mass. However, since the BBR data is georeferenced to address point locations while the independent and dependent variables are located across the uniform 100-metre grid, the high resolution contributes to local divergence between variables.

The aggregation to square kilometre levels all indicate significantly higher coefficients of determination, and thereby a higher confidence on this scale. The impact on the estimation of heating and cooling demands is hence that within one square kilometre the estimated values are representative but only 10% – 30% correctly located. It is assumed here that the impact on the final results is levelled out for areas as large as a medium-sized town or a typical municipality. Further scrutiny on the statistical analysis is required.

2.1.4 Heating and cooling demand density models

To arrive at raster representations of heating and cooling demand densities in the 14 EU MS´s studied, the above calculated floor areas for residential and service sectors were used together with several kinds of additional input data and complementary factors and quantities. In the following, the basic equations, relationships, and assumptions used for the calculations of residential and service sector heat and cold demand densities are accounted for together with some map illustrations and tables.

Once again, due to the hectare level resolution of these density rasters, i.e. the core outputs from the demand modelling and mapping activities of WP2, it is quite senseless to present these outputs graphically in continental static map images. Although some illustrative case examples are shown below (see e.g. Figure 2.6 and Figure 2.7), the main dissemination format for these results is that of the Peta4 web application.

2.1.4.1 Residential sector heat demand density

Residential heat demand was originally intended to be calculated using the floor area models of the previous section in combination with regional (NUTS3) data of specific heat demand, as described in section 2.1.1.1. However, it turned out that the simple distribution of national heat demands by the NUTS3 level population, which has been the preferred method in previous HRE studies (i.e. in previous versions of Peta), would be inferior to the improved modelling of floor areas in the bottom-up manner described in the previous subsection.

Meanwhile, as the heat demand on the national level would still be measured per capita, the novel approach introduced here begins by estimating the population in single-family houses, $P_{ha,SFH}$ (and accordingly for multi-family houses, $P_{ha,MFH}$), in each considered hectare grid cell:

$$P_{ha,SFH} = \frac{A_{floor,ha,SFH}}{\alpha_{SFH}} \quad \left[\frac{n}{ha}\right] \tag{7}$$

For this, input data on specific national average floor areas (per capita) for single-family housing, α_{SFH} (m^2/n), and multi-family housing, α_{MFH} (m^2/n), was gathered from available census data in the form of "density standard (floor area)" of dwellings by nation and type of building (ES, 2011). This approach was necessitated mainly by a general mismatch between determinants of sectoral heat demand (i.e. area versus population).

Next, this estimated single-family housing (and multi-family housing) population per hectare grid cell was corrected ($P_{ha,SFH,corr}$ and $P_{ha,MFH,corr}$ respectively) by use of the hectare grid cell population data in the Global Human Settlement (GHS) layer ($P_{ha,GHS}$) of the JRC (JRC, 2017c), according to:

$$P_{ha,SFH,corr} = \frac{P_{ha,SFH}}{P_{ha,SFH} + P_{ha,MFH}} \cdot P_{ha,GHS} \quad \left[\frac{n}{ha}\right] \tag{8}$$

Next, by summation of all corrected single-family and multi-family hectare population counts per country, as expressed in Equation 9 for single-family housing (n being the number of considered hectare grid cells per country), total national population counts per each building type category ($P_{tot,SFH}$ and $P_{tot,MFH}$ respectively) could be established.

$$P_{tot,SFH} = \sum_{i=1}^{n} P_{ha,SFH,corr} \quad [n] \tag{9}$$

From this, finally, residential sector heat demands by hectare grid cells, i.e. residential sector heat demand densities ($q_{L,res}$), was established and further adjusted for regional climate and demographical conditions by use of nationally weighted (arithmetic mean) heating indexes per NUTS3 region ($NHI_{N3R,WAM}$), as described in subsection 2.1.1.2.

For the final calculations, as shown in Equation 10, total residential building heat demands by the two building categories ($Q_{res,SFH}$ and $Q_{res,MFH}$ respectively, as detailed in Table 2.1), were used:

$$q_{L,res} = \left(\frac{P_{ha,SFH,corr} \cdot Q_{res;SFH}}{P_{tot,SFH}} + \frac{P_{ha,MFH,corr} \cdot Q_{res,MFH}}{P_{tot,MFH}} \right) \cdot NHI_{N3R,WAM} \quad \left[\frac{GJ}{ha}\right] \tag{10}$$

A snapshot example of the final and complete heat demand density raster of HRE4 (i.e. both residential and service sector heat demands combined) is shown in Figure 2.6.

This project has received funding from the European Union's Horizon 2020 research and innovation programme under grant agreement No. 695989.

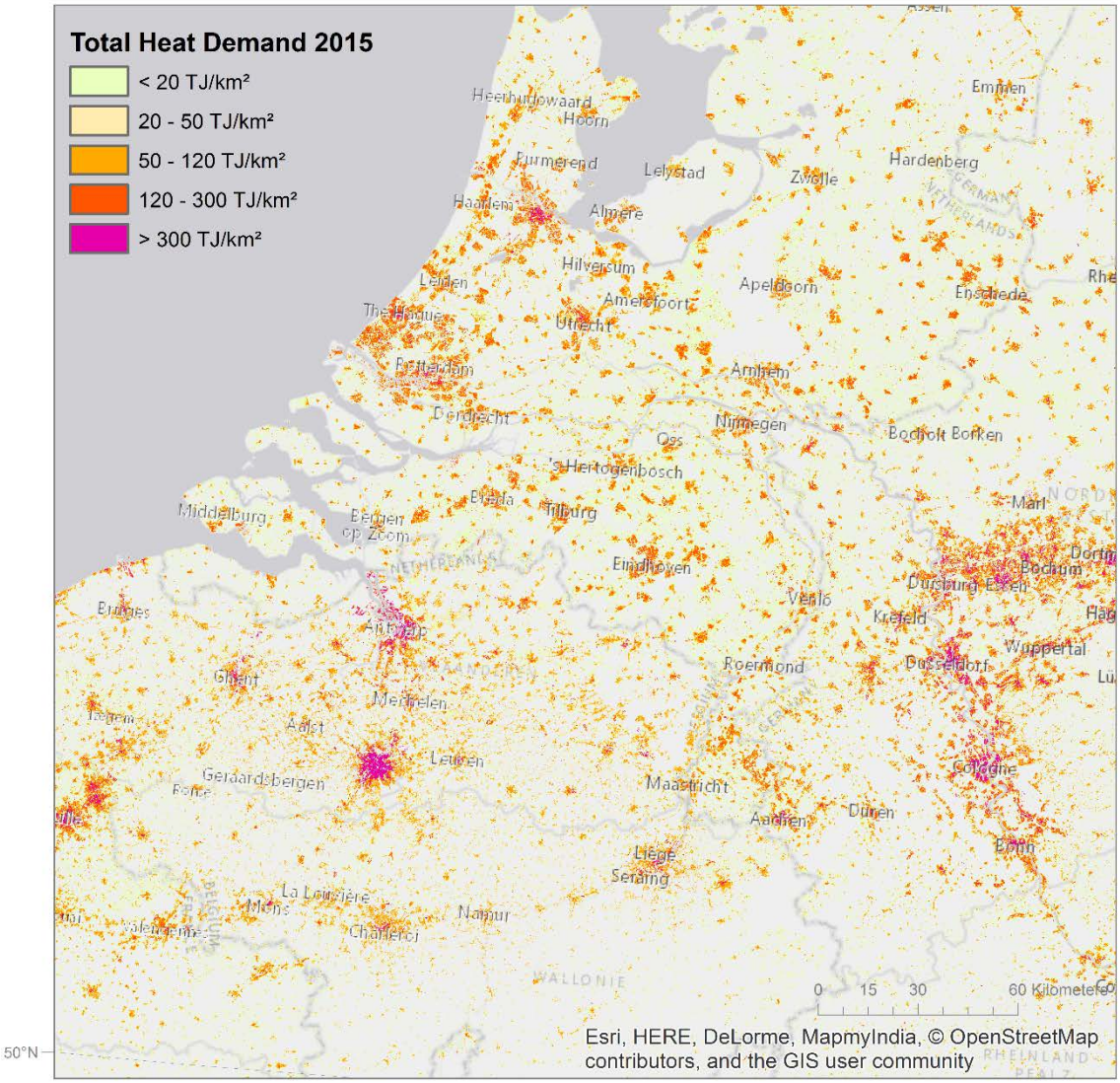

Figure 2.6. Mapping of residential and service-sector heat demand densities for year 2015. Snapshot overview of Belgium, northern France, the Ruhr, and the Netherlands areas of western central Europe.

2.1.4.2 Service sector heat demand density

For the service sector heat demand density assessment ($q_{L,ser}$), a more straight-on approach could be used. Here, the service sector hectare floor areas described above was used together with regionally distributed (NUTS3 region) national heat demand data ($Q_{ser,N3R}$, as described in subsection 2.1.1.1 above), and regionally distributed (NUTS3 region) service sector floor areas, $A_{floor,ser,N3R}$ (m^2), according to:

$$q_{L,ser} = \frac{Q_{ser,N3R} \cdot A_{floor,ha,ser}}{A_{floor,N3R,ser}} \quad \left[\frac{GJ}{ha}\right] \tag{11}$$

For all grid cells with an ESM built-up value of zero, the service sector hectare floor area was correspondingly set to zero. The final output raster is part of the combined residential and service sector raster displayed for Belgium, northern France, the Ruhr, and the Netherlands areas of western central Europe in Figure 2.6.

2.1.4.3 Residential sector cooling demand density

Residential cooling demand was calculated for single-family houses and multi-family houses combined, since the national cooling demand data delivered from the project partners did not differentiate between types of residential buildings. Subsequently, the floor areas for single and multi-family houses were added for each raster cell to generate total residential floor areas per hectare ($A_{floor,ha,res}$):

$$A_{floor,ha,res} = A_{floor,ha,SFH} + A_{floor,ha,MFH} \quad \left[\frac{m^2}{ha}\right] \tag{12}$$

A national correction factor was considered necessary to introduce in this context, since the assumed floor areas that WP2 received from project partners were discrepant and sometimes greatly different from the ones derived by the bottom-up methods described in this report. Since the discrepancies originated in different statistical methods, but also in somewhat different residential floor area definitions, namely those of gross floor area, $A_{floor,tot,res}$ (m^2) and merely net indoor floor area, $A_{indoor,tot,res}$ (m^2), this residential sector correction factor was defined as:

$$corr_{res} = \frac{A_{indoor,tot,res}}{A_{floor,tot,res}} \quad [-] \tag{13}$$

Residential sector cooling demand density ($q_{L,res}$) was then calculated using the residential hectare floor areas ($A_{floor,ha,res}$) , the correction factor ($corr_{res}$), the local national cooling index (NCI_{1000m}), and a market share of cooled area ($Share_{cooledArea,res}$) to be multiplied with the specific residential cooling demand on the national scale, $q_{res,national}$ (GJ/m^2), according to:

$$q_{L,res} = A_{floor,ha,res} \cdot corr_{res} \cdot NCI_{1000m} \cdot q_{res,national} \cdot Share_{cooledArea,res} \quad \left[\frac{GJ}{ha}\right] \tag{14}$$

National cooling index data by square kilometres was derived from the data presented in subsection 2.1.1.2 above, while the share of cooled residential areas and the data on specific (indoor floor area) residential cooling demands were supplied by project partners in WP3 (Fleiter et al., 2017, Dittmann et al., 2017). A corresponding snapshot example of the final and complete cold demand density raster of HRE4 (i.e. both residential and service sector cold demands combined) is shown in Figure 2.7.

This project has received funding from the European Union's Horizon 2020 research and innovation programme under grant agreement No. 695989.

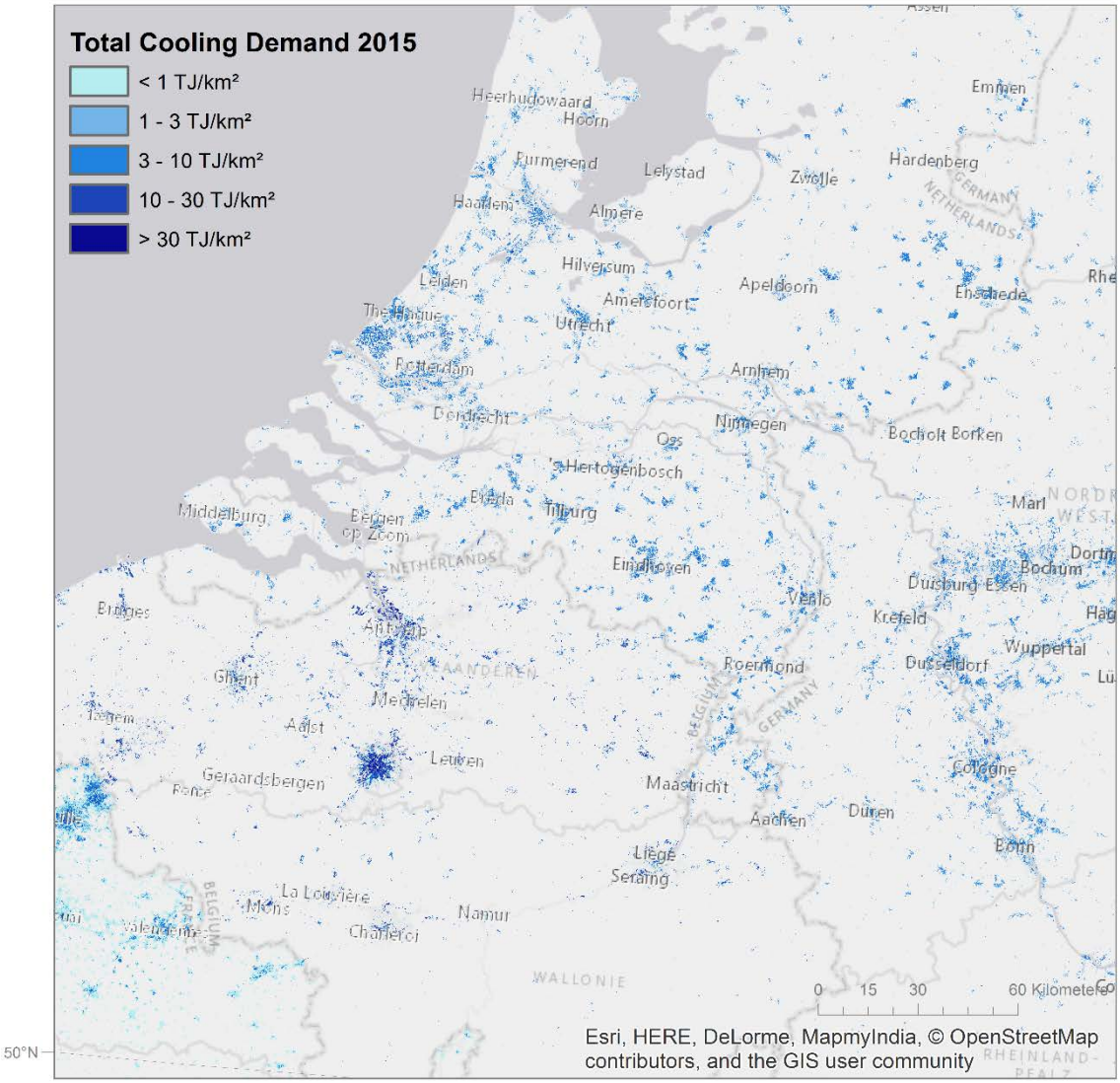

Figure 2.7. Mapping of residential and service-sector cooling demand densities for year 2015. Snapshot overview of Belgium, northern France, the Ruhr, and the Netherlands areas of western central Europe.

2.1.4.4 Service sector cooling demand density

The cooling demand density of the service-sector ($q_{L,ser}$) was estimated in perfect accordance with the approach used for the residential sector. Hence, it was calculated using the service sector hectare floor areas ($A_{floor,ha,ser}$), a corresponding correction factor ($corr_{ser}$), the same national cooling index (NCI_{1000m}), and a market share of cooled service sector area ($Share_{cooledArea,ser}$) to be multiplied with the specific service sector cooling demand on the national scale, $q_{ser,national}$ (GJ/m^2), according to:

$$q_{L,ser} = A_{floor,ha,ser} \cdot corr_{ser} \cdot NCI_{1000\,m} \cdot q_{ser,national} \cdot Share_{cooledArea,ser} \quad \left[\frac{GJ}{ha}\right] \tag{15}$$

Where the corresponding correction factor for the service sector floor areas was defined as the quota of indoor service sector floor areas, $A_{indoor,tot,ser}$ (m^2), and total service sector floor areas , $A_{floor,tot,ser}$ (m^2), according to:

$$corr_{ser} = \frac{A_{indoor,tot,ser}}{A_{floor,tot,ser}} \quad [-] \tag{16}$$

2.1.4.5 Modelling remarks

Given the many complexities associated with the task of mapping heating and cooling demands, population densities, floor area distributions etc., at high levels of spatial resolution, there certainly are areas of improvements among the many approaches and methods applied here. Still, to our current knowledge, the resulting raster data of heating and cooling demand densities for the residential and service sectors that are presented here are the hitherto most detailed and comprehensive attempt to map the spatial distribution of thermal demands in European buildings.

The produced raster datasets from this section constitute furthermore in many instances crucial input data for subsequent calculations in the project, especially those resulting for example in district heating and cooling systems investment costs, as described in subsection 2.4. Still, solely in themselves, they certainly also constitute main outputs of this project.

As also mentioned above, however, there is not much meaning in presenting these highly resolved raster data sets as static report images. The simple reason for this is that at such zoomed-out scales their content is not at all visible or comprehensible. For this reason, the main format by which to experience these layers, i.e. the most appropriate reporting format, one might say, is to activate and observe them as operational layers in the Peta4 web map application.

For reasons of storage space preservation, moreover, all demand raster data layers available at Peta4 have been further processed to unsigned 16 bit pixel depth, which means that they can hold integer values from 0 to 65535. A few higher demand figures had to be cut off, with negligible impact on the results. For heating and cooling demands, a classification by few and clear intervals of heating and cooling demand per hectare was also introduced for the purpose of faster visualization.

Finally, while in these calculation models all energy units were adjusted to the area unit of one hectare because the model uses the one hectare grid cell size (100-metre by 100-metre), the units are in some instances adjusted from GJ/ha to TJ/km² (by dividing by a factor 10). The general rationale for this was to obtain conformity with the heat demand density classification shown in Table 6.1 in the Appendix subsection 6.3.

2.1.5 Delineation of prospective DH supply areas

A quantification of heat demands within specified neighbourhoods is required to map areas, which could form prospective DH (district heating) supply areas, or parts of those. While the heat demands are modelled for individual 100-metre grid cells, several of those cells can form a coherent and contiguous zone. In ArcGIS Spatial Analyst, the Region Groups tool was used to identify individual clusters of grid cells, which are connected to at least one of four direct neighbour cells. This method forms individual zones of areas with a heat demand higher than a threshold value. For prospective supply zones here, the threshold was set at 50 TJ/km², while for the identification of rural heat demand in very small and sparse clusters this value was as low as 20 TJ/km².

This process has led to a delineation of prospective DH supply areas, which consequently are used as a geographical entity to summarize heat demands, to allocate excess heat, and to establish a spatially explicit connection between heat demands, district heating and cooling investment costs, as well as heat sources. It should be noted that these prospective DH areas are independent of the coherent DH areas (UMZ_DH), which are described in subsection 2.2.2.2. While the former are based on the heat demand densities established in this study, the latter consist of urban morphological zones that currently have district heating systems in operation.

2.2 Task 2.2: Mapping the Renewable Heat Resources (Resource atlases)

To the resource atlases of HRE4 belong not only the mapping of straight-out renewable heat resources, such as solar thermal, biomass, and geothermal heat sources, but also the spatial charting and assessment of excess heat annually available from activities in energy and industry sectors. For as long as such energy and industry sector activities remain operational[10], the excess heat emanating from them may be regarded – if not as renewable in the true sense of the word – at least as assets subject to continuous replenishment. Consequently, although a more proper label for this section would have been merely “Resource Atlases”, all locally available heat resources accounted for in the following are treated under the heading “renewable heat resources”.

In terms of actual quantification of annual availabilities, excess heat from energy and industry sector activities have proven more feasible to determine in comparison to the three studied categories of distinctive renewable resources. One, among several, reasons for this is the fact that while excess heat availabilities exist as point sources on the map, biomass availabilities, as well as the potential availabilities of solar radiation and geothermal heat, appear spatially rather as indistinct and discontinuous fields of opportunities. It has therefore been a subject for intense and recurring discussions among the WP2 researchers, how most appropriately to display and illuminate renewable heat resources given the available project hours and priorities.

As will be described in the following, the general resolution in HRE4 regarding mapping of renewable resources has thus been partly to establish cooperation with other contemporary, state-of-the-art, EU projects dedicated to these topics, by which the project has obtained access to datasets of a quality much higher than that which could have been achieved internally. Partly, the mapping strategy itself, i.e. the forms and means by which spatial relationships between the renewable resources themselves and the corresponding demand centres are identified, relies here entirely on the interactivity of the HRE4 Peta Online web map application.

In contrast to previous HRE studies, where for example, biomass and geothermal resources were displayed by e.g. relative availability or suitability levels and other types of fabricated “potential”-layers, these assets are here deliberately presented directly as is, i.e. as local, regional, annual availabilities, preferably in energy units where so possible. The main reason for this standpoint is that actual availability levels of renewable resources, and especially so for those of biomass, is subdued under such a great variety of factors[11] that the production of credible, general “potential

[10] This is in itself a critical and relevant area of consideration and future research; however, it is not the focus of the current section and therefore not elaborated further upon in this context.
[11] For example, alternative uses other than for energy purposes, sustainable usage levels, a transportable resource (locally, nationally, internationally), preferable usage level (household boilers, block boilers, power plants), preferable conversion types (combustion, gasification), etc.

assessments" for their regional availability requires attention and resources in excess of what has been allocated to the task in this project.

Hereby our resolution, namely to make the core geographical data layers of renewable resources, as conceived by the most recent, dedicated EU projects on these topics (here referring to sustainably available biomass (BioBoost) and geothermal heat (GeoDH)), directly accessible on the HRE4 online web service for any user of the interface. By the inherent measurement tools and opportunities to superposing other mapping output layers present in the map interface, any user, any local energy planner, any utility or regional coordinator, will have direct access to information on location, magnitude, and character of whatever resources and demands are locally present in any given case.

Regarding opportunities for solar thermal heat in the 14 MS´s, that is opportunities for installations of large-scale solar thermal collector fields directly in city vicinities, the approach here also includes collaboration with an external project (Task 52 of the IEA-SHC project), but constitute an exception in terms of the forms and means by which its spatial relationship is represented. In this instance, WP2 has performed an ordinary potential assessment, referring to an investigation of available suitable land for 20% and 50 % solar thermal heat shares in a selection of candidate district heating cities and towns, which is described in section 2.2.3 below.

In the following sub-sections 2.2.1 to 2.2.5, the methodologies and assumptions used in WP2 for the mapping of renewable resources are accounted for with focus on main input datasets, core theories, key concepts, with references to complementary publications where appropriate, while a selection of main results are summarised in section 3. Included in the resource atlas, finally, as present in subsection 2.2.2 below, is also a presentation of the fifth version of the Halmstad University District Heating and Cooling database (HUDHC_v5, 2016), which has provided vital information on current district heating and cooling infrastructures in Europe, vital for the feasible mapping of district heating and cooling cities in HRE4.

2.2.1 Energy and industry sector excess heat

A critical condition for the initial development of the HRE methodology to assess annually available excess heat volumes from European energy sector and energy-intensive industrial sector activities is the fact that no such data is readily available in ordinary international energy statistical sources. Recovered energy as such has remained a concept foreign to the common and historical structures of such statistics, since they by resorting to principles of thermodynamics (energy conservation and entropy) reflect the idea that conversion efficiencies above one is an impossibility.

There are likely many other reasons as well for the apparent contemporary scarcity of qualitative data on excess heat magnitudes to be expected from European power plants and industries, of which perhaps the very modest recoveries that are actually taking place so far in the European context might be one of the more reasonable explanations. However, among the publications of previous HRE studies (Connolly et al., 2012,

Connolly et al., 2013, Connolly et al., 2014b), and those of several others during recent years (Brueckner et al., 2014, Morandin et al., 2014, Eriksson et al., 2015, Broberg et al., 2012, Ivner and Broberg Viklund, 2015, Sandvall et al., 2015, Persson and Werner, 2012), it is clear that the interest and awareness is increasing by a considerable rate. Whether this increase in (academic) interest, e.g. methodologies by which to assess their magnitudes and spatial distribution, is reflected in a corresponding (practical) interest in the utilisation of the vast opportunities associated with recovery of secondary energy flows from these facilities, remains an open question yet to be settled.

As for the assessment made here, the methodological approach and assumptions made differs from those of the latest European scale HRE assessment of the second pre-study (Persson et al., 2014) only in terms of reference years for used input data, a narrowed scope to the 14 HRE4 MS´s, and the addition of Mining and Quarrying among considered industrial sectors. Hence, the ninth version of the European Pollutant Release and Transfer Register, the E-PRTR_v9 dataset (EEA, 2016a), publicly available as set of data tables in a relational database in the Microsoft Office Access format, constitute the core basis for the estimate at hand.

This version of the emissions database of the European Environment Agency (EEA), holds, among other emission types, quantitative data on facility specific carbon dioxide emissions from stationary combustion and other processes in European energy and industry sector facilities. However, since the E-PRTR database is of cumulative nature (meaning that for every new release, new information is added to the old but none is removed[12]) (EU, 2006), it is necessary to perform an extraction from the database in order to obtain the relevant data. As in previous HRE studies, this data extract is used – by applying a reversed calculation sequence – to assess annual primary energy supplies at facility level and – by additionally applying default main activity sector recovery efficiencies – to assess annual excess heat volumes available at these facilities.

2.2.1.1 Carbon dioxide emission factors

The methodological sequence begins by using standard carbon dioxide emission factors, sf_{co2}, from stationary combustion, as available in (IPCC, 2006), for ordinary fuel types, see Table 2.6, as well as for waste and biofuel fuel types, as shown in Table 2.7.

Table 2.6. Standard carbon dioxide emission factors from stationary combustion, by fuel type. Source:(IPCC, 2006)

Fuel type	**Sf_{CO2} [g,CO2 / MJ]**
Coal and coal products	94.6
Peat	106.0
Oil shale and oil sands	107.0
Crude, NGL and feedstocks	73.3
Oil products	74.1
Natural gas	56.1
WTE	77.5[a]

[a] Note, calculated value based on emission and energy statistics.

[12] The first annum in the E-PRTR database series consists of the prevailing 2001 EPER records, which is followed by the EPER 2004 data. From 2007 and forward, after the 2006 establishment of the E-PRTR regulation, the records refer to the E-PRTR context only and are now reported annually.

For waste fuels, or Waste-to-Energy (WTE), a fuel category that in the IPCC context extends over a wide array of different sub-types, and which further may be difficult to assess since statistical accounts hereof often are mixed with that of other biofuels, a separate assessment was made involving the extended energy balances from the International Energy Agency (IEA, 2016a). The purpose of this assessment was to create one uniform benchmark value representative as a common standard carbon dioxide emission factor for the heterogeneous WTE concept. In short, by utilising EU28 carbon dioxide emissions data from E-PRTR_v9 (annual volumes from waste incineration in transformation processes (heat and power generation)[13]) combined with known primary energy supplies[14] to these activities for the four-year period 2010 to 2013, an empirical, weighted arithmetic mean value of 77.5 g,CO_2/MJ could be established, as applied in Table 2.6.

Table 2.7. Standard carbon dioxide emission factors from stationary combustion, by waste and biofuel fuel type. Source: (IPCC, 2006)

Fuel type	**Sf_{CO2} [g,CO2 / MJ]**
Industrial waste	143.3
Municipal waste (renewable)	100.0
Municipal waste (non-renewable)	91.7
Primary solid biofuels	112.0
Biogases	54.6
Biogasoline	70.8
Biodiesels	70.8
Other liquid biofuels	79.6
Non-specified primary biofuels and waste	100.0
Charcoal	112.0

Hereafter, the standard carbon dioxide emission factors of Table 2.6 were assigned to each corresponding fuel type in the national energy balance sheet of each considered Member State, as available for the reference year 2013 in (IEA, 2014)[15]. By calculating a sum-product consisting of the primary energy (fuel) supply volume of each considered main activity sector times the corresponding standard emission factor for each fuel type, and then subsequently dividing this sum-product with the total primary energy supply volume for each main activity sector, specific carbon dioxide emission factors, f_{co2} (g,CO_2/MJ), could be established.

These specific carbon dioxide emission factors then, as detailed for each considered Member State and main activity sector in Table 2.8, provide unique main activity sector accounts with respect to the carbon intensity of domestic generation and production in energy and industry sector activities for each of these nations. For the main activity sector FSR (Fuel supply and refineries), an exception similar to that of the WTE sector

[13] 2010: 61.3 Mt, 2011: 52.3 Mt, 2012: 48.4 Mt, and 2013: 53.2 Mt.
[14] 2010: 667.7 PJ, 2011: 694.9 PJ, 2012: 719.7 PJ, and 2012: 731.4 PJ.
[15] At the time of completing this part of the study (summer of 2016), the 2016 edition of the IEA energy balances (incorporating data up to year 2015) had not yet been published, nor was any 2015 data available at Eurostat. The total EU28 primary energy supply for 2013 was given at 18,906 TWh (68,062 PJ) in the referenced 2014 edition of the IEA energy balances. The subsequently published 2016 version gives a corrected value of 18,914 TWh (68 092 PJ) for the year 2013. For the year 2014, the value is given at 18,201 TWh (65 522 PJ). Since the extract of carbon dioxide emission data from the E-PRTR_v9 includes excess heat activities mainly from the three-year period 2012 to 2014, this difference, although considerable in terms of total primary energy supply reductions in only one year, is expected to be negligible with respect to the established specific carbon dioxide emission factors.

was made. For FSR, the standard carbon dioxide emission factor of the IPCC fuel type "Crude, NGL, and feedstocks" (73.3 g,CO_2/MJ) was assigned homogenously to all Member State activities in this sector. See also Table 2.9 for complete labels and abbreviations for the eleven main activity sectors considered.

Table 2.8. Specific carbon dioxide emission factors by main activity sectors for the 14 HRE4 MS´s. Average values established based on standard carbon dioxide emission factors and national compositions of fuel use per main activity sectors. Sources: (IEA, 2016b, IPCC, 2006).

MS	TP-WTE[a]	TP–MA	TP–AP	FSR	IS	CPC	N-FM	N-MM	MQ	FT	PPP
AT	77.5	86.4	93.3	73.3	68.8	70.8	60.6	82.5	59.7	62.4	88.9
BE	77.5	74.4	75.4	73.3	76.0	56.8	63.3	76.7	-	60.2	89.9
CZ	77.5	93.3	92.1	73.3	86.1	74.0	59.2	73.9	58.7	61.5	97.6
DE	77.5	90.5	76.1	73.3	79.5	64.1	59.2	78.4	70.2	60.9	72.4
ES	77.5	81.4	67.3	73.3	78.6	59.1	67.6	67.0	65.5	69.8	74.8
FI	77.5	94.2	98.3	73.3	83.5	75.4	90.2	78.6	75.0	78.0	99.2
FR	77.5	82.6	89.0	73.3	80.9	65.8	57.4	65.9	72.2	62.4	74.6
HU	77.5	80.4	76.3	73.3	81.6	58.0	56.1	67.0	64.8	59.3	57.0
IT	77.5	74.6	61.9	73.3	76.8	63.6	57.3	68.4	63.5	59.2	57.8
NL	77.5	74.5	80.4	73.3	82.0	65.3	56.1	59.1	59.3	57.2	56.4
PL	77.5	94.4	90.0	73.3	81.5	83.4	62.9	80.5	69.8	76.1	100.5
RO	77.5	84.6	69.9	73.3	73.7	64.3	-	75.9	73.7	66.0	58.9
SE	77.5	102.3	107.6	73.3	86.2	67.2	82.3	84.3	92.1	69.5	109.8
UK	77.5	83.3	79.1	73.3	82.2	58.9	59.4	70.9	-	58.0	61.0
HRE4	**77.5**	**85.5**	**82.6**	**73.3**[b]	**79.8**	**66.2**	**64.0**	**73.5**	**68.7**	**64.3**	**78.5**

[a] Separate analysis and data used for this main activity sector, see e.g. Table 2.6.

[b] Standard carbon dioxide emission factor of 73.3 g,CO_2/MJ for crude, NGL, and feedstock´s used for main activity sector FSR in all 14 MS´s where activity is present, according to (IEA, 2016b).

2.2.1.2 Basic concepts

The basic theory and concepts used in the reversed calculation sequence, where annual, facility level, main activity specified, carbon dioxide emission data, $m_{CO2,a}$ (kg/a), extracted from the emissions database, is divided by corresponding specific emission factors to assess the primary energy supplies ($E_{prim,a}$) to these activities, have previously been published e.g. in (Persson et al., 2014):

$$E_{prim,a} = \frac{m_{CO2,a}}{f_{CO2}} \qquad \left[\frac{J}{a}\right] \tag{17}$$

Hereby, an assessment of theoretically available annual excess heat volumes from these activities is conceivable with the introduction of some kind of main activity sector specific weights, by which to determine general levels of primary energy utilisation (i.e. default recovery efficiencies, η_{heat}, as presented in Table 2.9). By this procedure and approach, it is clear that excess heat here is understood – and thus defined – as all rejected heat in thermal power generation that is not absorbed as electricity, and rejected heat in industrial processes not added or maintained in industrial products conceived available for recovery.

Consequently, it should be noted that this HRE assessment, which is in line with previous HRE studies, estimates maximal available excess heat volumes in the studied Member States. For practical, thermo-dynamical, economical or other eventual reasons, lesser volumes than these may in many instances prove realistically available for recovery, which has been noticed among others by (Brueckner et al., 2014, Miró et al., 2016).

Table 2.9. Main activity sector labels and corresponding main activity sector default recovery efficiencies. Note that default values have been set to reflect the maximal excess heat recovery potential at current conditions.

Main activity sector category	Abbreviation	η_{heat} [-]
Thermal Power Generation - MA	TP-MA	0.5
Thermal Power Generation - AP	TP-AP	0.6
Thermal Power Generation - WTE	TP-WTE	0.6
Fuel supply and refineries	FSR	0.5
Iron and steel	IS	0.25
Chemical and petrochemical	CPC	0.25
Non-ferrous metals	N-FM	0.25
Non-metallic minerals	N-MM	0.25
Mining and quarrying	MQ	0.1
Food and tobacco	FT	0.1
Paper, pulp and printing	PPP	0.25

On facility level, the application of default recovery efficiencies, which builds entirely on the linkage to main activity sector categories, generates the sought assessed annual excess heat volume, $E_{heat,o}$ (index "o" to indicate "theoretical"), as the product:

$$E_{heat,0} = E_{prim,a} \cdot \eta_{heat} \quad \left[\frac{J}{a}\right] \tag{18}$$

2.2.1.3 Facility extract

The E-PRTR_v9 dataset includes verified emission data up to 2013 and submitted, yet to be verified, data for 2014. Since, as mentioned above, the database is cumulative and continuously grows in size, it counts today approximately 58 000 unique Facility ID´s (many of which no longer are in use). On a yearly basis, as shown in Table 2.10, around 33,000 facilities with emissions to either land, water, or air, are currently in operation in the EU28 (plus Switzerland, Iceland, Lichtenstein, Norway, and Serbia).

However, since many of these facilities have reported continuously over the years, the total amount of unique "Facility Report ID´s" now exceed 265,000, and – since most of these facilities report more than one emitted substance per year – the total amount of unique "Pollutant Release ID´s" surpassed 350,000 in the ninth version of 2016. Hence, in this massive presence of data, a strategy is needed in order to request – by SQL commands and algorithms – and obtain a desired extract of information.

Table 2.10. Total count of Facility ID´s reported in the E-PRTR_v9 dataset, for all reporting years available (2001 and 2004 refers to the EPER dataset), by main Annex I activity sector (Note: (i) sector names are partly shortened here, (ii) this sector classification is not identical to the main activity sector classification of this study). Source: (EEA, 2016a)

Main IA Sector	2001	2004	2007	2008	2009	2010	2011	2012	2013	2014
1. Energy sector	1066	1466	1879	1969	2016	2048	1995	2009	2011	1963
2. Metals industry	824	1045	4047	4289	4372	4437	4492	4476	4564	4588
3. Mineral industry	684	993	2168	2294	2228	2222	2165	2156	2221	2149
4. Chemical industry	1109	1190	2635	2770	2846	2865	2840	2869	2870	2898
5. Waste sector	1219	1524	6404	7421	7805	8575	8990	9366	9881	10158
6. Paper and wood	-	-	839	882	861	852	835	835	840	844
7. Livestock & aqua	-	-	5668	5940	6154	6109	6355	6519	6787	7133
8. Food & beverage	-	-	1785	1955	2017	2058	2110	2192	2235	2284
9. Other activities	4281	5408	1131	1227	1281	1350	1308	1313	1322	1329
Grand Total	**9183**	**11626**	**26556**	**28747**	**29580**	**30516**	**31090**	**31735**	**32731**	**33346**

As for the relevant extract here, information on facilities with carbon dioxide emissions to air, since these are interpreted as originating essentially in combustion and incineration processes (which in turn generate heat), were sought for by the proper SQL scripts. The first extraction step resulted in a raw, uncorrected excerpt for EU28 amounting to 15,603 facilities (in total, over the period 2007 to 2014). If only looking at the year 2014, 1877 facilities appear to have been in operation, representing a total carbon dioxide emission volume of 1730 Mt, which in turn corresponded to an estimated primary energy supply of 5889 TWh.

Now, by cross-referencing with the 2013 energy balances for EU28, as reported in the 2014 edition from IEA (IEA, 2014), strictly limiting the focus to the eleven main activity sectors at hand, it was established that a total primary energy supply of 6493 TWh was provided to these sectors in this year. Hence, a pure 2014 extract would constitute quite an underestimate of the actual excess heat potential (only 91% of the primary energy supply control-volume). For this reason, the next step involved the identification of facilities reported as operational in previous years, however not for 2014[16], which were added to the point where the sum of their total primary energy supplies came as close as possible to match the official statistical record of 2013.

The final selection in this validation process came to consist of 2222 EU28 facilities from the years 2012 (155), 2013 (190), and 2014 (1877), together representing 1865 Mt of carbon dioxide emissions and corresponding to a total 6378 TWh of primary energy supply (98% of the statistical control volume). Hereby, it was settled that the final HRE4 excess heat extract would refer primarily to facilities reporting for the year 2014, and secondly, to non-duplicate facilities relative to this year added from the years 2013 and 2012.

However, since throughout the HRE project series, WTE facilities have been studied as a separate phenomenon[17], special attention was given to this sector also here. In short, this involved an update of the HRE WTE list of previous HRE studies and consisted firstly in the removal of all facilities belonging to the main IA sector 5 (Waste and waste water management) from the intermediate extract. Instead and secondly, after having been prepared as a mixture of unique old (previous HRE WTE list, with data mainly up to year 2011) and non-duplicate new (present in the E-PRTR_v9 dataset) facilities, a list of 449 EU28 WTE facilities conceived as being in operation was added to the extract.

Hereby, the final HRE4 excess heat extract was completed by limiting the selection to the 14 MS´s under study, resulting in all to 2188 facilities, as presented in Table 2.11.

[16] There may be several likely reasons for why still operational plants are absent in one reporting year but present in the other. One aspect refers to occasional or seasonal changes in operational conditions, which also relates to instances of facility closures and the introduction of new installations. Another, more general aspect, refers to the used datasets or statistical records themselves, which seldom are perfect and completely void of erroneous entries and other possible flaws – an aspect to which the E-PRTR dataset certainly does not constitute an exception.

[17] During the HRE2 pre-study, leading up to Stratego (HRE3) in the autumn of 2013, Halmstad University developed a specific HRE project database on European WTE facilities. This work relied heavily on that of CEWEP, ISWA etc. (referenced elsewhere in the text), and aimed mainly at linking their published data on current WTE facilities with the geo-coded facility data in the E-PRTR dataset (version 4.2 as it were at the time). This work resulted in the "HRE WTE list", which in 2014 counted 410 dedicated and geo-referenced WTE facilities in EU28.

Table 2.11. HRE4 excess heat extract: count of excess heat facilities and corresponding volumes of annual carbon dioxide emissions for the 14 HRE4 MS´s as reported in E-PRTR_v9, data mainly for the years 2014, 2013, and 2012. Thermal power generation activities > 50 MW. Sources: (ISWA, 2012, CEWEP, 2014, EEA, 2016a)

	Thermal Power		Industrial activities		WTE		Total	
MS	**Count of facilities**	**CO2 [Mt/a]**	**Count of facilities**	**CO2 [Mt/a]**	**Count of facilities**	**CO2 [Mt/a]**	**Count of facilities**	**CO2 [Mt/a]**
AT	15	6	27	23	11	2	53	31
BE	24	16	47	29	16	2	87	47
CZ	45	50	26	16	3	1	74	67
DE	155	318	209	136	99	21	463	476
ES	84	64	109	50	11	1	204	115
FI	48	24	30	25	4	0	82	49
FR	48	30	136	71	129	12	313	113
HU	24	12	20	7	2	0	46	19
IT	97	96	119	53	55	5	271	154
NL	43	53	40	31	12	7	95	91
PL	79	165	56	45	1	0	136	210
RO	24	24	25	15	-	-	49	39
SE	39	11	54	33	30	5	123	50
UK	74	139	80	55	38	8	192	202
HRE4	**799**	**1006**	**978**	**590**	**411**	**64**	**2188**	**1661**

Industrial activities dominate the selection in terms of facility count, followed by thermal power generation and WTE facilities (411 in the 14 MS´s). A map illustrating the locations, the main activity sectors, and the assessed annual excess heat volumes associated with these facilities is presented in section 3.2.1; see Figure 3.1, where also a summary table (Table 3.2) can be found.

2.2.2 Heating and cooling infrastructures

In terms of spatial mapping, being the core activity of WP2, two separate and distinct areas of heating and cooling infrastructures have been the focus in the HRE4 project. Primarily, work has been dedicated to the subject of European district heating and cooling systems, as they represent key infrastructures for the realisation of efficient solutions for urban environments in the conceptual HRE philosophy. Secondly, and likewise central in the HRE toolkit, are the so called individual heating alternatives (e.g. local household boilers, small-scale heat pumps, building level solar energy etc.), applicable for city solutions as well, but perhaps more crucially perceived as key for rural and countryside applications in the HRE context.

While the first area concerning the mapping of European district heating and cooling systems is accounted for in the following, the second area, due to it being thematically associated with Task 2.5 (Quantifying the potential mix of rural heating solutions), has been moved from its plausible place here and instead inserted under section 2.5. However, it is important to realise that the distinction made between central (heat and cold distribution networks) and local (individual heating technologies) heating and cooling infrastructures here, refer not in principal to utilised heat and energy sources (e.g. fuels, biomass, solar radiation, excess heat etc.), but rather to by what means energy is distributed and supplied to its users. Since, for the latter, this distribution can be achieved by a multitude of different alternatives, while for the former only alternative exists, the focus here is essentially that of district heating and cooling systems.

2.2.2.1 District heating and cooling systems database

A key asset of the Swedish HRE partner Halmstad University is a comprehensive database on European cities with district heating and cooling systems currently in operation, the Halmstad University District Heating and Cooling Database (HUDHC). This data assembly, conceived initially in 2010 and continuously developed ever since, has been built mainly on the basis of national energy and heat sector statistics, publicly available utility reports, Internet sites, and personal communications. In total, it consists of 4843 systems and it has been used and referenced in several previous HRE studies, mainly so in (Persson, 2015a, Connolly et al., 2014b, Persson et al., 2014).

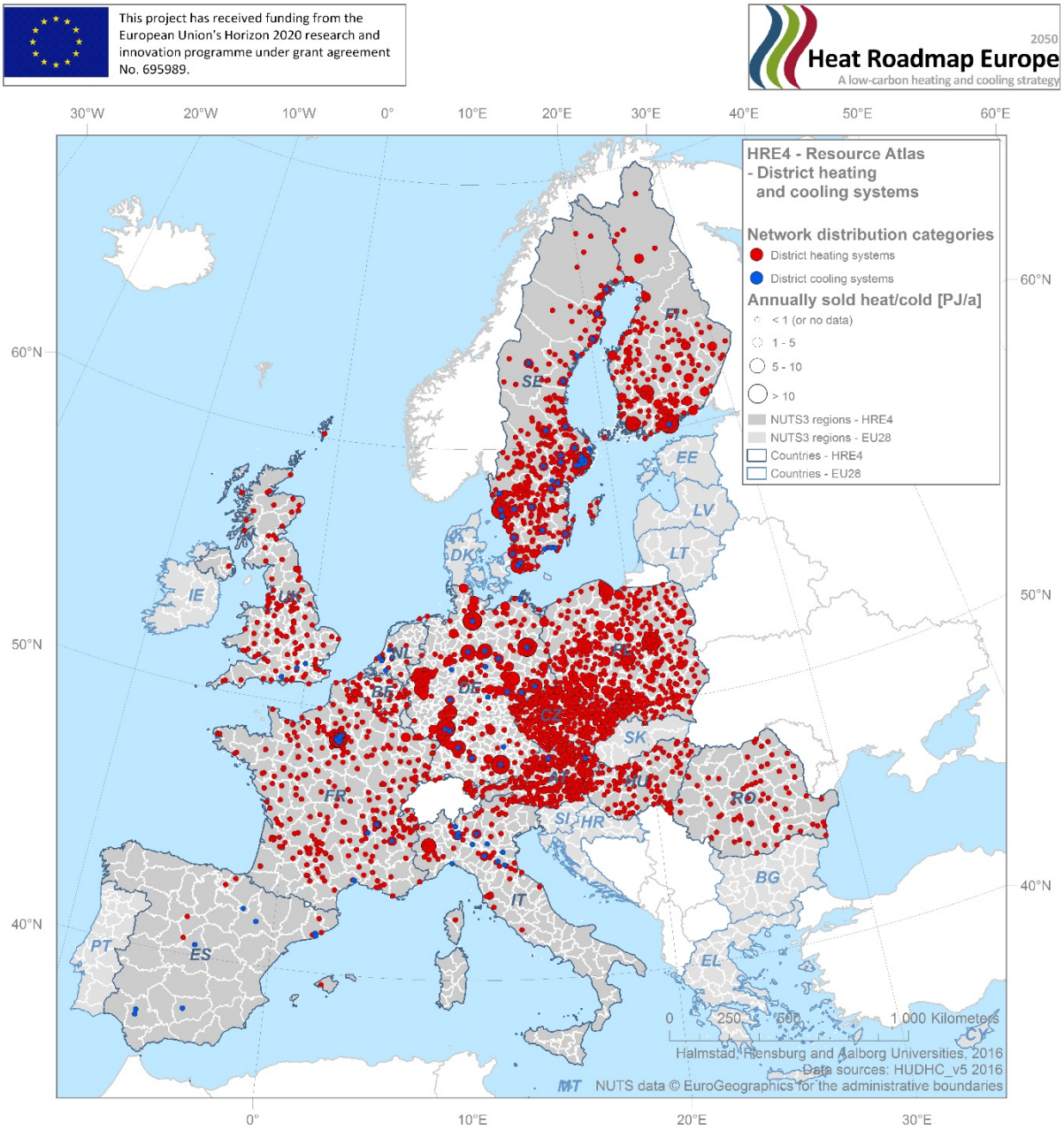

Figure 2.8. Map of 3207 district heating (3106) and cooling (101) systems in 2737 cities among the 14 HRE4 MS´s, by network distribution category, and annual volumes of heat and cold sold. Source: (HUDHC_v5, 2016)

After its most recent update (performed in the spring and summer of 2016), the fifth version of the dataset (HUDHC_v5, 2016) has been available and used in the current HRE4 project. It is noteworthy that quantitative data on e.g. system heat and cold annual sales, system pipe lengths etc., i.e. attribute values of the database, although frequently projected and published in the form of static maps, never before has been shared publicly. The background for this is twofold: partly because the database has been maintained strictly for internal research purposes at the university, partly since for a few Member States (AT, CZ, ES, SK, and PL) stored system specific information is subject to certain confidentiality constraints.

In the recognition of mutual benefit and interest, however, the research staff at Halmstad University decided early on in the start of the HRE4 project to make the HUDHC database accessible, including its system specific attribute values (except of course those referring to the four HRE4 MS´s AT, CZ, ES, and PL, for which quantitative data remains concealed).

Hereby, the project has had at its disposal information on a total count of 3207 district energy systems (3106 heating and 101 cooling) present in 2737 cities within the 14 HRE4 MS´s, as illustrated in Figure 2.8 and detailed in Table 2.12. For approximately 68% of these systems (2167), attribute values in terms of annually sold heat and cold are available (Q_{dh}) , while data on system pipe lengths (L) are less frequent and only present in 27% of the instances (878 systems).

Table 2.12. District heating systems in the 14 MS´s, by count, sum of annually sold heat (Q_{dh}), and sum of pipe lengths (L). (Info on district cooling systems in parenthesis where present). Source: (HUDHC_v5, 2016)

MS	No. of DH systems [n]	Sum of Qdh [PJ/a]	Sum of L [km]
AT	473 (2)	- (-)	- (-)
BE	38	2.4	3.1
CZ	391	56.1	-
DE	254 (20)	277.6 (-)	19032.5 (-)
ES	17 (8)	0.6 (0.7)	78.8 (-)
FI	178 (1)	115.7 (-)	14493.8 (-)
FR	456 (15)	78.6 (3.2)	3404.6 (151.9)
HU	109	-	-
IT	81 (12)	22.6 (0.4)	2259.4 (-)
NL	20 (5)	1.0 (-)	-
PL	429	239.7	-
RO	75	-	-
SE	386 (35)	169.5 (3.0)	220.0 (-)
UK	199 (3)	1.5 (-)	-
HRE4	**3106 (101)**	**965.2 (7.2)**	**39492.2 (151.9)**

As is also recognisable in Figure 2.8, the spatial feature characteristic by which the HUDHC database historically has geo-referenced any stored system, has been that of fixed point sources (i.e. by the geographical coordinates of the city centres). For reasons that will be made further clear in the following section, this database structure has been improved during the course of this project, namely by the conversion of such point sources to areal polygons features, by which the geographical extent and outstretch of these district heating and cooling cities have been made graspable and possible to map.

2.2.2.2 *Converting point source data to areal data*

For the HUDHC database information to become practically usable in geographical analyses of spatial relationships (such as distances, overlaps, connectivity etc.), it was essential to transform its historical form of spatial representation from feature point sources to feature polygon areas. Initial methodology discussions considered several different routes whereby to achieve such a transformation.

An early idea, however not pursued, which very likely still represents the approach that would have produced the most optimal output, was that of utilising information on energy demand densities, which in this project is established at hectare level (see e.g. section 3.1). Since it is well established from earlier studies that conventional district heat and cold distribution is economically feasible only above certain heat and cold demand density threshold levels (Persson and Werner, 2011), a spatial allocation of the database systems to all such sufficiently high demand density areas would presumably have produced the closest possible adaption to their actual geographical spread.

Another approach that was proposed, which aspired to the same logic but suggested the use of another information source (especially since at this early stage of the project no progress had yet been made with respect to demand density data), recognised the publicly available Urban Morphological Zones (UMZ) dataset as a suitable proxy for high demand density areas (EEA, 2016b). Since UMZ´s consist chiefly of the four defined urban category land use classes of the Corine Land Cover dataset (EEA, 2017a)[18], these certainly reflect coherent high demand density conditions in Europe. However, although the UMZ dataset is accessible by high spatial resolution formats[19], they are established on satellite imagery of the built-up environment and not on dedicated energy demand information. Hence, their status as proxies for heat and cold demand density clusters in this context.

Table 2.13. District heating systems in the 14 MS´s as converted from feature point sources to feature polygon areas (coherent DH areas (UMZ_DH)), by count and by number, population, sum of annually sold heat (Q_{dh}), and sum of pipe lengths (L), in these coherent DH areas.

MS	No. of DH systems [n]	Coherent DH areas (UMZ_DH) [n]	Population (UMZ_DH) [Mn]	Sum of Qdh [PJ/a]	Sum of L [km]
AT	473	327	4.7	-	-
BE	46	23	7.2	4.5	73.7
CZ	394	370	6.7	56.6	-
DE	257	195	32.1	278.2	19032.5
ES	17	14	10.2	0.6	78.8
FI	179	149	4.2	115.9	14493.8
FR	448	230	28.5	76.5	3334.0
HU	107	93	5.0	-	-
IT	81	62	11.1	22.6	2259.4
NL	20	16	5.2	1.0	-
PL	424	379	20.4	238.6	-
RO	74	70	7.4	-	-
SE	385	339	6.4	169.3	220.0
UK	199	93	28.8	1.5	-
HRE4	**3104**	**2360**	**177.9**	**965.2**	**39492.2**

[18] These are continuous urban fabric, discontinuous urban fabric, industrial or commercial units, and green urban areas.
[19] The UMZ data is available at EEA either by 250 x 250 meter grid cells or by 100 x 100 meter grid cells (i.e. hectares), the latter being the one used here.

As presented in Table 2.13, the conversion, which included district heating systems only, resulted in the identification of 2360 UMZ polygon areas, many of which host more than one system. Since the conversion itself was achieved by performing a spatial join between the HUDHC and the UMZ datasets, utilising a “closest” algorithm – and since, further, UMZ polygons does not conform to national boundaries – some discrepancies regarding count and country code association, compared to the original dataset in Table 2.12, are present in the output. It should further be noticed that for a selection of larger UMZ areas (mainly those hosting more than one system), total polygon populations were re-assessed by use of additional data sources (ES, 2015).

This project has received funding from the European Union's Horizon 2020 research and innovation programme under grant agreement No. 695989.

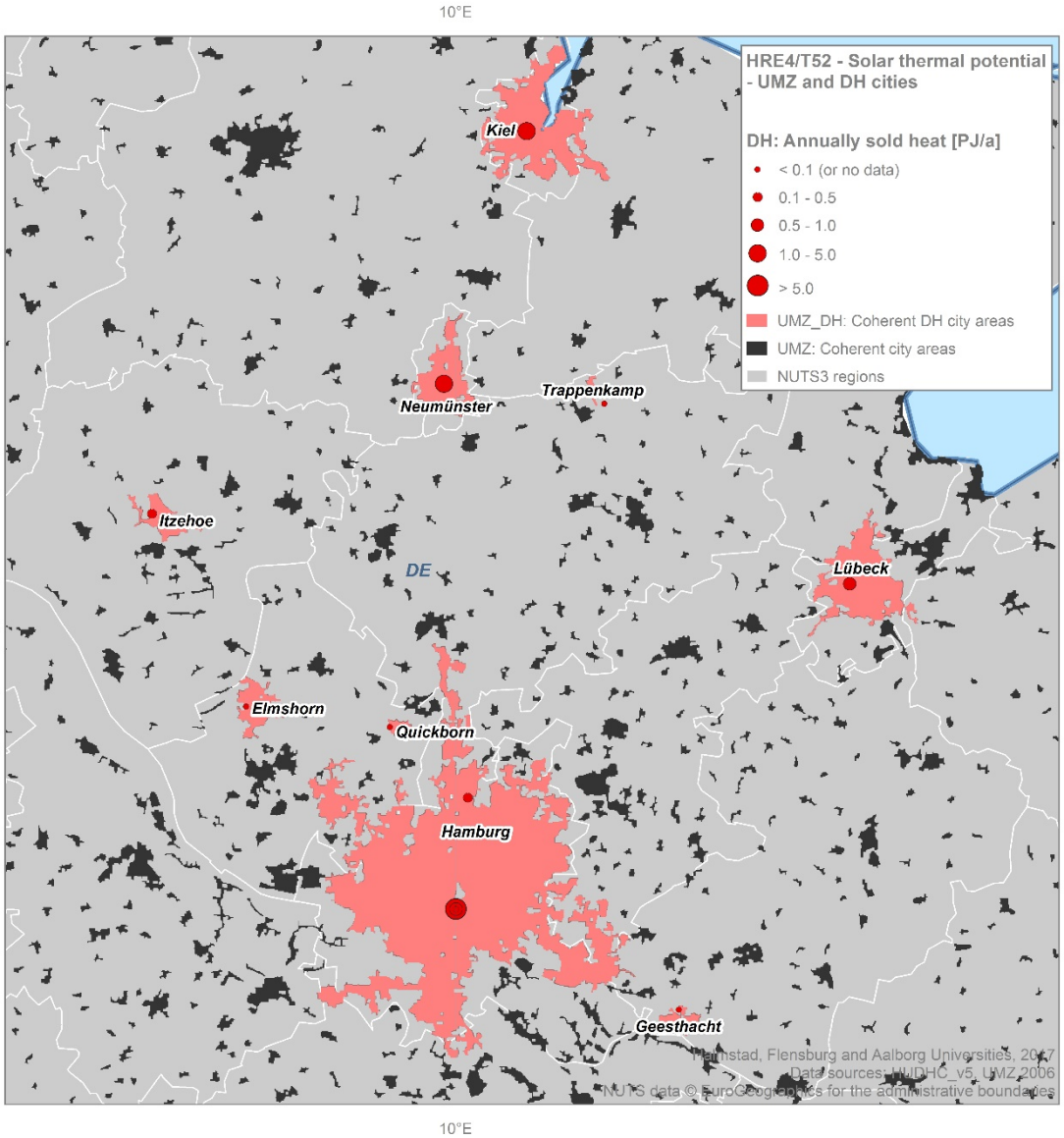

Figure 2.9. Illustration of the spatial conversion of HUDHC database feature point source data of city centres to feature polygon areas for corresponding city areas (UMZ_DH areas). Urban Morphological zones (UMZ) in black, UMZ_DH polygons (in light red), HUDHC point source city data (in dark red). Detail of the Hamburg and Kiel region in Germany.

The conversion process is exemplified by a close-up of the Hamburg and Kiel region in Germany, as presented in the map of Figure 2.9. By the performed spatial association of known district heating cities as feature point sources to their corresponding UMZ polygon areas, some 98% of the total count of recorded polygon areas in the UMZ dataset (130,932), where accordingly no district heating systems are currently in operation, could be deselected. The remaining ones represent our current knowledge of operational district heating systems in the 14 MS´s, not only by attribute values, but also by their spatial extension. The implications of this have proven very beneficial for the project in several aspects, not least with reference to the assessment of land available for large-scale solar thermal heat installations.

2.2.3 Large-scale solar thermal heat: Land availability

In this section, the collaboration between WP2 and the IEA-SHC Task 52 project (IEA-SHC-T52, 2017, IEA-SHC, 2017), represented by HRE4 partner PlanEnergi (DK), is presented in terms of input data, analysis, and intermediate outputs. As part of the HRE4 Resource atlases, the objective of the collaboration was to develop a conceptual and spatial methodological approach whereby to assess the theoretical and economical potential for large-scale solar thermal installations in current district heating towns and cities in Europe.

The initial inspiration, that is to say, the systemic and technical set-up that provided a role model for the assessment, is that of the typical contemporary Danish application of large-scale solar thermal heat in district heating systems, i.e. smaller towns (population average:~4000, max: ~40,000 (PlanEnergi, 2016)) with suitable land available close to the town edges (Mauthner and Herkel, 2017). According to data reported by the EU Horizon 2020 project Solar District Heating (SDH 2016) (SDHp2m, 2016, SDH, 2017), 252 large-scale solar thermal installations were in operation in all of Europe during 2016, of which most were connected to district heating systems in this Danish fashion, as can be seen in Figure 2.10.

Denmark has deservedly earned a remarkable front position in the European context in terms of applying this technological concept: large-scale solar thermal installations feeding renewable heat in the form of heated water to district heating systems equipped with either or both diurnal and seasonal thermal energy storages. Here, this has been proven an efficient system solution for the utilisation of renewable energy from the sun; although in Denmark, the average intensity of solar irradiation on a horizontal surface is only about half of that characteristic for the southern part of the European continent.

Hereby, large-scale solar thermal installations coupled with district heating systems may be considered a proven technology that are applicable in all regions of Europe. For the assessment in this study, therefore, the central idea has been to identify suitable cities with district heating systems currently in operation, to which large-scale solar thermal installations could be realistic alternatives. However, since different cities and urban areas are subject to very different opportunities in terms of locally and regionally

available heat resources, the identification of such a list of candidate solar district heating cities were subdued the following core criteria:

- The city does not have access to excess heat from excess heat activities (EHA)
- The city does not have access to Waste-to-Energy (WTE) incineration facilities
- Suitable land for solar collector installations are available in the city vicinity

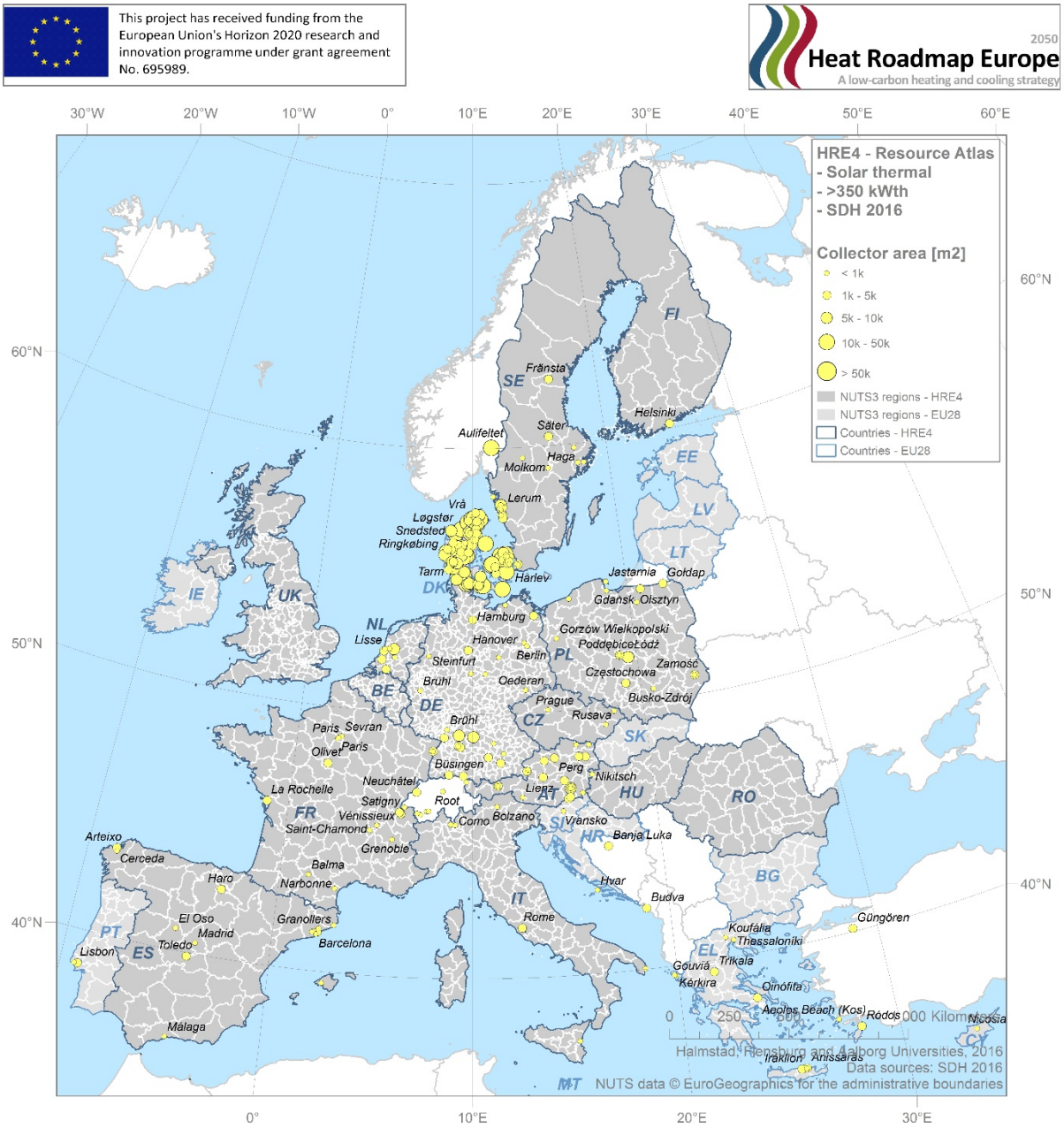

Figure 2.10. SDHp2m data for 2016 in EU: 252 large-scale solar thermal installations in Europe 2016. Source: (SDH-dataset, 2016).

It may be rightly argued that the two former of these criteria imposes unjust or even illogical limitations on the selection of candidate cities, since there is no formal rule that prohibit a combination of excess and solar heat utilisation in the same location. The rationale for the chosen criteria, however, resting on the two main arguments that,

firstly, excess heat recovery should have higher priority than that of solar heat, and, secondly, that the explicit focus is smaller cities, makes good sense in fostering a first, comprehensive assessment of wherefrom an expansion of solar heat in Europe according to Danish practise could begin.

The work presented here, further, consists of two out of three main steps: Firstly, the identification and selection of a candidate list of district heating cities for which large-scale solar thermal installations would constitute viable heat supply alternatives given the aforementioned core criteria. Secondly, the evaluation of availability of suitable land in vicinity of these candidate district heating city areas where solar collectors could be installed.

A third step, the final estimation of economic feasibility and technical viability of a full or partial realisation of the (spatial) expansion potential outlined here, will have to be presented and published under other circumstances in another context than this. The reason being that the work on this final step of the assessment is still in progress, under the auspices and main responsibility of the IEA-SHC T52 project (expected finalisation by the end of 2017).

2.2.3.1 Selection of candidate cities

The approach to identify and select a list of candidate DH cities utilised three main data sets: the Halmstad University District Heating and Cooling Database (HUDHC_v5), the European Pollutant Release and Transfer Register (E-PRTR_v9), and the Urban Morphological Zones (UMZ) dataset, all as referenced above. The selection sequence itself hence started by asking the first data source whether there is district heating in the city today, since a precondition to qualify to the candidate list was that a district heating system is in place and operating in the city at current.

Next, the second data source was consulted to answer whether there is excess heat from large-scale thermal power generation plants, from energy-intensive industries, or from WTE facilities[20] in the city or in the city vicinity (within 20 km). All cities with, or with opportunities for, such large-scale excess heat recoveries were to be removed from the list since they, according to the first and second criteria, were considered compelled to utilise these heat resources prior to that of solar thermal heat.

By projecting all used datasets in a GIS and then performing spatial cross-referencing between these map layers by their superimposing of each other, a candidate list of suitable cities for large-scale solar thermal installations would principally be obtainable. An initial and important step to make this feasible was that which is described in section 2.2.2.2 above, namely the spatial conversion of HUDHC database feature point source data to feature polygon areas for corresponding district heating city areas (UMZ_DH areas), with which the spatial extent of these cities could be apprehended and geographically outlined.

[20] As described in section 2.2.1 above, the additional data available in the HRE4 WTE List, counting 411 dedicated and operational WTE facilities in 14 MS´s (449 for the EU28), was used here.

Now, with information on the geographical extent of the district heating cities under study, the examination of how many of these coherent district heating city areas that have direct (or vicinity) access to excess heat from the three main sources at hand could be carried out. As depicted in Figure 2.11, keeping to the Hamburg and Kiel region example in Germany, a series of spatial join operations in the used GIS, distinguished by the three spatial contexts: inside, within 20 km, and others (i.e. candidate cities), identified 1676 coherent district heating areas in the 14 MS´s that qualified to the solar candidate list. In summary, as presented in Table 2.14, this selection process corresponded to 1831 unique district heating systems in these city areas.

This project has received funding from the European Union's Horizon 2020 research and innovation programme under grant agreement No. 695989.

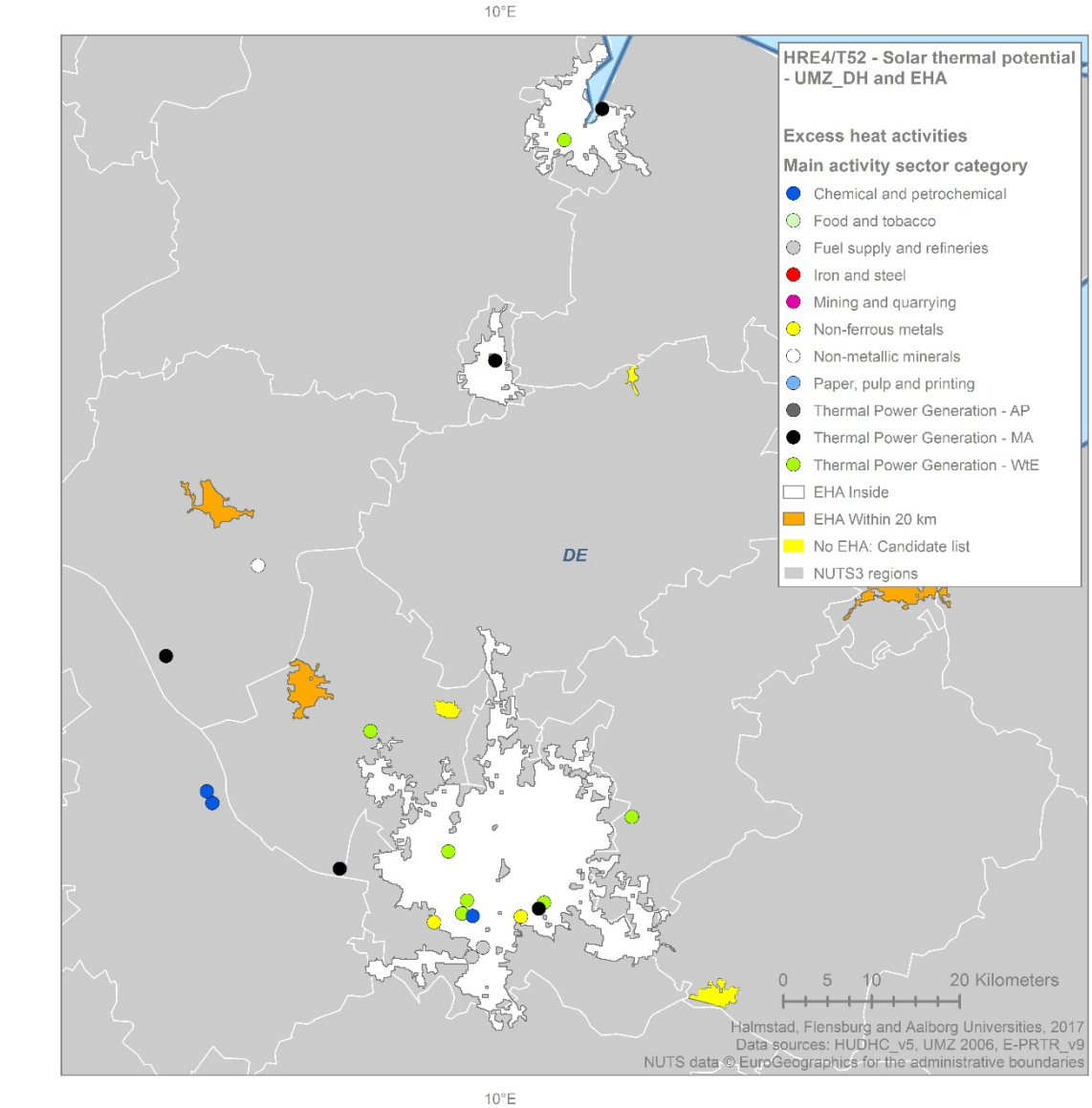

Figure 2.11. Coherent DH city areas (UMZ_DH) by vicinity to excess heat activities (EHA): within polygon borders (white), within 20 km of polygon borders (gold), or no EHA available (yellow), corresponding to candidate cities for large-scale solar thermal installations. Detail of the Hamburg and Kiel region in Germany.

Table 2.14. Summary of selection process to identify a list of candidate cities for the assessment of large-scale solar thermal heat in the 14 MS´s. Number of DH systems and coherent DH urban areas (UMZ_DH) without excess heat activities inside or within 20 km of their polygon borders. Additional data on annual heat sales (Qdh) and total population

Selection	No. of DH systems [n]	Coherent DH areas (UMZ_DH) [n]	With Qdh data [n]	Sum of Qdh [EJ/a]	Population [Mn]
All	3104	2360	1695	0.97	178
Excess heat: Inside	895	383	304	0.71	130
Excess heat: within 20 km	378	301	208	0.07	20
Candidate list	**1831**	**1676**	**1183**	**0.18**	**28**

As can be further seen in Table 2.14, 383 of all 2360 coherent district heating areas under study (16%), hosting in total 895 unique district heating systems, have immediate access to excess heat activities inside their polygon borders (as for example the city of Hamburg in Figure 2.11). Another 301 city areas (13%), corresponding to 378 unique systems, have access to excess heat within a 20 km distance. In terms of attribute values, approximately 65% (1183 out of 1831) of the identified candidate list cities were found having data on annually sold heat (Q_{dh}), which amounted to 0.18 EJ in total. The candidate list summary is further specified and detailed on Member State level in Table 2.15.

Table 2.15. Specification of selected candidate list cities for the assessment of large-scale solar thermal heat in the 14 MS´s: Number of DH systems and coherent DH urban areas (UMZ_DH) without excess heat activities inside or within 20 km of their polygon borders. Additional data on annual heat sales (Qdh) and total population

MS	No. of DH systems [n]	Coherent DH areas (UMZ_DH) [n]	With Qdh Data [n]	Sum of Qdh [PJ/a]	Population [Mn]
AT	361	285	-	-	1.68
BE	9	8	4	0.38	0.06
CZ	323	314	314	18.39	2.82
DE	87	83	78	19.35	2.69
ES	4	4	4	0.13	0.04
FI	109	104	104	18.20	0.99
FR	145	124	79	6.04	3.14
HU	70	66	5	0.04	1.83
IT	40	32	32	1.55	0.54
NL	5	4	3	0.62	0.19
PL	308	306	306	82.12	7.27
RO	46	45	5	0.05	2.16
SE	271	255	249	35.93	1.47
UK	53	46	-	-	3.08
Candidate list	**1831**	**1676**	**1183**	**182.81**	**27.96**

With respect to excess heat activities as such, 845 of the 2188 large-scale facilities included in the HRE4 extract, as described in section 2.2.1 and specified in Table 2.11, hence constituting ~39% of the total count, were found within coherent district heating city areas. Another 562 were found within 20 km of these city areas (~26%), meaning that the remaining part (some 35%) of the considered excess heat facilities were completely out of reach under the given circumstances.

This would indicate that, in the context of the studied 14 MS´s, approximately 64% ((845+562)/2188) of all large-scale excess heat activities in these countries are located in, or in close vicinity to, cities with district heating systems currently in operation. For this reason, it is fair to say that excess heat recovery represents real opportunities for structural energy efficiency improvements in many European district heating cities.

2.2.3.2 Identifying required and available land for solar collectors

The identification of required[21] and available land for the installation of solar collectors in the outskirts and surroundings of the 1676 coherent district heating city areas on the HRE4 solar candidate list, was based partly on a set of theoretical concepts and relationships, partly on spatial analysis in the used GIS. For the calculation of land surface area required to generate an annual solar heat volume, Q_{sol}, as a given share of the annual district heat delivery, Q_{dh} (kWh/a), a solar fraction (S_f), here set at 20% for the current estimate and at 50% for a future 2050 projection, was used in a first step:

$$Q_{sol} = S_f \cdot Q_{dh} \qquad \left[\frac{kWh}{a}\right] \tag{19}$$

Since this quantity, the annual solar heat volume, Q_{sol}, also is the product of a given solar collector area, A_{col} (m^2), solar radiation on a horizontal surface, G (kWh/m^2a), and a conversion factor referring to solar collector yield at an optimally oriented surface relative to the solar radiation at a horizontal surface, $C_{hor\text{-}to\text{-}col}$ (set here to a conservative average value of 0.4, according to (IEA-SHC, 2011)), A_{col} may be solved according to:

$$Q_{sol} = A_{col} \cdot C_{hor-to-col} \cdot G \Rightarrow A_{col} = \frac{Q_{sol}}{(C_{hor-to-col} \cdot G)} \qquad \left[m^2\right] \tag{20}$$

Now, depending on the set value of the solar fraction to determine the annual solar heat volume in Equation 19, the corresponding required collector area is obtainable for each candidate city, given that data on specific solar irradiation intensities, G, are available for each location. For this purpose, the publicly available dataset on solar radiation on horizontal surfaces provided by the Joint Research Centre (JRC), available at (JRC, 2017b), was used and spatially associated to each candidate list city.

Hereby, to determine the land area required, $A_{land,req}$, in extension to the solar collector area required, an additional factor, $f_{land\text{-}to\text{-}col}$ (-), which according to Danish practice and experience averages at the value 3.5, as concluded in (Nielsen and Battisti, 2012), may consequently be added to arrive at a final expression for required land area:

$$A_{land,req} = A_{col} \cdot f_{land-to-col} = \left(\frac{S_f \cdot Q_{dh}}{(C_{hor-to-col} \cdot G)}\right) \cdot f_{land-to-col} \qquad \left[m^2\right] \tag{21}$$

From this, required land area for 20% and 50% solar thermal heat shares of current annual district heat sales could be calculated and established – however only for the

[21] For a 20% solar heat share of current annual district heat deliveries that is. Based on experience (especially the Danish one), this level of solar heat contribution is practically viable without the introduction of seasonal thermal energy storage, only requiring diurnal storage capacity in general. For a conceived 2050 scenario, a 50% solar heat share was included in the performed assessments, however in the understanding that such high shares would presuppose access to seasonal storage options.

1183 coherent district heating city areas for which Q_{dh} data was available, as specified in Table 2.14 and Table 2.15. Despite this unfortunate loss of 493 city areas from the initial candidate list (29%), for which the subsequent land area calculations could not be performed (but which nonetheless constitute suitable cities for future solar projects), the remaining qualifiers were considered a population large enough for a continued pursuit of the study objectives.

Consequently, the second step of evaluating the availability of suitable land in direct vicinity of these remaining candidate city polygon areas where solar collector fields could be built, focused on 1183 coherent district heating city areas, for which a sequence of GIS modelling, additional data, and assumptions were applied. One initial and important assumption being that the assessment solely focused on land installations, hence disregarding possibilities for roof-mounted systems and other plausible in-city installations (such as those along motorways, in park areas etc.).

Central for the subsequent spatial analyses thus performed, was the core objective to identify suitable land for large-scale solar thermal installations in direct vicinity to the city area borders, as represented by the edges of the corresponding polygon areas. Now, it might be in place here to mention briefly that these analyses, such as is commonly the case in pioneering research activities, involved several iterations and testing of many different possible approaches, of which most eventually were discarded and abandoned[22].

Common for them all, however, was the idea to use – once again – the Corine Land Cover dataset of the European Environment Agency (EEA) as a coherent information source on land character and use (EEA, 2017a). As a special assignment, PlanEnergi analysed the land use classes present in the Corine dataset (44 classes in all) and settled for a selection of seven categories thought to resemble land types suitable for solar collector installations, i.e. fairly flat, not build-up land covered neither by forests nor by waterways, as presented in Table 2.16.

Table 2.16. Selected Corinne Land use classes as representative of suitable land categories for large-scale solar collector installations, by code and label levels, and general comments on suitability. Source: (EEA, 2017a)

Code Level 3	Label Level 1	Label Level 2	Label Level 3	Comment
211 (12)	Agricultural areas	Arable land	Non-irrigated arable land	Very suitable
212 (13)	Agricultural areas	Arable land	Permanently irrigated land	Very suitable
231 (18)	Agricultural areas	Pastures	Pastures	Very suitable
243 (21)	Agricultural areas	Heterogeneous agricultural areas	Land principally occupied by agriculture	Suitable
321 (26)	Forest and semi natural areas	Scrub and/or herbaceous vegetation	Natural grasslands	Very suitable
322 (27)	Forest and semi natural areas	Scrub and/or herbaceous vegetation	Moors and heathland	Suitable
333 (32)	Forest and semi natural areas	Open spaces with little or no vegetation	Sparsely vegetated areas	Suitable

[22] What is referred to here is mainly a first set of mapping techniques, involving for example proximity tools such as Thiessen polygons and multiple ring buffers, by which delineation of vicinity land areas were sought, but never sufficiently found. Among these was also an initial idea to use “dynamic” distances (as functions of city district heat deliveries), to determine radii (feasible transmission distances) of circular buffer zones emanating from polygon point source centres.

For the establishment of buffer corridor areas, eventually, i.e. the delineation of vicinity areas in which suitable Corine land use classes were to be sought, a straight-on approach using pre-defined distances emanating from the polygon edges was the preferred choice. These pre-defined distances were set to 200 metres and 1000 metres respectively, for each of which spatial analysis (extract by attribute, extract by mask, and zonal statistics) was carried out by superimposing each buffer layer over each of the seven selected Corine land use classes, hereby generating the outputs of the assessment, as illustrated in the map of Figure 2.12.

This project has received funding from the European Union's Horizon 2020 research and innovation programme under grant agreement No. 695989.

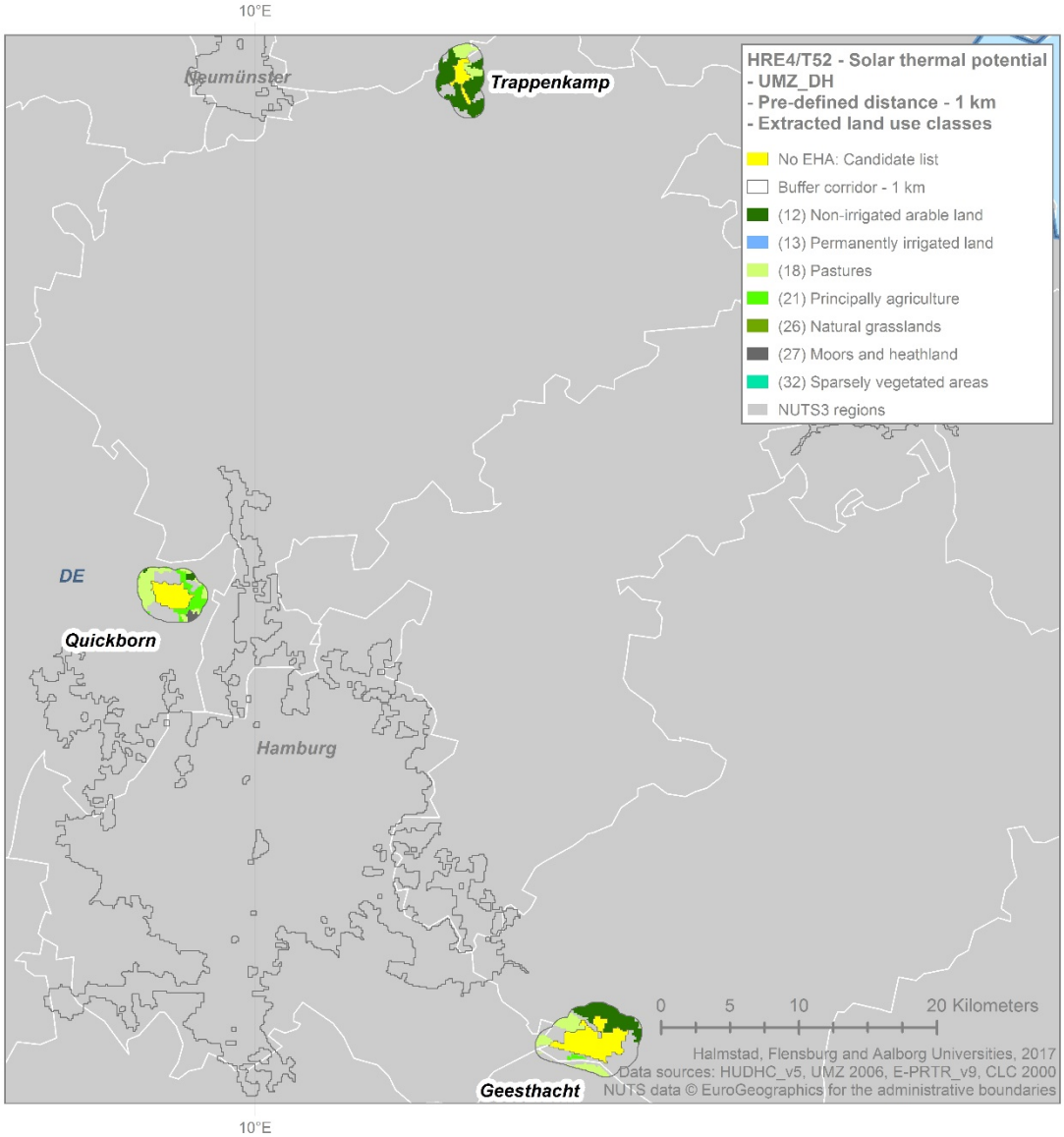

Figure 2.12. Extracted Corine land use classes as representing suitable land areas for large-scale solar thermal installations within 1000-metre buffers of solar candidate list cities. Enhanced detail for three solar candidate list district heating city areas in the Hamburg and Kiel region in Germany.

The outputs of the assessment accordingly contains information on buffer areas and required land areas for solar thermal shares of 20% (diurnal storage at current conditions) and 50% (seasonal thermal storage as representative of a future 2050 scenario) out of annual district heat deliveries for each studied district heating city on the candidate list, as presented in Table 2.17. For each of these city areas, further (as detailed and summarised per MS in Table 2.18), the area sum and the area specific of all and each of the seven considered Corine land use classes, i.e. the suitable land in their direct vicinity, is established and spatially determined for both the 200 and 1000-metre buffer scenarios.

Table 2.17. HRE4/IEA-SHC T52 solar thermal assessment: Output information on the selected coherent district heating city areas in the 14 MS´s, required land areas for 20% and 50% solar heat shares out of current annual district heat sales, and buffer land areas at 200 metre and 1000 metre corridor distances

	Candidate list cities	Required land area		Buffer land area	
MS	**with Qdh Data [n]**	**20% [km2]**	**50% [km2]**	**200 metre [km2]**	**1000 metre [km2]**
BE	4	0.2	0.5	11.6	57.3
CZ	314	8.7	21.8	933.7	4596.0
DE	78	9.4	23.5	503.3	2053.0
ES	4	0.0	0.1	6.9	40.6
FI	104	10.2	25.4	499.0	2166.2
FR	79	2.4	6.0	540.5	2120.6
HU	5	0.0	0.0	20.3	90.5
IT	32	0.6	1.4	97.8	450.6
NL	3	0.3	0.8	11.6	55.0
PL	306	39.5	98.8	1749.1	7331.0
RO	5	0.0	0.0	17.1	81.4
SE	249	18.9	47.3	760.3	3637.8
HRE4	**1183**	**90.2**	**225.6**	**5151.3**	**22680.0**

Additionally, as also presented in Table 2.18, a complementary concept, representing the minimum value of required vs. (sum of) suitable land area for each candidate city, is established to pinpoint the share of required land areas that are possible to "require" out of available suitable land areas actually at hand. This concept, hence labelled "Potential land area", signifies the amount of land surface area, present in the form of available suitable Corine land use classes, needed to exploit within the specified vicinities to realise the solar heat shares conceived in the assessment.

Table 2.18. HRE4/IEA-SHC T52 solar thermal assessment: Summary on suitable land use class areas and potential land areas, by MS´s and by 200 metre and 1000 metre buffer land areas respectively

	200 metre			*1000 metre*		
MS	**Suitable land area [km2]**	**Potential land area: 20% [km2]**	**Potential land area: 50% [km2]**	**Suitable land area [km2]**	**Potential land area: 20% [km2]**	**Potential land area: 50% [km2]**
BE	7.9	0.2	0.5	40.2	0.2	0.5
CZ	721.7	8.7	21.6	3261.9	8.7	21.7
DE	323.6	9.4	23.5	1286.7	9.4	23.5
ES	5.3	0.0	0.1	30.2	0.0	0.1
FI	177.5	8.8	18.5	714.9	9.8	21.9
FR	293.1	2.4	6.0	1135.6	2.4	6.0
HU	10.1	0.0	0.0	54.0	0.0	0.0
IT	50.6	0.6	1.4	207.4	0.6	1.4
NL	9.3	0.3	0.8	47.6	0.3	0.8
PL	1252.5	38.8	97.0	5031.0	39.3	97.5
RO	10.8	0.0	0.0	64.4	0.0	0.0
SE	262.2	17.9	43.5	1218.5	18.2	45.2
HRE4	**3124.4**	**87.2**	**213.0**	**13092.3**	**89.0**	**218.6**

2.2.4 Geothermal heat: Visualisation of parameters

Generally, it is difficult to quantify possible heat magnitudes and to locate spatially the volumetric and geographical potentials for geothermal heat as a source for district heating. The main reasons for this is because available information on geological formations often is incomplete and because drilling for geothermal heat still has high failure rates. Mapping of geothermal resources can therefore only be indicative and based on the visualisation of several geological parameters such as temperature gradient, heat flow, and the presence of favourable deep rock formations such as aquifers, as illustrated in Figure 2.13.

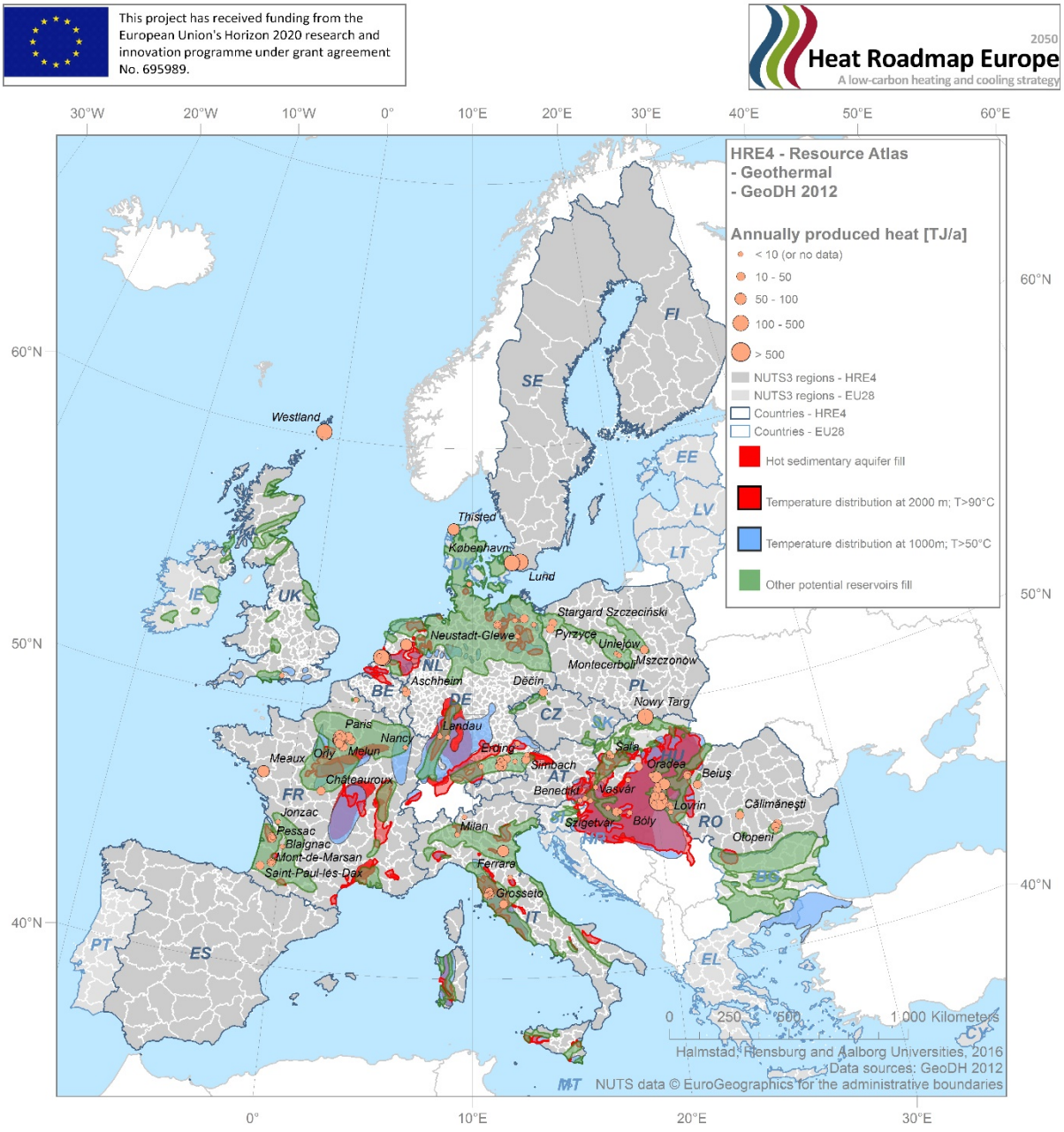

Figure 2.13. Projection of original GeoDH data on geothermal district heating systems in operation (by annually produced heat), and several geological parameter layers; e.g. hot sedimentary aquifers and other possible reservoirs.

The GeoDH project has prepared maps of Europe with these conditions, which allow for visual recognition and qualitative assessments of the presence of geothermal heat at any given location in Europe. Since these GeoDH maps have been kindly shared with the HRE4 project, where they subsequently has been added to the online mapping tool (these are available as operational layers in Peta4.2), they provide enhanced possibilities for the identification of viable geothermal heat projects since they appear here together with a multitude of other information layers.

An indicative example, illustrative both of opportunities for superposing different operational layers at the Peta4 web map application, and of the general difficulty to assess geothermal potentials in quantitative terms, is presented in Figure 2.14. As can be seen, several geothermal assets are within reach for many of the depicted prospective DH supply areas (indicating coherent areas suitable for district heating due to sufficiently high and concentrated heat demand densities). Since this rich diversity often is the local case, site-specific inquiries must be considered the standard approach to distinguish between prevailing opportunities and thereby to assess local geothermal potentials.

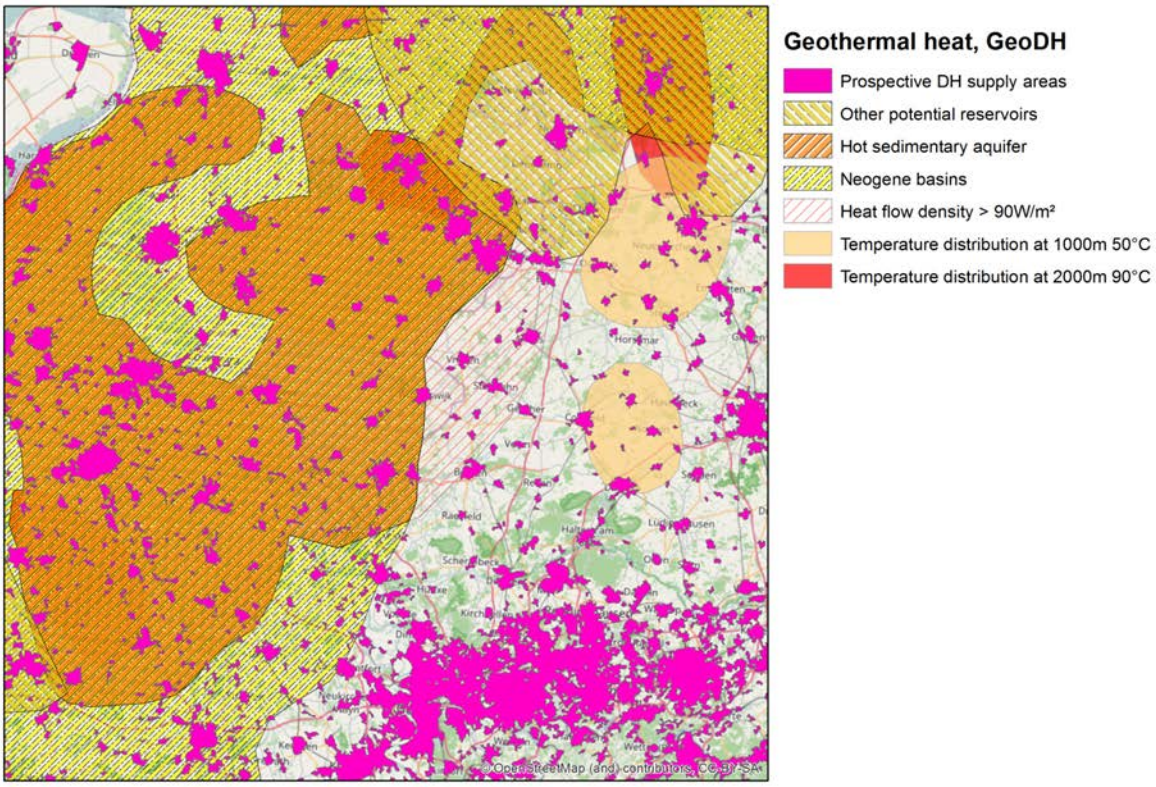

Figure 2.14. Principal extract from Peta4 illustrating the superposing of prospective DH supply areas (areas suitable for district heating (precursor concept of coherent DH areas (UMZ_DH)) with several geothermal resource layers as prepared by the GeoDH project.

2.2.5 Biomass: Regional availabilities

Data on regional biomass resources from main biomass-generating activities such as forestry, agriculture, and households, were sourced in the HRE4 project from the BioBoost project (2012 to 2015), as mentioned in the introduction (Pudelko et al., 2013). The BioBoost project was the first ever to map the technically and economically feasible and accessible residual biomass resources among EU member states (EU27 plus Switzerland) on the NUTS3 level, as illustrated for the resource category straw in Figure 2.15. (Three complementary maps referring to categories forest, biodegradable municipal waste (BMW), and pruning are presented in subsection 6.3).

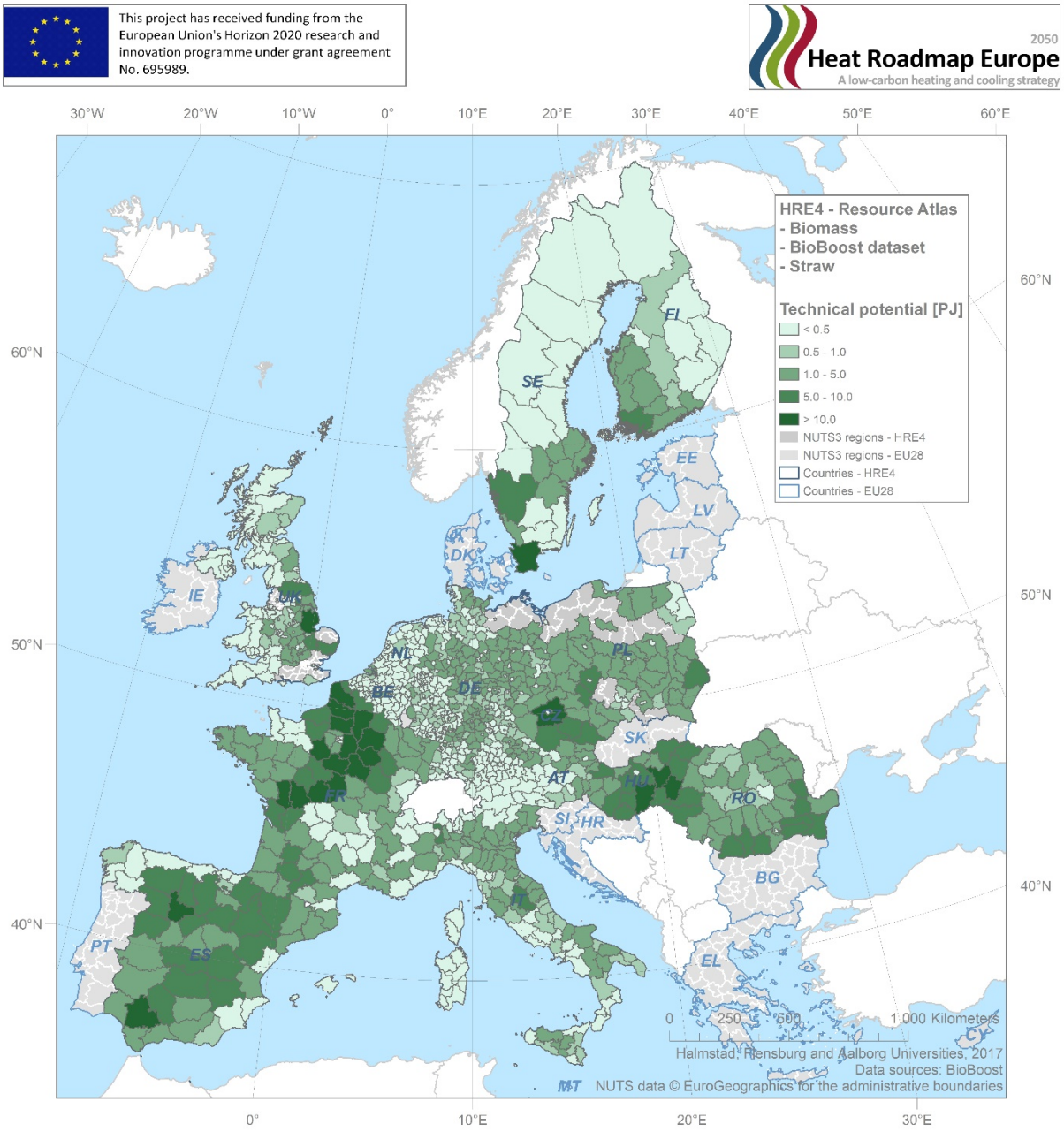

Figure 2.15. BioBoost NUTS3 region data on annual technical potential for straw among the 14 MS´s of the EU. Source: (Pudelko et al., 2013).

In the associated BioBoost work package “Feedstock, potential, supply and logistics”, eleven biomass resource categories in all were originally assessed of which four subsequently were included in the HRE4 biomass resource maps. Categories straw and orchard’s pruning from agriculture where selected together with forestry residues from operations such as thinning and cutting, along with biodegradable municipal waste (BMW) from urban and industrial waste; these four categories representing the major volume of the BioBoost data, as presented in Figure 2.16.

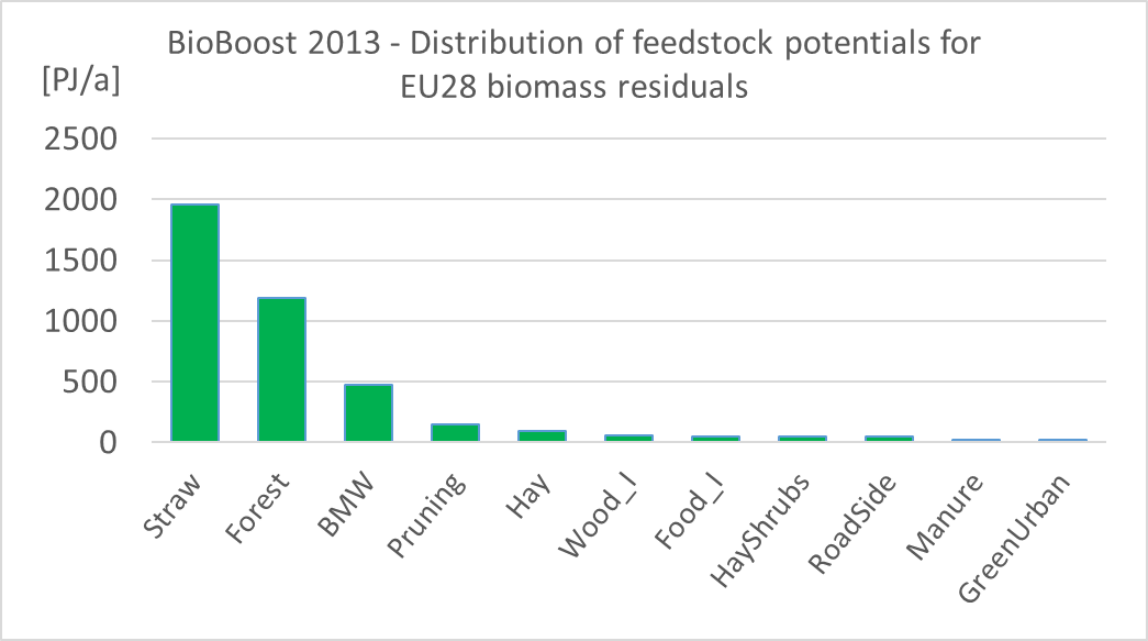

Figure 2.16. Summary of the BioBoost dataset for eleven studied residual biomass categories, by annual technical potential for the EU28. Source: (Pudelko et al., 2013).

Excluded from this HRE4 study, consequently, were residual biomass categories such as wastes from the food and wood industry, hay as well as manure. Also roadside vegetation and biomass derived from natural conservation activities such as urban maintenance of green areas, hay and shrubs were not included. The main reason for these exclusions was the very small amounts of biomass in total that these categories comprise, furthermore at high-perceived sensitivity to costs and availability.

In terms of dissemination, apart from the four continental maps presented in this report, the four selected BioBoost data categories (i.e. straw, forestry, biodegradable municipal waste, and pruning), have been transferred directly to the Peta4 online mapping platform via an attribute table from the BioBoost project partner IUNG (Instytut Uprawy Nawozenia I Gleboznawstwa, Panstwowy Instytut Badawczy). In the ArcGIS Online platform, the four types of biomass are further scaled at appropriate intervals, and made available as individual and transparent operational layers.

From an economic potential perspective, the economic availability of biomass in the BioBoost project was based on the assessment of feedstock costs at the national levels, assuming variable roadside costs and a fixed supply-price function to determine the relation between feedstock price and the degree of sourcing. While the BioBoost project

also included the logistics aspects of biomass supply and demand, these were not included here, mainly so because of the unknown relationship between supply on one side and the demand in the European heating sector on the other.

It is the belief of the HRE4 WP2 team that biomass markets exist at three levels: local, regional and global. While the global biomass markets are not directly relevant in terms of regional and local availability assessments (since biomass is a transportable item), a determination of viable future utilisation levels at these scales presupposes a feedback information mechanism between regional markets and the level at which these local biomass categories are used e.g. in local heating plants. In a later phase of the HRE4 project, when the future national energy mixes are known from the energy systems analyses in the modeling of WP6, it will be possible to quantify regional biomass demands and to weigh these against the known availabilities.

As an alternative approach for spatial representation, WP2 has also elaborated on the idea of distributing NUTS3 regional biomass data to hectare levels using a reverse-engineering approach, where biomass amounts are spatially disaggregated to land use types from the above referenced Corine land use dataset (such as forests, arable land and orchards etc.). Figure 2.17 shows an illustrative example of local biomass density modelling where regional data on straw availabilities are distributed to a hectare raster grid representing information on arable land.

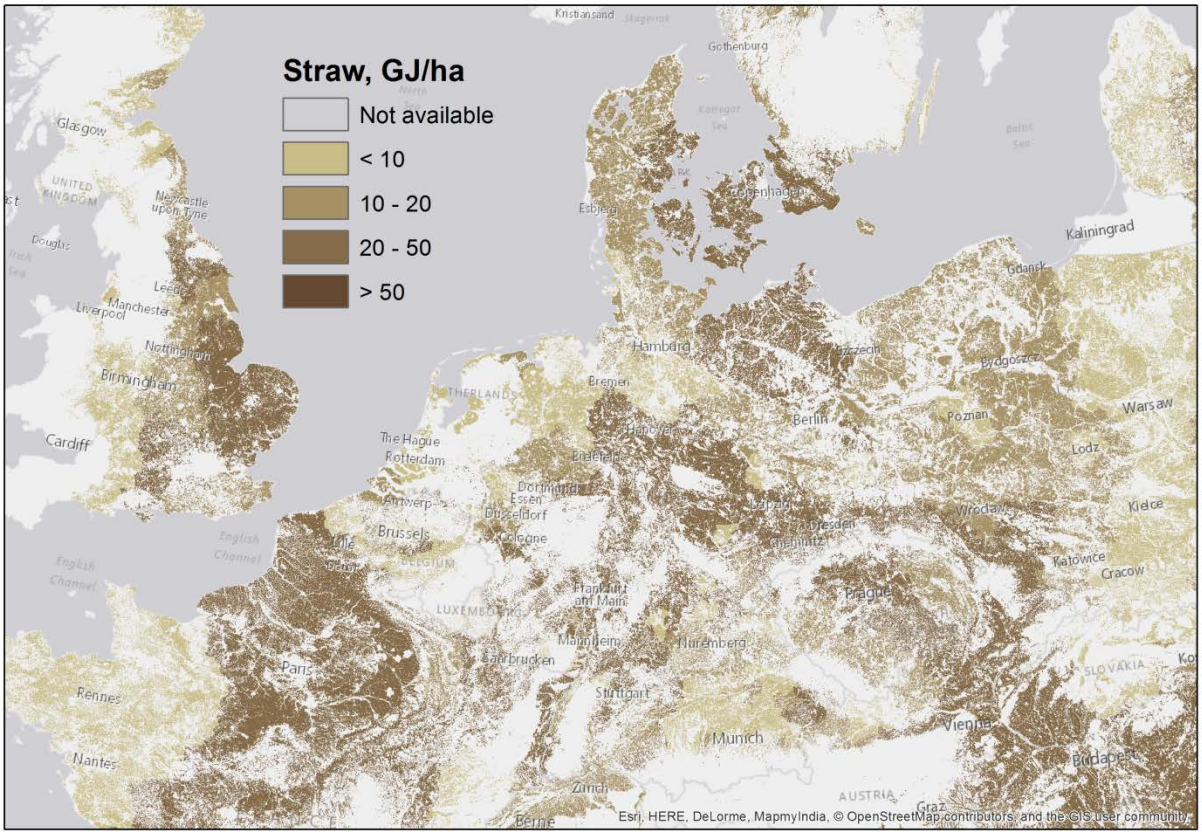

Figure 2.17. Local biomass density modelling: distribution of biomass resources (here: straw from agriculture) from NUTS3 regions to a 100-metre grid. The distribution happens uniformly on the basis of land use classification, using the 100-metre Corine land use classification grid (here: arable land).

2.3 Task 2.3: Heat synergy regions (hot spots)

The concepts of regional heat balances (or “excess heat ratio”) and heat synergy regions (or “hot spots”) were first conceived and introduced in the second HRE study in 2013 ((Connolly et al., 2013). The approach, later refined and developed as the project progressed, has been incorporated and applied in several continental EU28 assessments, as documented inter alia in (Persson et al., 2014, Persson, 2015a, Persson, 2015b). Given that the above references already give comprehensive accounts for the theoretical context and background of these concepts, the following section will focus explicitly on key quantities and, where so applicable, on new methodological developments with reference to these.

The primary purpose of establishing regional quotas of available excess heat assets vs. building heat demands is to provide overview indications of where, in what regions, total magnitudes of these assets and demand are in balance with each other. Secondary to this, a more general purpose is to identify regions with extremely high – as well as extremely low – ratio values, which both signifies less feasible areas for large-scale excess heat recovery projects. The point being that, for viability, regions with simultaneous presence of highly concentrated demand centres as well as considerable volumes of excess heat from large-scale energy and industry sector facilities, are more suited than those plentiful in one but not in the other respect.

The approach accounted for in the following, therefore, aims first at establishing regional heat balances for all 1140 NUTS3 regions studied in the 14 MS´s (this figure excludes seven Spanish and five French Atlantic and overseas NUTS3 regions respectively), and subsequently – on the basis of these balances – determine the suitability for excess heat recovery of these regions. For the identification of the latter, i.e. the heat synergy regions, a novel approach involving so called “priority groups” is used and presented for the first time in this study.

2.3.1 Regional heat balances

From the HRE4 WP2 estimate on theoretically available excess heat from large-scale energy and industry sector facilities in operation, $E_{heat,o}$, as described above in section 2.2.1 (see Equation 18) and summoned in section 3.2 below, we have seen that the 14 MS´s host a total of 2188 large-scale facilities located in 732 NUTS3 regions in these countries. Since we, from the regional distribution of total national building heat demands in residential and service sectors, as presented above in section 2.1.1, further know the magnitudes and annual volumes of NUTS3 region heat demands for space heating and hot water preparation, $Q_{tot,N3R}$ (see Equation 2), calculations of excess heat ratios, $\xi_{heat,o}$, are made possible:

$$\xi_{heat,o} = \frac{\Sigma E_{heat,o}}{Q_{tot,N3R}} \qquad [-] \tag{22}$$

Accordingly, by dividing the sum of all excess heat volumes assumed available per NUTS3 region with the total sum of building heat demands per corresponding NUTS3 region, 732 regional heat balances were found among the study population of 1140 NUTS3 regions. It should be briefly noted that initial discussions considered the inclusion also of low temperature industrial heat demands in $Q_{tot,N3R}$ here (that is space, hot water, and below 100 °C process heat demands), but for reasons explained further in sections 1.3, these were not included in the final assessments. However, one can rest assure that most of the low temperature industrial heat demands present in contemporary Europe, for which WP3 has supplied detailed sub-sectoral in-data, is spatially consistent with the excess facilities identified within the 732 NUTS3 regions.

In Figure 2.18, all 732 NUTS3 regional excess heat ratio values are projected in a scatter plot, with regional heat demands on the abscissa and the sum of regional excess heat on the ordinate. Since the dotted diagonal line indicates a ratio value of one, it is clear that a majority of region values are below this level, while a lesser share is above it[23]. The maximum ratio value was found at 55.0 (German NUTS3 region of Spree-Neisse (DE40G)), the average mean at 1.44, the median at 0.83, while the lowest was that of French NUTS3 region Cantal (FR722), at 0.004. Twenty-five regions have annual excess heat volumes in excess of 20 TWh (maximum at 70.5 TWh in German region DEA27 (Rhein-Erft-Kreis)), while 50 regions were found to have corresponding values below 0.1 TWh per year.

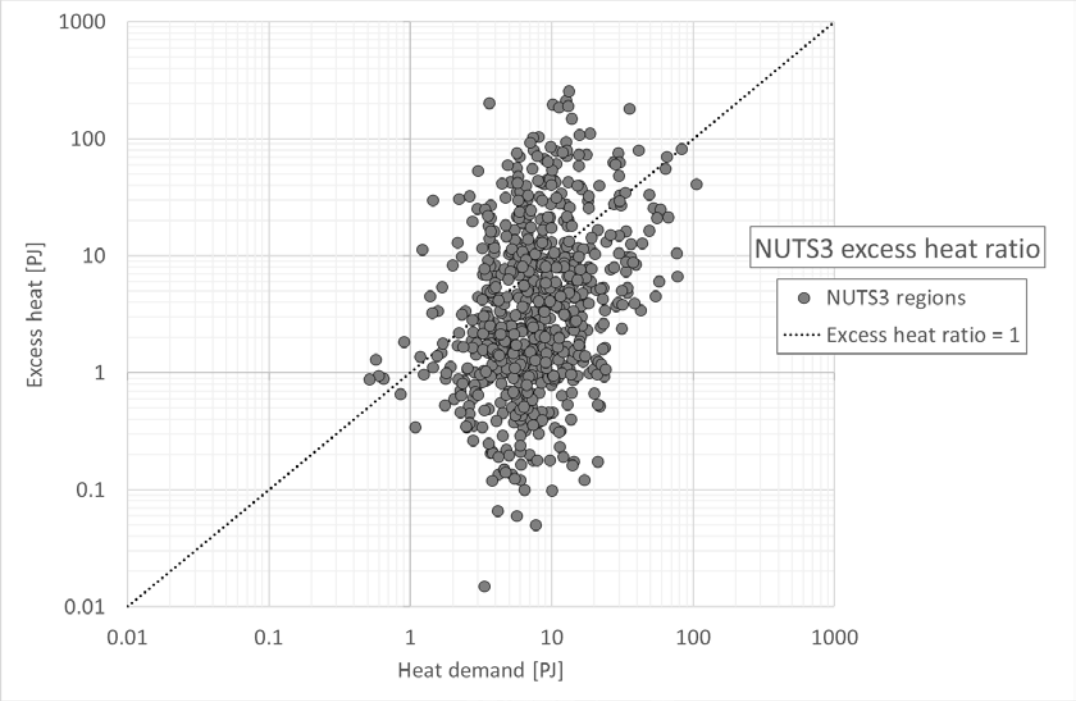

Figure 2.18. Scatter plot showing the excess heat ratios of 732 the 14 HRE4 MS NUTS3 regions with an excess heat ratio value above zero.

[23] Five hundred and twenty four NUTS3 regions, harboring 1631 TWh of annual heat demands and 503 TWh of excess heat, have ratio values below one. Two hundred and eight regions, with total heat demands of 494 TWh per year and 1923 TWh of excess heat, have ratio values above one.

Now, if projected on the map, as shown in Figure 2.19, the 0.83 median value of the total output is clearly visible throughout the studied 14 MS´s, and, since considerable variations of regional ratio values are present, it is understood that these primarily serve as intermediate quantities by which to identify the heat synergy regions. Once again, the key objective here is primarily not to locate high nor low ratio value regions, but instead to target those where both demands and assets are plentiful. In contrast to this, however, 408 NUTS3 regions (36%) completely lack access to large-scale excess heat activities, as studied here, and these regions are habituated by some 100 million people, representing heat demands in the order of ~600 TWh per year (22%).

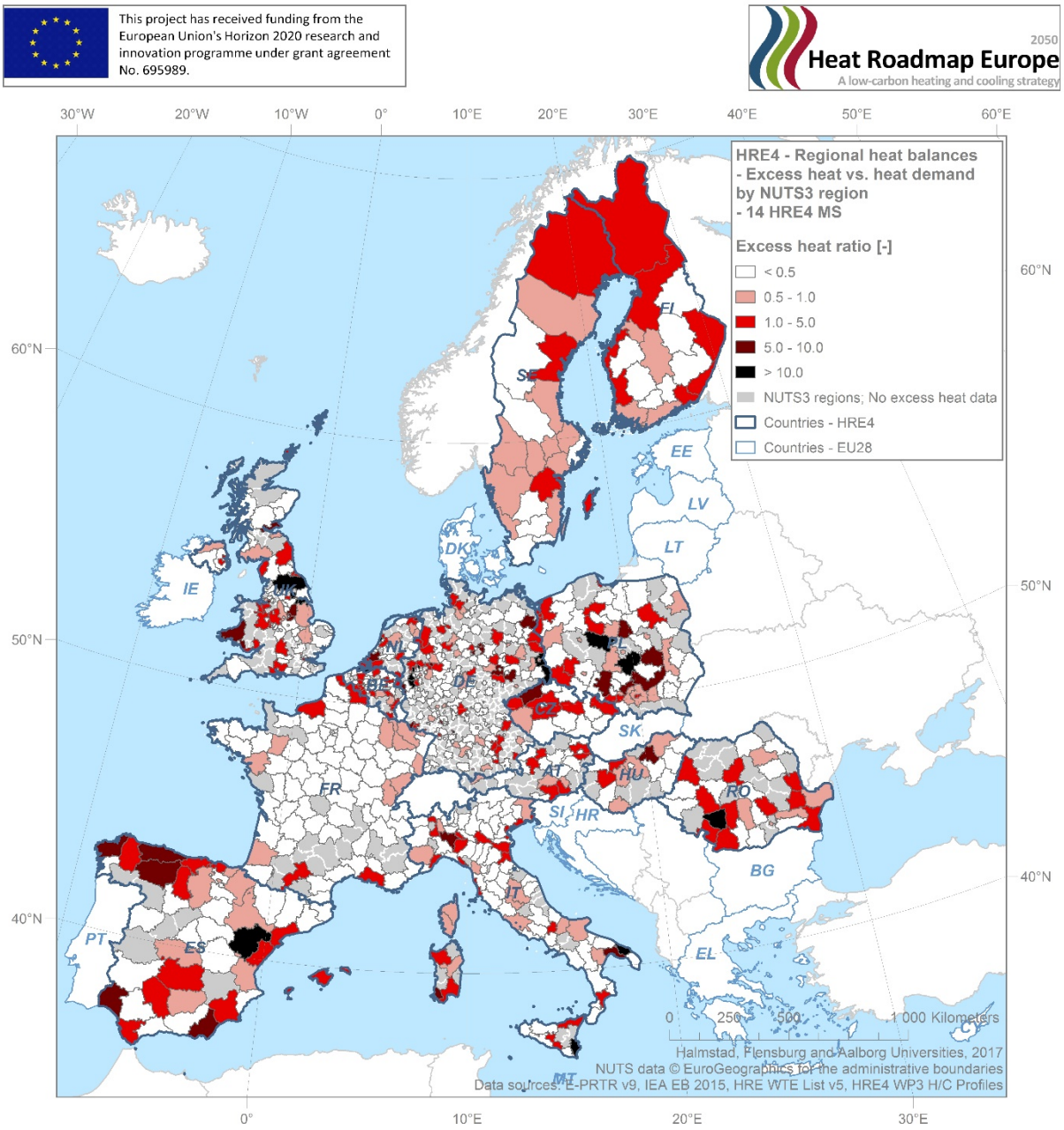

Figure 2.19. Map with excess heat ratio values for 732 NUTS3 regions in the 14 HRE4 MS. Ratio values, based on theoretically available excess heat and residential and service sectors heat demands, are divided into five classes ranging from below 0.5 to above 10.0.

2.3.2 Heat synergy regions: Priority groups

The main objective by which heat synergy regions, or "hot spots", are introduced is to identify NUTS3 regions (or clusters of NUTS3 regions) which simultaneously host high heat demand concentrations as well as large magnitudes of excess heat. In theory, such regions should constitute the most favourable regions and districts for feasible recoveries of secondary heat flows, why they represents primary target regions for structural energy efficiency projects in contemporary Europe. In previous HRE studies, this identification process was never formalised in a repeatable methodological approach, but often achieved merely on manual spatial analysis and ocular observations within the GIS at hand.

For this reason, a set of priority groups, whereby to distinguish NUTS3 regions according to their suitability for excess heat recoveries and heat synergy projects, is arranged and employed. The priority grouping is determined by the excess heat ratio characteristics (numerator and denominator quantities of the ratio) for each region, and consist itself of five distinct priority status categories, as detailed in Table 2.19.

Table 2.19. Excess heat ($E_{heat,o}$) and heat demand (Q_{tot}) characteristics for the definition of priority groups to identify heat synergy regions

	Characteristics			
Priority group	**Excess heat[a] [PJ/a]**	**Heat demand[b] [PJ/a]**	**Priority status**	**Comment**
1	$\sum E_{heat,o} > 10$	$Q_{tot} > 10$	Very high	High levels of both $E_{heat,o}$ and Q_{tot}
2	$1 < \sum E_{heat,o} < 10$	$Q_{tot} > 10$	High	Moderate levels of $E_{heat,o}$ and high Q_{tot}
3	$\sum E_{heat,o} > 10$	$1 < Q_{tot} < 10$	Moderate	High $E_{heat,o}$ and moderate levels of Q_{tot}
4	$1 < \sum E_{heat,o} < 10$	$1 < Q_{tot} < 10$	Low	Both $E_{heat,o}$ and Q_{tot} at moderate levels
0	$\sum E_{heat,o,max} < 2.5$	$Q_{tot,max} < 25$	No priority	Both $E_{heat,o}$ and Q_{tot} at low levels

[a] Maximal theoretical levels of annually available excess heat.
[b] Space heating and domestic hot water preparation in residential and service sectors.

The first priority group (priority status "Very high") represents the real crème-de-la-crème of suitable NUTS3 regions for excess heat recovery projects, including only such regions where both heat demands and excess heat volumes exceed 10 PJ (or 2.78 TWh) annually. In Figure 2.20, viewed again, as in the scatter plot format of Figure 2.18, this first group consists of the top-right segment of black dots, and from Table 3.3 in section 3.3, it can be seen that almost half of all available excess heat (47%) is included in this group.

The second and third group, priority status "High" and "Moderate", respectively, both represent suitable regions and captures either above 10 PJ heat demand regions (with lesser excess heat availabilities) or above 10 PJ excess heat regions (with smaller heat demand concentrations). Eventually, the fourth priority group (priority status "Low") signifies possible excess heat recovery regions, however where both heat demands and excess heat availabilities are below 10 PJ per year.

The fifth and final priority group ("No priority") assembles those regions where excess heat activities very well are present, although either at very low levels or in combination with comparatively huge heat demands, far too large to be fully satisfied with the present excess heat. From Table 3.3 in section 3.3, once again, it is evident that this

group, while representing 15% of the total heat demands, only hosts one per cent of the annual excess heat volume in study. In section 3.3, further, is presented a corresponding European continental map, see Figure 3.2, which illustrates the spatial distribution of the identified heat synergy regions.

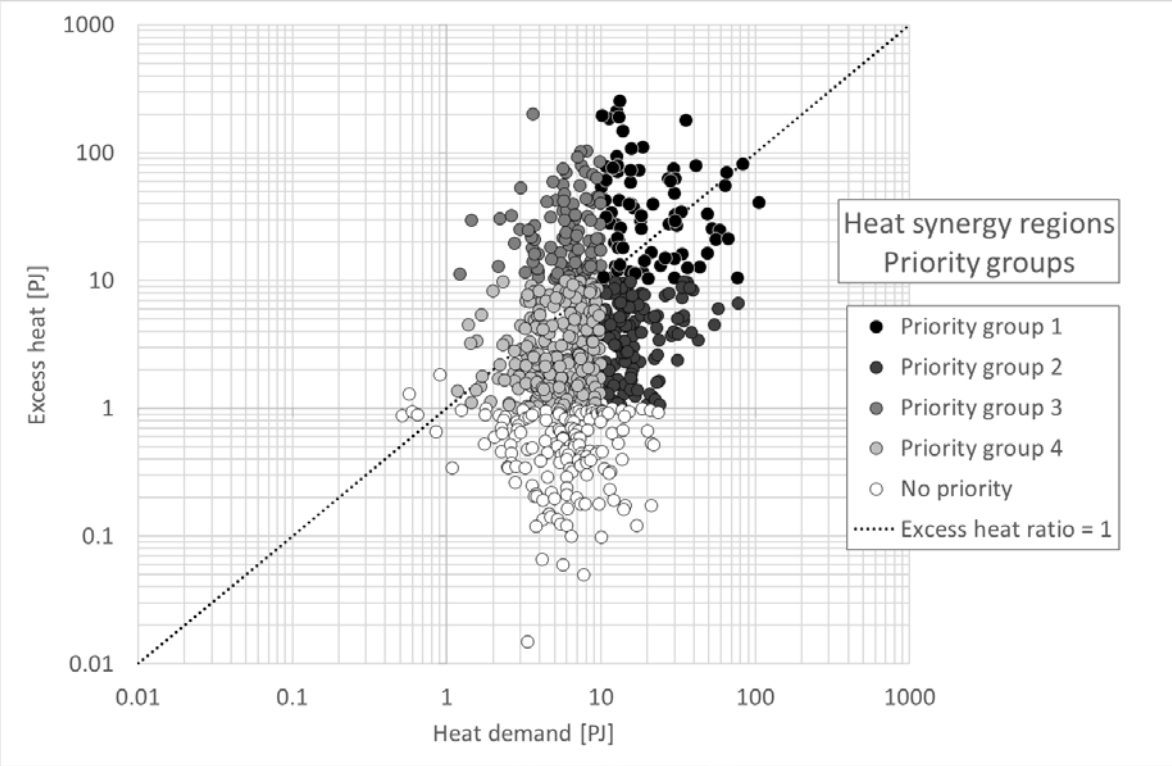

Figure 2.20. Scatter plot showing the excess heat ratios of 732 HRE4 14 MS NUTS3 regions with an excess heat ratio value above zero and their division into priority groups to identify heat synergy regions.

2.4 Task 2.4: Connect heat and cooling densities with district heating and cooling network costs

The connection between heat and cooling demand densities and the investment costs for district heating and cooling networks rests in the HRE4 project partly on fundamental theory of district heating and cooling investment costs, partly on advanced spatial analysis in a GIS. On the direct basis of the prepared hectare grid cell heat and cold demand density rasters from the demand atlases accounted for in section 2.1.4, and the use of additional complementary input data, the corresponding investment costs for district heating and cooling pipe networks has feasibly been established for all corresponding grid cells in the 14 MS´s of the EU.

From a pure research perspective, it might be appropriate to recognise that this is quite a bold ambition that, to our current knowledge, never has been neither attempted nor accomplished earlier at the level of detail and scope at hand here. It should also be added that the realisation of this ambition provides site-specific, novel, and coherent information on the economic feasibility of extending district heating and cooling network throughout contemporary Europe, which is illustrated in Figure 2.22 and Figure 2.23 of this section and as well in the figures of subsection 6.6 and 6.7.

Moreover, by the aggregation of found specific investment costs to national cumulative market share curves, as shown e.g. in Figure 3.3 of the result summary in subsection 3.4, it also brings along renewed understanding and insight into currently feasible extension levels for these thermal infrastructures. However, it must also be recognised that the found cost levels, just like the heat and cold demand density models that provide their main source of input data, are modelled and thus anticipated values – hence, not real world values gathered empirically as statistical records. For this reason, these outputs should be interpreted as indicative only, why they should not substitute for the ever-necessary case-by case feasibility studies that should accompany any heat or cold infrastructure project.

2.4.1 Theory of district heating and cooling investment costs

According to the fundamental theory and concepts related to district heating and cooling systems investment costs, as presented by Fredriksen and Werner (2013), the basic equation for the heat distribution capital cost (C_d), i.e. the annualized investment cost per unit sold heat or cold, can be written as:

$$C_d = \frac{a \cdot I}{Q_s} = \frac{a \cdot \left(\frac{I}{L}\right)}{\left(\frac{Q_s}{L}\right)} \quad \left[\frac{€}{GJ}\right] \tag{23}$$

Where the chosen annuity (based here on 3% real interest rate and a 30 year investment lifetime) is denoted “a”, the total investment cost is symbolized by “I” (€), and the annual heat and cold sales respectively are denoted “Q_s” (J/a). By insertion of the pipe system route length, L (m), the numerator parenthesis expresses the specific investment cost (investment cost by route meter) and the denominator expresses the linear heat density (annual heat sales by route meter).

To meet the objective of calculating this cost on hectare grid cell level[24], the available input data, namely the heat (and cold) demand densities of these hectare grid cells (q_L), were connected to the cost function in Equation 23 by a transformation of linear heat density, as originally presented in (Persson and Werner, 2011) and subsequently developed in (Persson, 2015a). By this transformation of the traditional expression of linear heat density (Q_s/L), to an analytical expression based on population density, p (n/m^2), specific building space, α (m^2/n), specific heat demand, q (GJ/m^{2}a), and effective width, w (m), the heat distribution capital cost can be re-written as:

$$C_d = \frac{a \cdot \left(\frac{I}{L}\right)}{p \cdot \alpha \cdot q \cdot w} = \frac{a \cdot \left(\frac{I}{L}\right)}{e \cdot q \cdot w} = \frac{a \cdot \left(\frac{I}{L}\right)}{q_L \cdot w} \qquad \left[\frac{€}{GJ}\right] \tag{24}$$

Where plot ratio, e (-), i.e. the share of building space area on a given land area, needs only to be multiplied with the specific heat demand to represent the sought connecting quantity (q_L). From here, to complete the transformation, linear heat densities may again be assessed if q_L is complemented by the effective width value of each corresponding hectare grid cell. For this, the plot ratio of each hectare grid cell was used to determine the corresponding effective width value, according to an adaption of their internal relationship as presented in previous studies (Persson and Werner, 2010) and expressed according to Equation 25:

$$0 < e \leq 0.4; w = 137.5 \cdot e + 5, e > 0.4; w = 60 \quad [m] \tag{25}$$

The connection between heat and cooling densities with district heating and cooling network costs thus exist within the denominator of the original distribution capital cost expression. For the numerator, it is known from experience that the specific investment cost (I/L) follows a linear relationship with respect to the average pipe diameter (d_a), which allows for a re-writing of the expression with the introduction of a construction cost constant, C_1 (€/m), and a construction cost coefficient, C_2 (€/m^2), according to:

$$C_d = \frac{a \cdot (C_1 + C_2 \cdot d_a)}{q_L \cdot w} \qquad \left[\frac{€}{GJ}\right] \tag{26}$$

[24] Hectare grid cells without demand density data, the majority of cells, were excluded from the calculations.

For this study, these construction costs, which in (Persson and Werner, 2011) were based on 2007 Swedish cost catalog values, were updated by use of a Swedish entrepreneur index (SCB, 2017a, SCB, 2017b, SDHA, 2007, SRB, 2017) to represent average 2015 cost levels. As can be seen in Figure 2.21[25], these cost levels were updated for three characteristic area categories: (A) Inner city areas, (B) Outer city areas, and (C) Park areas, where after an adapted average function on the basis of these three categories was assessed for pipe diameters up to 0.3 meters.

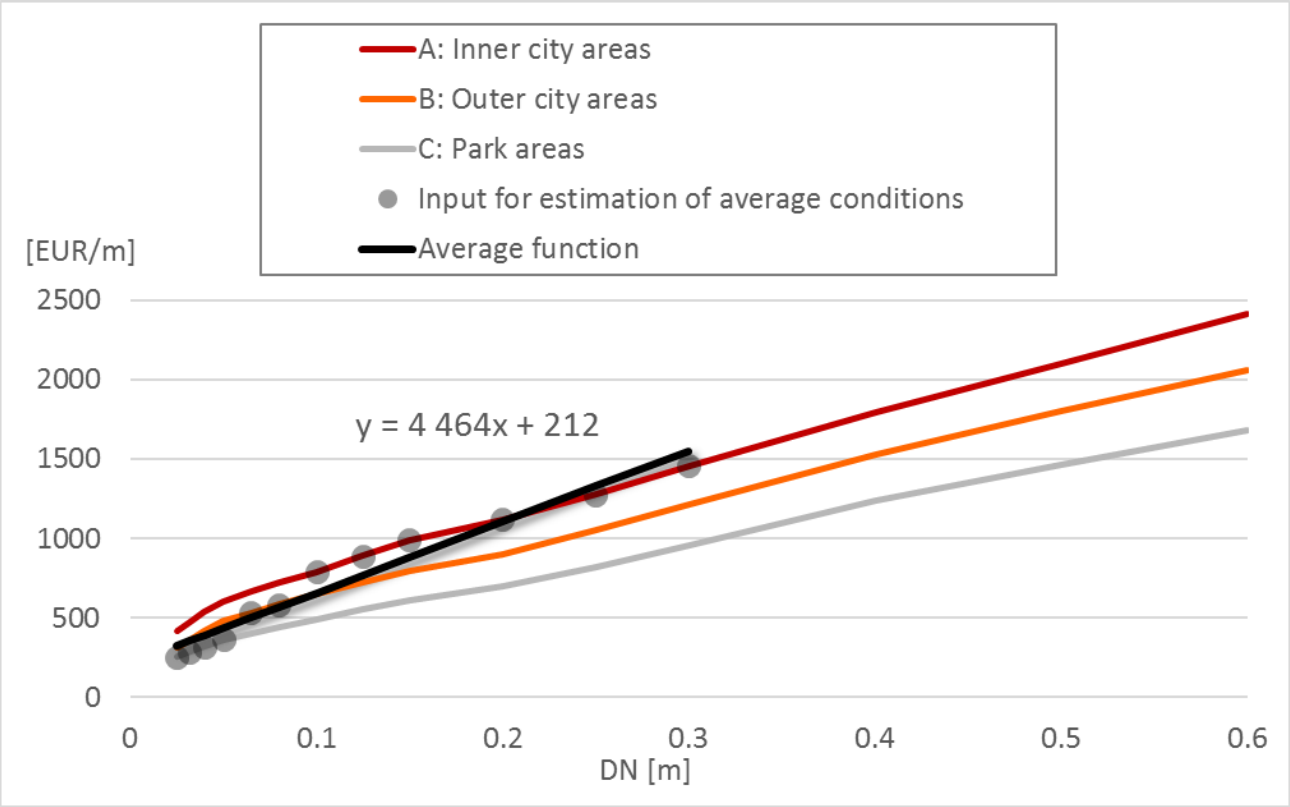

Figure 2.21. Average construction cost function based on assessed 2015 construction costs levels for three characteristic area categories: (A) Inner city areas, (B) Outer city areas, and (C) Park areas. Sources: (SDHA, 2007, SCB, 2017b, SCB, 2017a, SRB, 2017)

Hereby, for this study, an average construction cost constant value of 212 €/m and an average construction cost coefficient value of 4464 €/m^2 have been used uniformly for all considered hectare grid cells as representative of average current construction costs conditions in Europe.

By use, finally, of the established logarithmic relationship between linear heat density and average pipe diameter (Equation 27), as originally presented by Persson & Werner (2011), all the necessary quantities and values to satisfy the study objective, i.e. to connect the heat and cooling demand densities with district heating and cooling network costs, were hereby obtained:

[25] Swedish pipe catalog cost data originally reported in [SEK] was converted to [EUR] by use of the 2015 average exchange rate (9.3562) between the two currencies. It is noted that this is a considerably lower rate level than that of 10.8 used in the referenced Persson & Werner 2011 study.

$$d_a = 0.0486 \cdot \ln(q_L \cdot w) + 0.0007 \qquad [m] \tag{27}$$

In the calculations of pipe diameters, a lower limit of linear densities at 1.5 GJ/m was set both for heating and cooling networks. Below this threshold, pipe diameters of 0.02 meters were applied uniformly for all grid cells with present demand values above zero.

Cooling pipe diameters further, were established by inserting a multiplying factor of √5 to the expression in Equation 27 when operating with linear cool densities. As applied and reported also in the earlier HRE3 project Stratego (Möller and Werner, 2015), this upscaling factor reflects the general circumstance that flows in district cooling networks are about five times higher than those in district heating networks at same demand levels[26], while flow as such is proportional to the square of a circular pipe diameter.

2.4.2 DHC investment costs: Spatial analysis

The spatial analysis to determine the district heating and cooling network costs consisted of a series of raster layer calculations (raster calculator), each of which fabricated intermediate outputs adding significant value to the WP2 catalogue of results. First, the floor area data supplied from WP3, as described in subsection 2.1.3, was used to establish the plot ratio of each hectare grid cell. Next, applying the conditions and relations of Equation 25, rendered raster layers with effective width values.

On this basis, corresponding raster layers for linear heat (and cold) densities could be produced by utilising the established connectivity to the heat and cold demand density layers of the WP2 demands atlases and that of the established effective width values. Hereafter, pipe dimensions were assessed on grid cell level for both district heating and district cooling networks according to Equation 27, after which three different aspects of the anticipated investment cost were calculated: (1) specific investment costs (€/m), (2) absolute investment cost (€/GJ), and (3) the sought output, namely the (heat and cold) distribution capital costs (€/GJ).

Now, as the number of unique hectare grid cells with other than “No data” values in any of these produced output rasters is roughly 34 million (thus representing approximately 9% of the total gross land area at 370 million hectares of the 14 studied EU MS´s, as detailed further in Table 3.4 in subsection 3.4), their production is both a time and process capacity consuming process.

However, after processing times well up to an hour – or more - in some instances, these highly detailed output maps where found well worth the wait, as illustrated for the city of Budapest in the city map of the Hungarian capital in Figure 2.22. In terms of outputs, although these certainly are at their best viewed through the Peta4 online map service, images like these still reveal the striking and spectacular detail of these results (for three additional examples (Manchester, Stockholm, and Brussels), see sub-section 6.6).

[26] Which is explained by the fact that temperature differences in district cooling networks, on average, are about one fifth of the temperature differences in district heating networks.

This project has received funding from the European Union's Horizon 2020 research and innovation programme under grant agreement No. 695989.

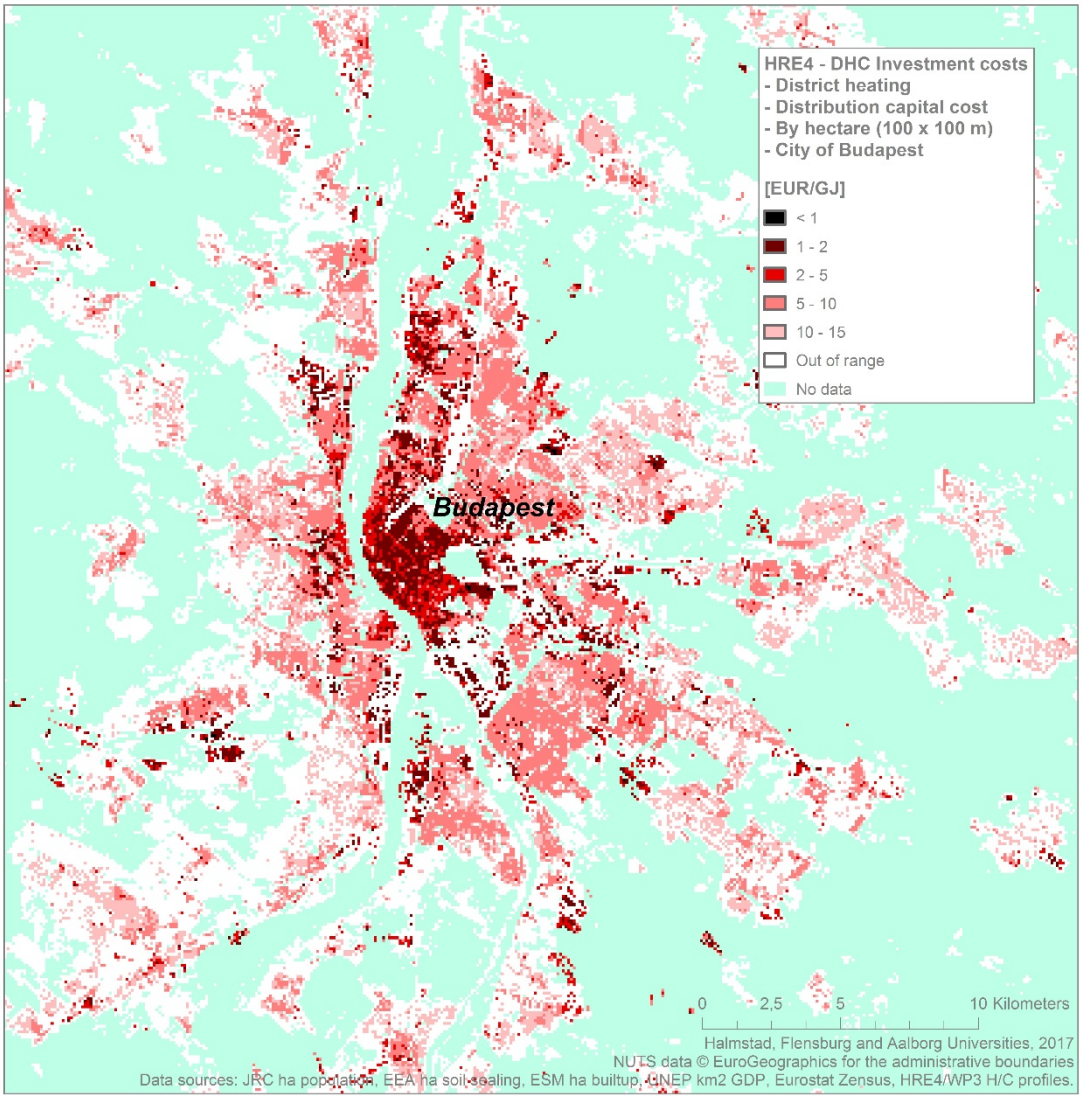

Figure 2.22. Close-up map of marginal distribution capital costs for district heating pipe networks by hectare grid cells; Case study example for the city of Budapest in Hungary.

As visible in the map of Figure 2.22, the selected level of resolution generates what, from a zoomed-out perspective, can be interpreted as coherent area segments with fairly uniform levels of investment costs. Clearly, a majority of inner city areas, here appearing mainly as dark umber (1 – 2 €/GJ) and poinsettia red (2 – 5 €/GJ), constitute highly feasible areas for district heat distribution. Towards suburban areas (medium coral light (5 – 10 €/GJ)) and beyond (rose quartz (10 – 15 €/GJ)), these opportunities may still be considerable, however steadily decreasing by distance to the city centre. Finally, rural areas with anticipated marginal heat distribution capital costs levels above 15 €/GJ were considered out of range (white).

For the corresponding marginal cold distribution capital costs, the city map in Figure 2.23 shows a case example of the Spanish city of Barcelona and its surroundings (see further subsection 6.7 for three additional city maps (Milan, Helsinki, and Brussels)). As can be seen, the city centre constitutes a rather homogenous area in terms of investment cost levels, which are found mainly in the range of 5 – 10 €/GJ and 10 – 15 €/GJ. It should be noted that principally no cold distribution capital costs below five €/GJ were found in the study population (with some few exceptions). Still, to make apparent the significant differences in general investment cost levels for heating and cooling networks, the chosen legend scale for cooling costs was deliberately set identical to that of heating costs.

This project has received funding from the European Union's Horizon 2020 research and innovation programme under grant agreement No. 695989.

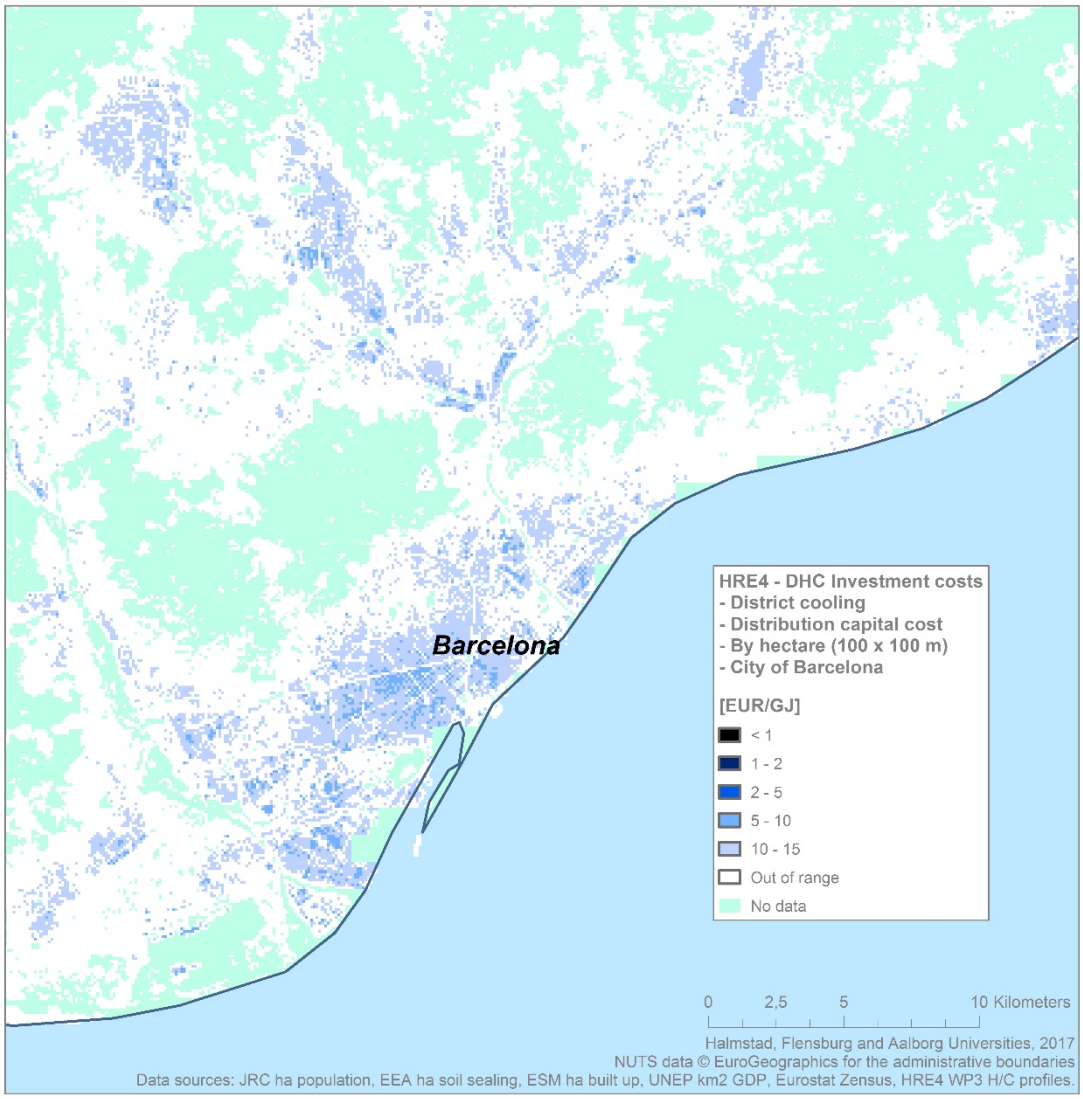

Figure 2.23. Close-up map of marginal distribution capital costs for district cooling pipe networks by hectare grid cells; Case study example for the city of Barcelona in Spain.

2.5 Task 2.5: Quantifying the potential mix of rural heating solutions

Heating and cooling supply technologies largely follow the pattern of settlements and the availability of heating and cooling sources. Sufficient demand densities render district heating and cooling technologies feasible, and access to low-cost sources make collective technologies more attractive than individual solutions. Finally, political, economic as well as socio-cultural, barriers have an influence on the practically available choices of heat demand technologies.

In this section, the mapping of rural heating solutions is sketched. Rural areas are on the one hand characterised by low heating and cooling demand densities, on the other hand, however, rural heating and cooling costs are often higher in comparison to urban areas. Issues of energy poverty may be addressed by utilizing some of the renewable energy potentials that are more readily available in rural areas. Rural heat markets moreover have largely remained uncharted and thus unknown for European countries. While urban areas are in the focus, and considerably easier to map, heat demand mapping in rural areas has much fewer data to use as input, and the sensitivities are often much higher in comparison to high demand density areas.

In section 2.1.3, a series of multilinear models of floor area were developed, which extend into all rural areas which also show some degree of build-up and presence of population, albeit at much lower levels and for much smaller areas at a time than in urban areas. Hence, the sensitivity associated to the correct mapping of these rural areas, and thus the potential for errors in the assessed heat demands, are much higher.

Geographically, the mapping of rural heat demands is further complicated by the choice of the geographical unit of one hectare. While such a high spatial resolution is a necessary requirement to model floor areas and heat demands to the required detail of heat supply analyses, it also means that in rural areas, single houses extend to the smallest possible land area of one hectare, making any heat demand density model highly insecure. Hence, the chosen unit of heat demand per hectare usually hides the presence of single buildings or small clusters of buildings.

2.5.1 Individual heating solutions

Individual heating solutions such as boilers and heat pumps are often the choice of technology in areas where collective district heating may not be feasible. By use of a predefined classification of heat demand densities by their most appropriate heating solution, as presented in Table 6.1 in Appendix section 6.3, the preferable choice of technology for any given area can be generally appreciated and modelled in alignment with these guidelines. Hereby, rural heat demands can be located on maps and summarised by administrative entities such as NUTS3 regions, by heat demand density classes in general, by the size of contiguous settlement areas, or by the proximity to favourable prospective DH supply areas, as illustrated in Figure 2.24.

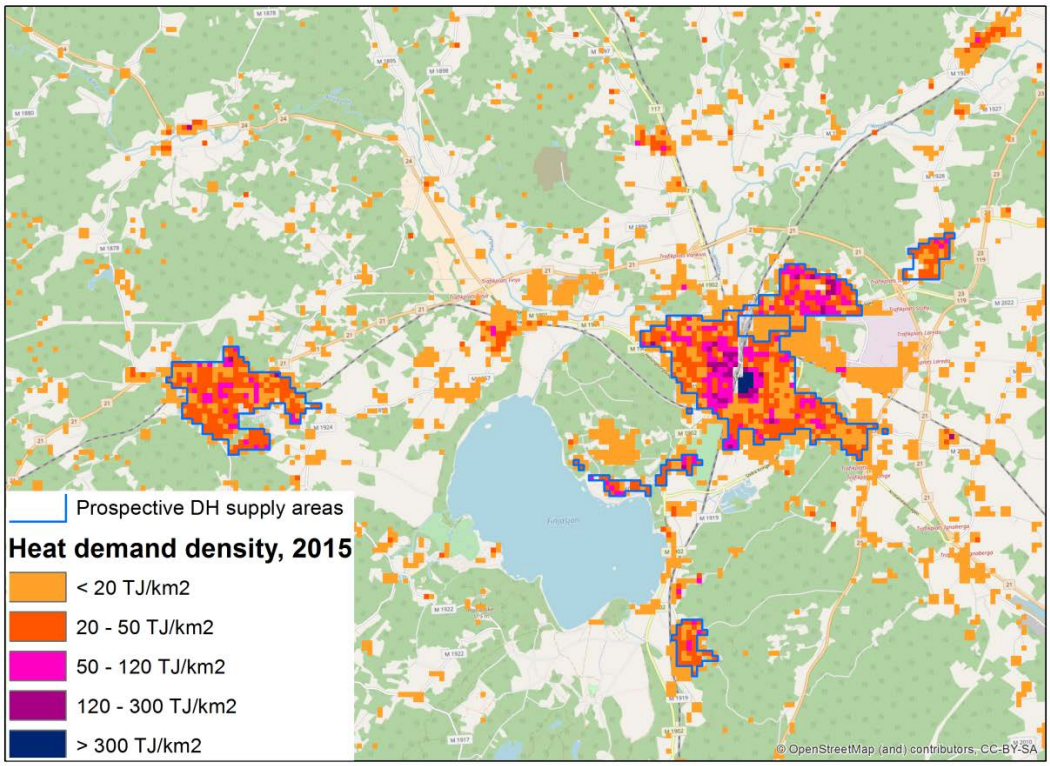

Figure 2.24. Local map of heat demand densities in a local area (here showing the area around the town of Hässleholm in Sweden). Rural heat demand density is usually below 20 TJ/km² due to the sparse distribution of buildings

Accordingly, rural areas with heat demand densities lower than 50 TJ/km² (outside coherent urban areas) are currently assumed as being dominated by individual heating solutions (e.g. boilers, micro-cogeneration, direct (radiators) and indirect (heat pumps) electrical installations).

It should be observed however, that collective heat distribution systems such as district heating networks still might be feasible and applicable in such low demand density areas. This may be explained by the fact that besides the heat demand density of individual rural locations, the size of each rural settlement itself is also an important parameter for the choice of heating technologies.

In rural areas in the range of 50 to 120 TJ/km², the choice is very much depending on the proximity to larger district heating systems and on their access to renewable or excess heat sources. In the present project, accordingly, prospective DH (district heating) supply areas consist of clustered grid cells that extend to coherent and contiguous larger areas with sufficiently high concentrations of heat demand density within them (often including significant shares of grid cells with values above the 120 TJ/km² level (corresponding to 1200 GJ/ha)), as is also visible in Figure 2.24.

For single heat demand densities above 120 TJ/km² in rural areas, it is assumed that these comprise of single buildings or small clusters of buildings with no substantial potential for district heating – except if they are located close enough to prospective district heating areas. However, within these areas as well, it should be noted that district heating should be assessed and compared to individual heating options.

If observed on the square kilometre level, it should thus be noted that areas with heat demand density values below 50 TJ/km^2, or even below 20 TJ/km^2, might still host sufficiently concentrated settlements where smaller district heating systems could be feasibly established. Built-up rural areas of coherent sizes smaller than one square kilometres may therefore occasionally provide sufficiently high total heat demands to facilitate network heat distribution, albeit their heat demand densities at square kilometre scales may read below 50 TJ/km^2.

Decision processes on rural heating solutions should hence include considerations not only of the heat demand density of any given area, but also recognise the geographical outstretch and neighbourhood conditions of this area. Hence, it should further be noted that rural settlements may be rather concentrated and that even small communities, of e.g. 200 households, may profit from investing in district heating. District heating should thus be carefully considered in rural areas as well.

Since the location of heat demand is of less importance for rural, individual, heat supply solutions than for district heating systems, it makes sense to summarise the heat demand by appropriate heat demand density classes, as is done for all 14 MS´s in Table 3.1, although it could be done at higher resolution or relative to other phenomena such as the delineation of grid operators etc. Further information on heat demand density classification by which to model the choice of heat supply solutions in urban versus rural areas is given in Table 6.1.

3 Summary of main results

For reasons that has been made clear in the introduction and further mentioned in several of the preceding sections, namely that the main means and format of results dissemination for WP2 in this HRE4 project is that of the Peat4 web map application, this section is limited to a brief summary of main findings and results. Among these, a few words are first said in subsection 3.1 on the modelled heat and cold demand density rasters of the demand atlases.

Next, the main findings of the work with the resource atlases are commented upon in subsection 3.2, focusing here exclusively on the assessed excess heat potential from large-scale excess heat activities in energy and energy intensive industrial sectors. Concerning the three renewable heat categories included in the study estimations, no explicit results are here put forward for biomass and geothermal resources, mainly since they have been mapped on regional and local levels and made available as such in transparent operational layers at Peta4.

For the third renewable category, solar thermal heat by large-scale solar collector installations in current district heating city areas, for which the work presented here consists of only two out of three intended steps (as described in section 2.2.3 above)[27], it can be concluded in general that land availability is not a limiting factor. Our findings suggest, after having selected a candidate list of 1183 coherent district heating city areas and subsequently evaluated the availability of suitable land in vicinity of these, that required land for 20% solar district heating shares at current conditions constitute merely ~3% of the suitable land available within the narrowest perimeter studied (200-metre buffers)[28]. However, as these numbers refer to accumulated total average values, which by no means are representative of every unique case, a closer study of each and every unique area is recommended. Once more, the study of these output layers at Peta4 provides the case-specific information needed for the preliminary evaluation of land availability in each particular city.

Subsection 3.3 presents the final output from the heat synergy region assessments, which in terms of methodological approaches and data was described above in section 2.3.2, while the final subsection 3.4 presents a conclusive account on the estimated marginal distribution capital costs for district heating systems in the 14 MS´s of the EU. In summary, it may be noticed from these outputs that the ~28% of excess heat NUTS3 regions that represent “very high” (priority group 1) and high (priority group 2) priority group statuses, together constitute more than 50% of both heat demands (57%) and excess heat availabilities (53%) in these regions – while simultaneously representing areas with lowest assessed investment costs.

[27] The third step, i.e. an estimation of economic and technical feasibility in accordance with the spatial expansion potential outlined in this study, is planned for completion within the IEA-SHC T52 project during the latter part of 2017.
[28] At 50% solar district heating shares out of current annual district heat sales, required land constitute ~7% of available suitable land areas. At the farther perimeter (1000-metre buffers), the corresponding numbers were found at ~0.7% (20% shares) and ~2% (50% shares).

3.1 Demand atlases

Heating and cooling demands for the reference year 2015 have been mapped for the residential and service sector in the 14 MS´s of the EU at 100-metre geographical resolution in a one hectare grid. First, national and regional heating and cooling demands were calculated using European heating and cooling indices, which adjust national averages to climatic, demographic and socio-economic conditions at the NUTS3-level. In a combined top-down and bottom-up approach, national heat and cooling demands by sectors, derived from the FORECAST model in WP3, were then distributed to a model of floor area distribution by hectare, which was generated using multi-linear regression models.

Exploratory regression analyses have identified the most promising independent variables and coefficients to arrive at functions, which allow for a quantitative and representative image of building intensity of urban and rural areas. In particular, the degree of built-up areas from the European Settlement Model by the EU JRC, the 100-metre population grid, as well as other phenomena available from public sources, have shown to be appropriate variables for the explanations of how buildings in various sectors are distributed across Europe.

Accordingly, the modelled floor areas of single and multi-family dwellings and service sector buildings were combined with specific heat and cold demands to derive hectare grid rasters with heating and cooling demand densities at 100-metre resolution for all participating countries. In Table 3.1, the total volumes of found heat demand densities are presented by five levels of heat demand density classes. As can be seen, approximately one fifth of the total HRE4 heat demand volume (8% + 13% = 21%), originate in lower demand density areas, i.e. rural and semi-suburban areas, while close to half of the total volume (28% + 21% = 49%) on average is found among high density areas (e.g. urban centres and inner city areas). Notably, for Italy, Spain, Sweden, and Germany, the share of the total heat demand that is concentrated to such high demand density areas reaches well above 50%.

Table 3.1. Heat demand by MS as per cent of total heat demand and by heat demand density. The quantification of heat demands by demand densities is essential for the assessment of heat supply strategies

MS	Q_{tot} [PJ/a]	<20 TJ/km² [%]	20-50 TJ/km² [%]	50-120 TJ/km² [%]	120-300 TJ/km² [%]	>300 TJ/km² [%]
AT	232	11%	17%	25%	17%	30%
BE	324	5%	15%	38%	18%	24%
CZ	237	9%	17%	19%	31%	24%
DE	2413	4%	9%	31%	32%	24%
ES	489	8%	14%	20%	35%	23%
FI	226	14%	13%	21%	15%	38%
FR	1562	11%	17%	32%	26%	14%
HU	210	10%	34%	23%	14%	19%
IT	1283	7%	9%	19%	35%	30%
NL	426	5%	5%	40%	47%	4%
PL	658	15%	23%	19%	23%	20%
RO	183	34%	18%	16%	30%	2%
SE	294	11%	14%	17%	17%	41%
UK	1363	4%	7%	53%	24%	11%
HRE4	**9900**	**8%**	**13%**	**30%**	**28%**	**21%**

The outcome of the WP2 efforts related to Task 2.1 is a Pan-European Thermal Atlas at 100-metre resolution, which, on the basis of a uniform input database from the public domain, arrives at a heating and cooling demand atlas that gives a realistic and representative image of the thermal demands in Europe. As shown in this report, this outcome have subsequently been used to calculate the costs of district heating and cooling infrastructures and to formulate strategies to meet heating and cooling demands with available excess heat and renewable sources.

3.2 Resource atlases

The HRE4 extract of large-scale excess heat facilities from the E-PRTR_v9 dataset builds on a selection of activities with carbon dioxide air emissions reported during the years 2012 to 2014, as described in section 2.2.1. In this context, although this data is a couple of years old, the extract is presented to represent facilities currently in operation. However, it is fair to withhold a general disclaimer here regarding the actual status of these activities, partly due to the age of the data itself, partly due to the extract being the result of a research process essentially performed from behind an office desk – and thus not from in situ accounts from each single activity.

The presented extract constitute the best conceivable assessment based on the used data, and is analogous to previous assessments made within the HRE project series. It should be noticed however, that the methodological approach aims at illustrating the maximal theoretical excess heat volume available from these facilities on an annual basis, and not necessarily the technically feasible volume possible to utilise by excess heat recovery processes. The aim, once again, is to illustrate the vast potential of this resource, and to make visible the great amount of secondary heat that is – still – being straight-out wasted in many European energy and industry sector activities.

It should also be noted, which is visible in the map of Figure 3.1 (where all 2188 facilities that constitute the HRE4 excess heat extract are present), that the selection refers mainly to large-scale activities in a limited set of main activity sectors, namely those generally referred to as “energy-intensive”. As the interest and prospects for excess heat recovery processes increases among the Member States of the EU, it is likely that also the scope of plausible excess heat sources will expand beyond these “classical” excess heat sectors.

Future studies, therefore, should focus also on the viability of recovering secondary energy flows from other sectors, e.g. from supermarkets, computer server stations, urban ventilation infrastructures, cooling processes in building etc. Nonetheless, in terms of sheer magnitudes, the sources accounted for here represent the core sample.

From the summary presented in Table 3.2, it is clear that the 14 MS´s of the HRE4 study resembles the major part of EU28 NUTS3 regions (86%), of EU28 population (88%), and – as pronounced already in the HRE4 project application – of EU28 heat demands in residential and service sector buildings (92%). It is further noticeable that, among the 14 HRE4 MS´s themselves, 64% of the 1140 NUTS3 regions herein (which

corresponds to 79% and 78% of total population and total heat demand respectively), host 89% of all the excess heat-generating activities in the whole of EU28. As expected, in terms of category distribution, thermal power generation (TP) dominates the total excess heat volume (67%), followed by industrial activities (IND) at 27%, and Waste-to-Energy (WTE) at 6%.

A general, concluding comment concerning these estimated European excess heat resources may be that they continue to appear as a vast, yet somehow disguised, grey area of huge opportunities that for their actual realisation will need more attention and support in the coming years than what have been the case historically.

This project has received funding from the European Union's Horizon 2020 research and innovation programme under grant agreement No. 695989.

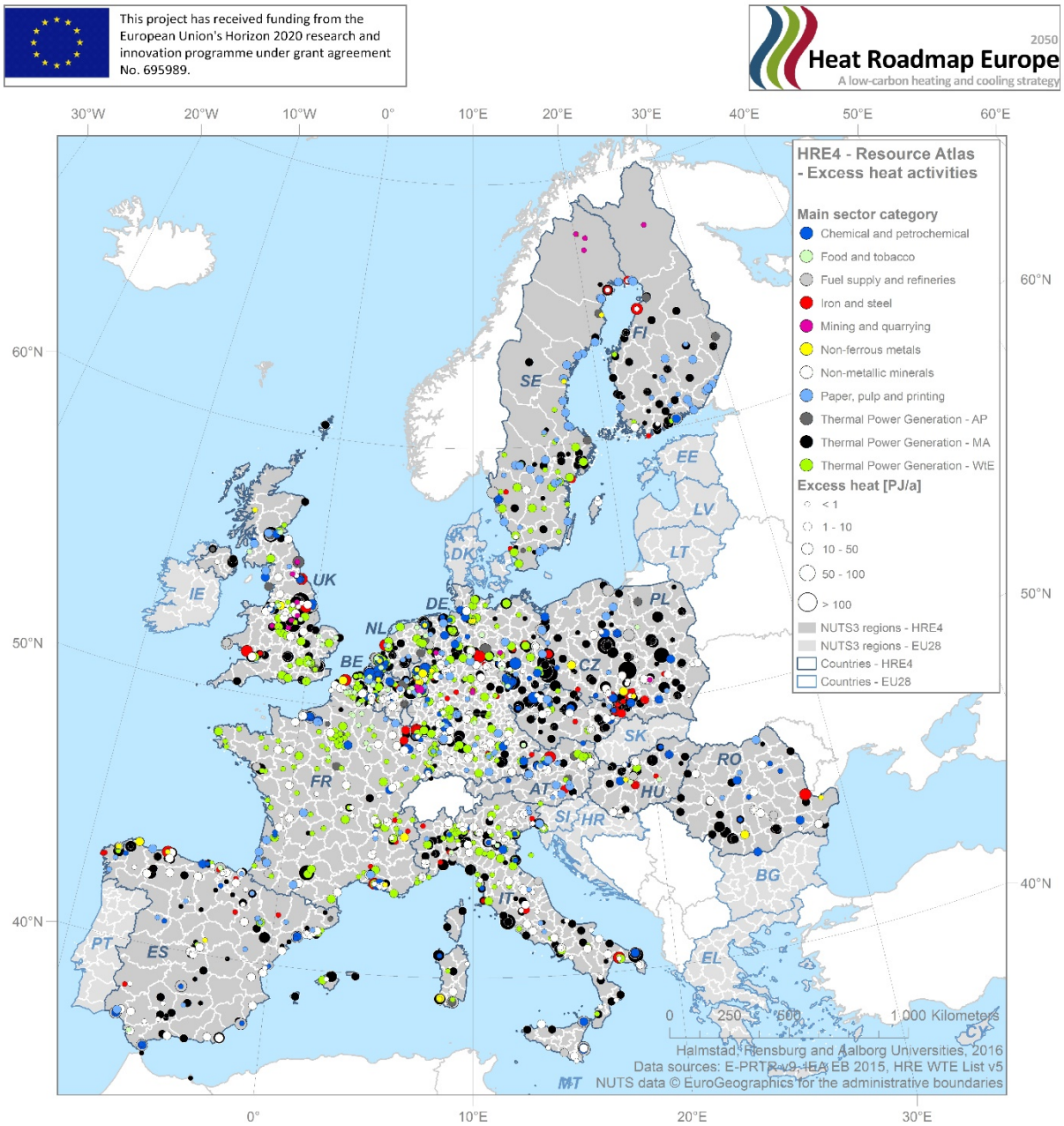

Figure 3.1. Map of the 2188 large-scale excess heat activities currently in operation in the 14 HRE4 MS´s, by main activity sector and assessed annual excess heat volumes. Thermal power generation activities > 50 MW. Sources: (EEA, 2016a, CEWEP, 2014, ISWA, 2012).

Table 3.2. NUTS3 regions (N3R) in the 14 HRE4 MS´s, all in study (left), all with excess heat activities in operation (right), by population (P), heat demand in residential and service sectors (HD), primary energy supply (PES), excess heat (EH), and references to corresponding EU28 totals. Excess heat specified by sectors: Thermal Power (TP), Industrial (IND), and Waste-to-Energy (WTE). Energy volumes in TWh/a. Population in millions

	HRE4 14 MS´s			HRE4 14 MS´s with excess heat ratio value > 0							
MS	**N3R**	**P**	**HD**	**N3R**	**P**	**HD**	**PES**	**EH**	***TP***	***IND***	***WTE***
AT	35	8.6	64.5	20	6.4	48.1	112.3	38.1	*9.0*	*24.2*	*4.9*
BE	44	11.3	90.1	31	9.8	78.4	182.6	68.2	*29.2*	*35.1*	*4.0*
CZ	14	10.5	65.9	14	10.5	65.9	207.0	90.3	*73.9*	*15.1*	*1.3*
DE	402	81.2	670.4	203	51.5	424.8	1575.4	686.2	*492.4*	*148.1*	*45.7*
ES	52[a]	44.3	130.8	46	42.7	125.7	420.2	174.2	*108.8*	*62.5*	*2.8*
FI	19	5.5	62.9	18	5.4	62.6	146.7	57.9	*35.5*	*22.0*	*0.4*
FR	96[b]	64.3	420.6	79	59.2	388.6	421.5	156.2	*50.5*	*79.0*	*26.7*
HU	20	9.9	58.3	14	8.0	47.5	71.2	29.3	*20.0*	*8.6*	*0.7*
IT	110	60.8	354.7	91	55.7	327.8	582.9	258.7	*179.6*	*69.3*	*9.7*
NL	40	16.9	118.1	25	11.8	82.2	345.3	155.3	*99.5*	*40.9*	*14.9*
PL	72	38.0	182.7	57	31.2	149.9	641.8	289.0	*242.2*	*46.7*	*0.0*
RO	42	19.9	50.8	27	14.4	36.6	138.2	56.7	*39.8*	*16.8*	*-*
SE	21	9.7	82.3	21	9.7	82.3	142.7	51.9	*15.5*	*26.0*	*10.5*
UK	173	64.9	378.6	86	34.9	204.6	700.5	313.8	*234.2*	*63.2*	*16.4*
HRE4	**1140**	**445.7**	**2730.8**	**732**	**351.2**	**2124.9**	**5688.3**	**2425.8**	*1630.1*	*657.5*	*138.2*
Share [%]	**100**	**100**	**100**	**64**	**79**	**78**	**100**	**100**	*67*	*27*	*6*
EU28 (Ref.)	1328[c]	503.7	2977.4	833	393.2	2316.7	6404.6	2729.5	*1853.8*	*731.5*	*144.2*
Share of Ref.	86	88	92	88	89	92	89	89	*88*	*90*	*96*

[a] Seven Atlantic Spanish NUTS3 regions (ES703 to ES709) are here omitted.
[b] Five overseas French NUTS3 regions (FRA10, FRA20, FRA30, FRA40, and FRA50) are here omitted.
[c] Two Atlantic Portuguese NUTS3 regions (PT200 and PT300) omitted from the EU28 continental land total. Including the ES, FR, and PT omissions, the total EU28 NUTS3 region count, according to NUTS 2013 classification, would be 1342.

3.3 Heat synergy regions

When distinguished by priority groups, that is according to suitability for excess heat recoveries and heat synergy projects (as defined in Table 2.19 above), the annually available excess heat in each of the 732 considered NUTS3 regions is noticeably concentrated to the first of these groups (Priority group 1), as is visible in Table 3.3. It is apparent that close to half of the total identified excess heat volume (47%) in all of the 14 MS´s of the EU (~4.1 EJ/a), while constituting approximately only one quarter of the total heat demand (27%, ~2.0 EJ/a), is concentrated to these “very high” priority regions. This in itself should be a signal for the general viability of significantly increased efforts to recover and utilise available excess heat in high heat demand density areas.

Table 3.3. Summary of NUTS3 regions (N3R), total volumes, and relative shares of heat demands (Q_{tot}) and excess heat volumes ($E_{heat,o}$) by priority group for the 14 MS´s of the EU

Priority group	**N3R**	**Q_{tot} [TWh/a]**	**$E_{heat,o}$ [TWh/a]**	**Q_{tot} [%]**	**$E_{heat,o}$ [%]**
1	80	564	1139	27	47
2	126	648	153	30	6
3	98	173	856	8	35
4	266	432	253	20	10
0	162	308	25	15	1
HRE4	**732**	**2125**	**2426**	**100**	**100**

Similarly, and to further emphasise this, low priority regions (i.e. low (4) and no (0) priority groups), represent more than half of the total count of NUTS3 regions (266 + 162 = 428 (~58%)), while hosting only 35% of the total heat demand (20% + 15%) and no more than one tenth of the available excess heat volume (10% + 1% = 11%).

As a first order appreciation of the geographical distribution of these excess heat opportunities, the results from the spatial mapping of NUTSD3 regions by their priority group classification is presented in Figure 3.2. Due to considerable differences in NUTS3 region sizes among different MS, attention should be given to the general increase of practical possibilities for excess heat recovery as the regional sizes decreases. At smaller sizes, further, the identification of regional clusters may become relevant.

The map layer of Figure 3.2 will be uploaded and made publicly available as an operational layer in Peta4.2.

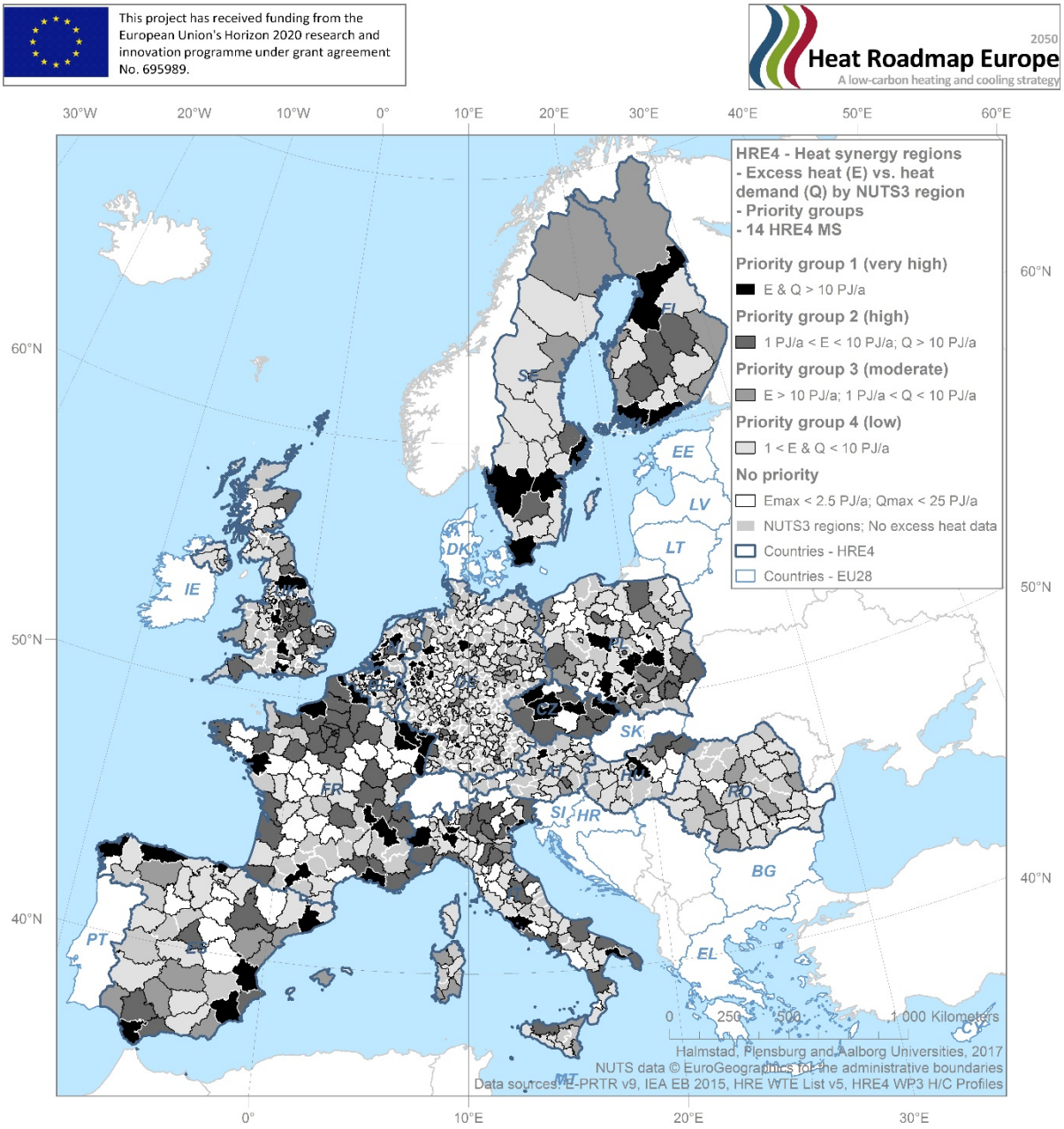

Figure 3.2. Map of heat synergy regions by five priority groups of excess heat ratio for 732 NUTS3 regions in the 14 HRE4 MS.

3.4 DHC investment costs

Finally, the national aggregates (zonal statistics as table) of the assessed hectare level heat and cold distribution capital costs for district heating and cooling networks are part of the main and essential outcomes resulting from this project phase. Calculated on the basis of the demand atlases and the investment costs theory described in above sections, and further prepared as cumulative cost curves indicating shares of total national heat markets (abscissa) at different cost levels (ordinate), these results for district heating networks may be illustrated as in Figure 3.3.

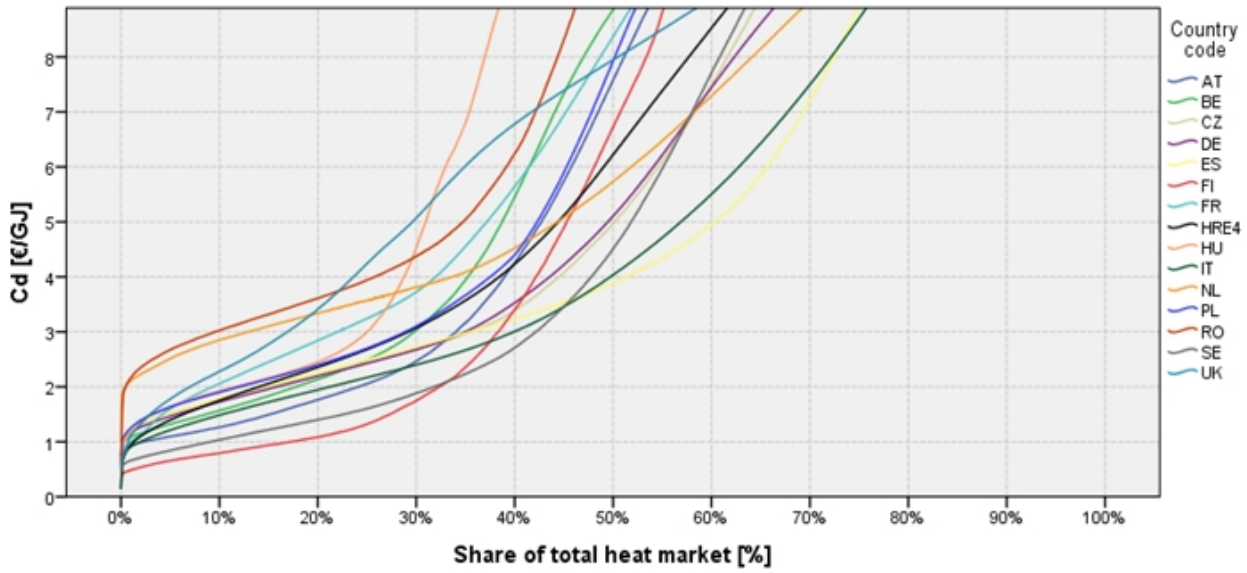

Figure 3.3. Marginal distribution capital costs levels and the corresponding district heat market shares in the 14 MS´s of the EU.

From this presentation, three distinct inferences can be made. First, heat distribution capital costs were successfully established on the hectare grid cell level for a selection representing 92% of the total EU28 building heat demand in residential and service sectors (i.e. the 14 MS´s of the EU). This in itself is a major, unprecedented research achievement that will be further elaborated in coming conference and journal papers.

Second, marginal distribution capital costs as low as below 1 €/GJ are rare but present in the study results, mainly so for high heat demand density areas in Scandinavian countries. In none of the studied countries is it feasible to expand district heating at marginal conditions beyond 20% total heat market shares at this very low cost level (the average HRE4 cost level being 2.3 €/GJ for this market share). For the same expansion level (20%), the most expensive circumstances appear in Romania (RO); 3.6 €/GJ, the United Kingdom (UK); 3.5 €/GJ, and the Netherlands (NL); 3.3 €/GJ.

Third, although national differences appear, the average grand total curve (HRE4) suggests approximately 49% district heating heat market shares at marginal cost levels of 6.0 €/GJ, which should correspond to the upper 49% share-segment of the total heat

demands specified in Table 3.1 (i.e. high heat demand density areas above 120 TJ/km² (~0.33 GWh/ha)). In energy units, this would translate into a directly feasible European district heating sector of approximately ~1350 TWh per year in terms of annual demands (49% * 9.9 EJ/a = 4.85 EJ/a), which roughly speaking represents a tripling from current levels.

Hereby, this study has developed a methodology not only to determine the distribution of heat demand both in spatial and heat demands density terms, it has further established the cost levels – and the locations of these costs – by which the corresponding share of the total heat demand could be suppled. By comparison to gross land areas of the 14 studied MS´s further, as presented in Table 3.4, it is noticeable that only 9% of this total land area constitute areas with recorded heat demands ($A_{Land,qL}$) at current conditions. In countries with relatively low population densities, like Finland, Sweden, and Spain, corresponding values are as low as a few percentages. On the other hand, in densely populated countries like the Netherlands and Belgium, one quarter of total land areas may be that of built-up heat demand areas.

Table 3.4. Total and heat demand gross land areas for the 14 MS´s of the EU

MS	**A_{Land} [Mkm²]**	**A_{Land} [Mha]**	**$A_{Land,qL}$ [Mha]**	**Share [%]**
AT	0.08	8.39	0.91	11%
BE	0.03	3.05	0.69	22%
CZ	0.08	7.89	0.86	11%
DE	0.36	35.74	5.77	16%
ES	0.51	50.59	1.55	3%
FI	0.34	33.84	0.83	2%
FR	0.63	63.32	7.95	13%
HU	0.09	9.30	0.77	8%
IT	0.30	30.21	3.96	13%
NL	0.04	4.15	1.09	26%
PL	0.31	31.27	3.68	12%
RO	0.24	23.84	1.61	7%
SE	0.44	43.86	1.36	3%
UK	0.25	24.85	2.77	11%
HRE4	**3.70**	**370.30**	**33.79**	**9%**

Finally, the deliberate reason for seeking to illustrate our current findings in the form of these aggregate national average curves, is to make them aligned and transparent to previously reported findings that used a similar disposition, see e.g. (Persson and Werner, 2011). Hereby these results are readily comparable with these and other studies pertaining to the same design format (Möller and Werner, 2015), although none of these mapped heating and cooling demand densities at the hectare level as was performed in this study.

4 Conclusions and discussion

In conclusion, this report has comprehensively described the methodologies and assumptions used in the mapping of WP2 during the first reporting period of the fourth Heat Roadmap Europe project, a work performed essentially during the period from March 2016 to August 2017. By the development, application, and use of these methods, approaches, toolboxes, datasets, and various reporting formats, the majority of topics and original research challenges included in the five work package tasks have been addressed and solved during this period.

Hereby, demand atlases (Task 2.1), including heat and cold demand densities in residential and service sectors at hectare grid cell level, have been conceived by using an enhanced demand model for the best possible representation of the spatial distribution of these demands. The assessed cooling demand distributions in both service and residential sectors deserve perhaps a special mention in this context, since they represent distinct progress in comparison to previous HRE atlases. Given the availability of proper input data, further, the enhanced Pan-European Thermal atlas (Peta4) is capable of projecting both current and future demand levels, and it has provided the core background settings for the estimations of district heating and cooling network costs, as performed in Task 2.4. Lastly, an online interactive web map application, where the corresponding demand data for each of the 14 MS´s of the EU are represented, has been arranged and is being maintained as the main results reporting format of WP2.

Resource atlases (Task 2.2), or mapping of the renewable heat resources, which is the formal task title, have been created with reference to excess heat, current district heating infrastructures, solar thermal heat, biomass residuals, and geothermal heat. For the first three of these, excess heat present in large-scale energy and industry sector facilities, district heating cities as urban morphological zones, and a candidate list of solar thermal district heating cities, quantified potential assessments have been performed. For biomass and geothermal resources (for which original data from other contemporary state-of-the-art EU projects have been incorporated), this report has settled for the visualisation of these resource categories, while their connectivity to potential district heating networks is assessable by inspection of the corresponding operational layers at the online map service.

As for heat synergy regions, or hot spots, (Task 2.3), this study has reported on an improved methodological approach compared to previous HRE assessments, by introducing the concept of priority groups. Here, all NUTS3 regions with excess heat activities currently in operation (power plants, waste incinerators, and industry) have been distinguished by their regional heat balance values (excess heat ratios) and sorted into one of five such groups, which reflect their general suitability for excess heat recovery projects. Hereby, policymakers and investors have been provided access to information on which regions where these opportunities are most palpable.

Connecting heat and cooling densities with district heating and cooling network costs (Task 2.4), has been achieved by linking the key outputs from Task 2.1, namely the demand density rasters, to the basic theoretical concepts of network investment costs by transformation of the linear heat density quantity. By advanced spatial analysis further, combining aggregated supply option totals (quantified resources of Task 2.2 and heat synergy regions of Task 2.3) and estimated investment costs, a first order assessment of the resource-efficient allocation of excess heat potentials to district energy grids has been performed. The costs for installing district heating and cooling pipelines was established for all 14 MS´s at the hectare grid cell level, which to our current knowledge is an unprecedented research achievement. The resulting output cost layers will be made available as operational layers at the online interactive map service (Peat4.2)

In terms of quantifying the potential mix of rural heating solutions (Task 2.5), which in essence truly is difficult to estimate, this report has settled for a principal sketching of the general parameters and issues associated to such estimates. A message from these investigations, with respect to heat planning and decisions of appropriate heating solutions in rural contexts, would be that heat demand density information in itself often is insufficient for proper evaluations. We conclude that also the spatial extent, i.e. the size, of rural built-up areas (and that of areas contiguous to these) needs to be recognised in such evaluations.

Finally, we would like to end this report by saying a few words on future mapping and to discuss briefly some of the approaches and findings we have presented here. In terms of future mapping within the current HRE4 project, we intend to include a model that reflects the 2050 conditions as modelled in WP6. For this purpose, it is not yet clear how to include the future spatial extent of urban areas, as well as phenomena such as urban sprawl, densification, and the ongoing process of urbanisation and the following depopulation of rural areas across Europe. There is very little knowledge available for this, and the best available point of departure may be the NUTS3 region projections of future demographics available from Eurostat. Additional input from within the project are the specific heating and cooling demands in buildings in 2050 and the total demands by sectors from WP3 (the 2050 heating and cooling profiles), as well as the feedback from the energy systems analysis in WP6.

More generally, the story of future heat mapping remains to be written. We see two clear trends: the improvement of local data by smart metering and advanced and automated surveys, which could be used for optimal designs of energy plants as an example. On the other hand, regional, national and EU-wide heat atlases will be developed that will increasingly respond to the needs of energy professionals at these levels. In this respect we recognize that continental mapping, i.e. top-down approaches as those represented in this project, and local mapping, i.e. bottom-up approaches, need and should constitute complementing perspectives in the ever-continuing charting of European heat and cold market conditions and opportunities. From a principal view point, one might say that continental mapping facilitates general understanding of

theoretical potentials, hence providing material for overviews and plausibility studies at national levels, while local mapping facilitates specific understanding of technical and economical potentials, hence supporting viability and feasibility studies at local and regional levels.

The present study has further exposed a clear interface to ongoing projects at the city level, e.g. the PlanHeat project and the Thermos project. From projects such as these, but also from a general trend to improve the mapping and the digital representation of urban areas, such as city topologies, BIM data, or 3D Modelling (CityGML), we further expect better and extended databases for the formulation of heating and cooling supply strategies in the future.

We would like to stress here, however, that the primary objective of the HRE4 project is to provide analyses and mapping, which work for all EU MS´s, and for cities, towns and rural areas at the same time. This covering analytical approach will have to do with the least common denominator in available data to be time- and cost effective. At the same time, we are confident that publicly available data from authoritative sources improves all the time, as we have seen in the development of population raster data in the past years. By making use of those, more resources can be put in the establishment, the continuous improvement and the quality control of such data, which eventually will form the common basis for an EU-wide information basis for energy planning and management.

5 References

BBR (n.d.). Bygnings- and Boligregisteret (Danish Register of Buildings and Dwellings). Retrieved 2017-04-17 from www.bbr.dk.

BROBERG, S., BACKLUND, S., KARLSSON, M. & THOLLANDER, P. 2012. Industrial excess heat deliveries to Swedish district heating networks: Drop it like it's hot. *Energy Policy,* 51**,** 332-339.

BRUECKNER, S., MIRÓ, L., CABEZA, L. F., PEHNT, M. & LAEVEMANN, E. 2014. Methods to estimate the industrial waste heat potential of regions – A categorization and literature review. *Renewable and Sustainable Energy Reviews,* 38**,** 164-171.

CEWEP. 2014. *Country Reports: 2010 Country Report on Waste Management* [Online]. Confederation of European Waste-to-Energy Plants. Available at: (http://www.cewep.eu/information/data/subdir/442._Country_Report_on_Waste_Management.html). [Accessed].

CONNOLLY, D., HANSEN, K., DRYSDALE, D., LUND, H., VAD MATHIESEN, B., WERNER, S., PERSSON, U., MÖLLER, B., GARCIA WILKE, O., BETTGENHÄUSER, K., POUWELS, W., BOERMANS, T., NOVOSEL, T., KRAJAČIĆ, G., DUIĆ, N., TRIER, D., MØLLER, D., ODGAARD, A. M. & LAURBERG JENSEN, L. 2014a. Enhanced Heating and Cooling Plans to Quantify the Impact of Increased Energy Efficiency in EU Member States. Translating the Heat Roadmap Europe Methodology to Member State Level. Work Package 2. Main Report: Executive Summary. Stratego: Enhanced Heating and Cooling Plans. Project No: IEE/13/650. Available at (2015-09-10): (http://heatroadmap.eu/resources/STRATEGO/STRATEGO%20WP2%20-%20Executive%20Summary%20%26%20Main%20Report.pdf).

CONNOLLY, D., LUND, H., MATHIESEN, B. V., WERNER, S., MÖLLER, B., PERSSON, U., BOERMANS, T., TRIER, D., ØSTERGAARD, P. A. & NIELSEN, S. 2014b. Heat Roadmap Europe: Combining district heating with heat savings to decarbonise the EU energy system. *Energy Policy,* 65**,** 475-489.

CONNOLLY, D., VAD MATHIESEN, B., ALBERG ÖSTERGAARD, P., MÖLLER, B., NIELSEN, S., LUND, H., PERSSON, U., WERNER, S., GRÖZINGER, J., BOERMANS, T., BOSQUET, M. & TRIER, D. 2013. Heat Roadmap Europe 2050 - Second pre-study for EU27. Euroheat & Power, Brussels. Available at: (http://www.euroheat.org/Heat-Roadmap-Europe-165.aspx).

CONNOLLY, D., VAD MATHIESEN, B., ALBERG ÖSTERGAARD, P., MÖLLER, B., NIELSEN, S., LUND, H., PERSSON, U., WERNER, S., NILSSON, D. & TRIER, D. 2012. Heat Roadmap Europe 2050 - First pre-study for EU27. Brussels. Available at: (http://www.euroheat.org/Heat-Roadmap-Europe-165.aspx): Euroheat & Power.

CORNELIS, E., HOLM, A. B., LAUERSEN, B. & LYGNERUD, K. 2016. Summary Report on WP3. Insights from drafting local heating and cooling action plans. WP3: National plan – local action: supporting local authorities. Deliverable 3.d (former Deliverable 3.7). Stratego: Enhanced Heating and Cooling Plans. Project No: IEE/13/650. Available at (2017-08-15): http://stratego-project.eu/wp-content/uploads/2016/11/D3.d-WP3-Final-Report-1.pdf.

DALIN, P., NILSSON, J. & RUBENHAG, A. 2005. Ecoheatcool. Work Package 2. The European Cold Market. Final Report. Brussels. Available at (2015-01-22): (http://www.euroheat.org/files/filer/ecoheatcool/documents/Ecoheatcool_WP2_Web.pdf).

DITTMANN, F., RIVIÈRE, P., STABAT, P., PAARDEKOOPER, S. & CONNOLLY, D. 2017. Space Cooling Technology in Europe: Technology Data and Demand Modelling. Deliverable No. D 3.2: Cooling Technology datasheets. Heat Roadmap Europe 2050, A low-carbon heating and cooling strategy.

DUMAS, P. & BARTOSIK, A. 2014. GeoDH: Geothermal DH Potential in Europe. Geo-DH project (Promote Geothermal District Heating Systems in Europe). Intelligent Energy Europe Programme. Available at (2017-08-27): http://geodh.eu/wp-content/uploads/2014/11/GeoDH-Report-D-2.2-final.pdf.

EEA 2014. Degree of soil sealing (2014-11-13). European Environment Agency. Available at (2016-11-12): https://www.eea.europa.eu/data-and-maps/data/eea-fast-track-service-precursor-on-land-monitoring-degree-of-soil-sealing#tab-european-data.

EEA. 2016a. *The European Pollutant Release and Transfer Register (E-PRTR). Downloaded data category (2016-06-19): eprtr_v9_mdb.zip* [Online]. European Environment Agency, Copenhagen. [Accessed].

EEA. 2016b. *Urban Morphological Zones 2006 (UMZ2006). Downloaded data category (2016-12-11): UMZ2006_f3v0_raster, UMZ2006_f3v0_vector, and UMZ2006_sqlite* [Online]. European Environment Agency, Copenhagen. [Accessed].

EEA. 2017a. *Corine Land Cover 2006* [Online]. European Environment Agency, Copenhagen. Available at (2017-08-10): https://www.eea.europa.eu/data-and-maps/data/corine-land-cover-2006-raster-2#tab-metadata. [Accessed].

EEA. 2017b. *Corine Land Cover 2012* [Online]. European Environment Agency, Copenhagen. Available at (2017-04-20): http://land.copernicus.eu/pan-european/corine-land-cover/clc-2012. [Accessed].

ENERGISTYRELSEN 2012. Individual Heating Plants and Energy Transport: Technology Data for Energy Plants, May 2012. Energistyrelsen (Danish Energy Agency).

ERIKSSON, L., MORANDIN, M. & HARVEY, S. 2015. Targeting capital cost of excess heat collection systems in complex industrial sites for district heating applications. *Energy,* 91**,** 465-478.

ES 2011. Eurostat Census Hub. Population and housing census. Eurostat. Luxembourg. Retrieved 2017-03-02 from http://ec.europa.eu/eurostat/web/population-and-housing-census/census-data/2011-census.

ES 2015. Map 1: Resident population in Urban Audit core cities, 1 January 2012. Eurostat Regional Yearbook 2015. Chapter 15 - European cities. Download date: 2017-01-16. Eurostat. Luxembourg. .

ES 2016. Population on 1 January by broad age group, sex and NUTS 3 region [demo_r_pjanaggr3]. Last update: 2016-08-05. Download date: 2016-08-16. Eurostat. Luxembourg. .

EU 2006. Regulation (EC) No 166/2006 of 18 January concerning the establishment of a European Pollutant Release and Transfer Register and amending Council Directives 91/689/EEC and 96/61/EC. Brussels: European Parliament and the Council.

FLEITER, T., ELSLAND, R., REHFELDT, M., STEINBACH, J., REITER, U., CATENAZZI, G., JAKOB, M., RUTTEN, C., HARMSEN, R., DITTMANN, F., RIVIÈRE, P. & STABAT, P. 2017. D3.1 Profile of heating and cooling demand in 2015. Heat Roadmap Europe 2050, A low-carbon heating and cooling strategy.

FREDERIKSEN, S. & WERNER, S. 2013. *District Heating and Cooling*, Studentlitteratur AB, Lund.

GEODH 2014. Manual on the use of the web-map service. Geo-DH project (Promote Geothermal District Heating Systems in Europe). Intelligent Energy Europe Programme.

GEODH. 2017. *GeoGH: Geothermal district heating* [Online]. Available at (2017-08-27): http://geodh.eu/. [Accessed].

GILS, H. C. 2012. A GIS-based Assessment of the District Heating Potential in Europe. *12th Symposium Energieinnovation, 15-17 Feb.* Graz, Austria. .

HUDHC_V5 2016. Halmstad University District Heating and Cooling Database_version 5 (2016 update). Halmstad University, Sweden.

IEA-SHC-T52. 2017. *Task 52 – Solar Heat and Energy Economics in Urban Environments. Solar Heating & Cooling Programme, International Energy Agency* [Online]. Available (2017-08-06): http://task52.iea-shc.org/description. [Accessed].

IEA-SHC. 2011. *Common Calculation Method: Solar Collector Energy Output* [Online]. Solar Heating & Cooling Programme, International Energy Agency. Available (2017-08-13): http://www.iea-shc.org/common-calculation-method. [Accessed].

IEA-SHC. 2017. *Solar Heating & Cooling Programme, International Energy Agency* [Online]. Available (2017-08-06): http://www.iea-shc.org/ [Accessed].

IEA 2014. Energy Balances of OECD and Non-OECD Countries (2014 Edition). Summary Energy Balances. Paris: International Energy Agency.

IEA 2016a. Energy Balances of OECD and Non-OECD Countries (2015 Edition). Extended Energy Balances. Paris: International Energy Agency.

IEA 2016b. Energy Balances of OECD and Non-OECD Countries (2015 Edition). Summary Energy Balances. Paris: International Energy Agency.

IPCC 2006. 2006 IPCC Guidelines for National Greenhouse Gas Inventories. Prepared by the National Greenhouse Gas Inventories Programme, Eggleston H.S., Buendia L., Miwa K., Ngara T. and Tanabe K. Published: IGES, Japan.

ISWA 2012. Waste-to-Energy: State-of-the-Art-Report, Statistics, 6th Edition, August 2012. International Solid Waste Association. .

IVNER, J. & BROBERG VIKLUND, S. 2015. Effect of the use of industrial excess heat in district heating on greenhouse gas emissions: A systems perspective. *Resources, Conservation and Recycling,* 100**,** 81-87.

JRC 2017a. European Settlement Map (ESM). Joint Research Centre, Institute for the Protection and Security of the Citizen, Global Security and Crisis Management Unit. European Commission, Brussels. Retrieved 2017-07-21 from http://land.copernicus.eu/pan-european/GHSL/EU%20GHSL%202014.

JRC 2017b. Ground-station based solar radiation data. Downloaded dataset (2017-01-13): hor_rad_PVGIS_classic_year_latlon. Joint Research Center, Institute for Energy and Transport (IET), European Commission.

JRC 2017c. Joint Research Centre Data Catalogue: GHS population grid, derived from EUROSTAT census data (2011) and ESM 2016. Joint Research Centre. European Commission, Brussels. Retrieved 2017-07-13 from http://data.jrc.ec.europa.eu/dataset/jrc-ghsl-ghs_pop_eurostat_europe_r2016a.

MAUTHNER, F. & HERKEL, S. 2017. Technology and Demonstrators. Technical Report Subtask C - Part C1. IEA-SHC-Task 52 Solar Heat and Energy Economics in Urban Environments. Solar Heating & Cooling Programme, International Energy Agency.

MIRÓ, L., BRUECKNER, S., MCKENNA, R. & CABEZA, L. F. 2016. Methodologies to estimate industrial waste heat potential by transferring key figures: A case study for Spain. *Applied Energy,* 169**,** 866-873.

MORANDIN, M., HACKL, R. & HARVEY, S. 2014. Economic feasibility of district heating delivery from industrial excess heat: A case study of a Swedish petrochemical cluster. *Energy,* 65**,** 209-220.

MÖLLER, B. 2008. A heat atlas for demand and supply management in Denmark. *Manag. of Environ. Qual.: An Int. J.,* 19**,** 467 - 479.

MÖLLER, B. & NIELSEN, S. 2014. High resolution heat atlases for demand and supply mapping. *Int. J. of Sustain. Energy Plan. and Manag.,* Issue 1. In press.

MÖLLER, B. & WERNER, S. 2015. Quantifying the Potential for District Heating and Cooling in EU Member States. Work package 2. Background report 6. Deliverable No. D 2.2. Stratego: Multi-level actions for enhanced Heating & Cooling plans.

NÁDOR, A., ZILAHI-SEBESS, L., SZEILER, R., SIMÓ, B., HOFMEISTER, M. & DUMAS, P. 2013. Matching geothermal potential and heat demand of Europe: the web-map tool of the Geo-DH project to promote geothermal district heating. *European Geothermal Congress 2013. Pisa, Italy, 3-7 June 2013.*

NIELSEN, J. E. & BATTISTI, R. 2012. Solar district heating guidelines: Feasibility study. Fact sheet 2.3, version id: 2.3-6. Solar District Heating (SDH). Available at (2017-08-11): http://solar-district-heating.eu/Portals/0/Factsheets/SDH-WP3_FS-2-3_FeasibilityStudy_version6.pdf.

OSM 2017. OpenStreetMap. Available at (2017-04-17): http://www.openstreetmap.org.

PERSSON, U. 2015a. *District heating in future Europe: Modelling expansion potentials and mapping heat synergy regions.* Energy and Environment, Chalmers University of Technology.

PERSSON, U. 2015b. Quantifying the Excess Heat Available for District Heating in Europe. Work Package 2. Background Report 7. Stratego: Enhanced Heating and Cooling Plans. Project No: IEE/13/650. Available at (2017-08-15): http://stratego-

project.eu/wp-content/uploads/2014/09/STRATEGO-WP2-Background-Report-7-Potenital-for-Excess-Heat.pdf

PERSSON, U., MÖLLER, B. & WERNER, S. 2014. Heat Roadmap Europe: Identifying strategic heat synergy regions. *Energy Policy,* 74**,** 663-681.

PERSSON, U., MÖLLER, B. & WIECHERS, E. 2017a. Maps manual for lead-users. WP2 – GIS mapping of heating and cooling within the 14 MS´s in the EU. Deliverable D.2.4. Heat Roadmap Europe 2050, A low-carbon heating and cooling strategy [to be published...].

PERSSON, U., MÖLLER, B., WIECHERS, E. & GRUNDAHL, L. 2017b. Map of the heat synergy regions and the cost to expand district heating and cooling in all 14 MS: Accessing the outputs of D2.2. Heat Roadmap Europe 2050, A low-carbon heating and cooling strategy.

PERSSON, U., MÖLLER, B., WIECHERS, E., GRUNDAHL, L. & CONNOLLY, D. 2016. Demand and Resource Atlases for all 14 MS: Accessing the outputs of D2.1. Heat Roadmap Europe 2050, A low-carbon heating and cooling strategy.

PERSSON, U. & WERNER, S. Effective Width - The Relative Demand for District Heating Pipe Lengths in City Areas. The 12th International Symposium on District Heating and Cooling, 2010 5th to 7th of September, Tallin. 128-131.

PERSSON, U. & WERNER, S. 2011. Heat distribution and the future competitiveness of district heating. *Applied Energy,* 88**,** 568-576.

PERSSON, U. & WERNER, S. 2012. District heating in sequential energy supply. *Applied Energy,* 95**,** 123-131.

PETA4. 2017. *Pan-European Thermal Atlas 4 (Peta4)* [Online]. Europa-Universität Flensburg, ArcGIS Online. Heat Roadmap Europe - A low-carbon heating and cooling strategy for Europe. Available at (2017-08-25): http://heatroadmap.eu/Peta4.php [Accessed].

PLANENERGI 2016. Trends in the deployment of solar district heating in Denmark: Identification of factors with impact on the development - An input for subtask C. Task 52 – Solar Heat and Energy Economics in Urban Environments. Solar Heating & Cooling Programme, International Energy Agency. (Internal project draft, June 2016, not published). Copenhagen.

PLANHEAT. 2017. *Planheat* [Online]. Funded by the European Union's H2020 Programme under grant agreement 723757. Available at (2017-08-27): http://planheat.eu/. [Accessed].

PUDELKO, R., BORZECKA-WALKER, M. & FABER, A. 2013. The feedstock potential assessment for EU-27 + Switzerland in NUTS-3. D1.2_v1.0. BioBoost: Biomass based energy intermediates boosting biofuel production. Co-funded by the European Commission FP7, Directorate-General for Transport and Energy. Grant No. 282873.

SANDVALL, A. F., BÖRJESSON, M., EKVALL, T. & AHLGREN, E. O. 2015. Modelling environmental and energy system impacts of large-scale excess heat utilisation – A regional case study. *Energy,* 79**,** 68-79.

SCB. 2017a. *Entreprenadindex för husbyggnad och anläggning (Entrepreneur index for buildning construction and premises)* [Online]. Sveriges Byggindustrier (Swedish

Construction Industries). Statistiska centralbyrån (SCB) (Central Statistical Agency). [Accessed].

SCB. 2017b. *Nya Entreprenadindex med bas januari 2011 och E84 (New Entrepreneur index with bases January 2011 and E84)* [Online]. Sveriges Byggindustrier (Swedish Construction Industries). Statistiska centralbyrån (SCB) (Central Statistical Agency). Available at (2017-08-29): http://www.byggindex.scb.se/art6.html. [Accessed].

SCOTTISH-GOVERNMENT 2014. Scotland Heat Map - User guide: 2.1 Manual. Version 1.0. Heat, Energy Efficiency and Low Carbon Investment, Energy & Climate Change Directorate, Scottish Government. Edinburgh. Available at (2017-08-15): http://www.gov.scot/Resource/0048/00489200.pdf.

SCOTTISH-GOVERNMENT. 2017. *Scotland Heat Map* [Online]. Heat, Energy Efficiency and Low Carbon Investment, Energy & Climate Change Directorate, Scottish Government. Edinburgh. Available at (2017-08-15): http://heatmap.scotland.gov.uk/. [Accessed].

SDH-DATASET 2016. European Large-Scale Solar Heating Networks. *WG 2E Solar District Heating - ESTTP/SDHTO, ELSSHN/ESTTP.* Internal database, not published. Solar District Heating.

SDH. 2017. *Solar District Heating* [Online]. Available (2017-08-06): http://solar-district-heating.eu/. [Accessed].

SDHA 2007. Kulvertkostnadskatalog (The district heating pipe cost catalogue). Report 2007:1. The Swedish District Heating Association, Stockholm.

SDHP2M 2016. Supplying Renewable zero-emission heat. Solar District Heating, Solites.

SRB 2017. Ackumulerat årsgenomsnitt 2015 (januari - december): SEK/EUR. (Accumulated annual average 2015 (January - December): SEK/EUR). Sveriges Riksbank (Swedish National Bank).

STRATEGO. 2014. *Stratego - Enhanced heating & cooling plans* [Online]. Web page available at (2014-10-29): (http://stratego-project.eu/). [Accessed].

THERMOS. 2017. *THERMOS: Thermal Energy Resource Modelling and Optimisation System* [Online]. Funded by EU Horizon 2020. Available at (2017-08-27): https://www.thermos-project.eu/home/. [Accessed].

UNEP/DEWA/GRID 2012. UNEP/DEWA/GRID-Geneva. Gross Domestic Product 2010. United Nations Environment Programme (UNEP). Retrieved 2017-05-29 from http://preview.grid.unep.ch/index.php?preview=data&events=socec&evcat=1&lang=eng.

WERNER, S. 2006a. ECOHEATCOOL: The European Heat Market. Available: http://www.euroheat.org/ecoheatcool.

WERNER, S. 2006b. The New European Heating Index. *10th International Symposium on District heating and Cooling.* Hannover, Germany. .

WERNER, S. 2016. European space cooling demands. *Energy,* 110**,** 148-156.

6 Appendices

6.1 Regional data

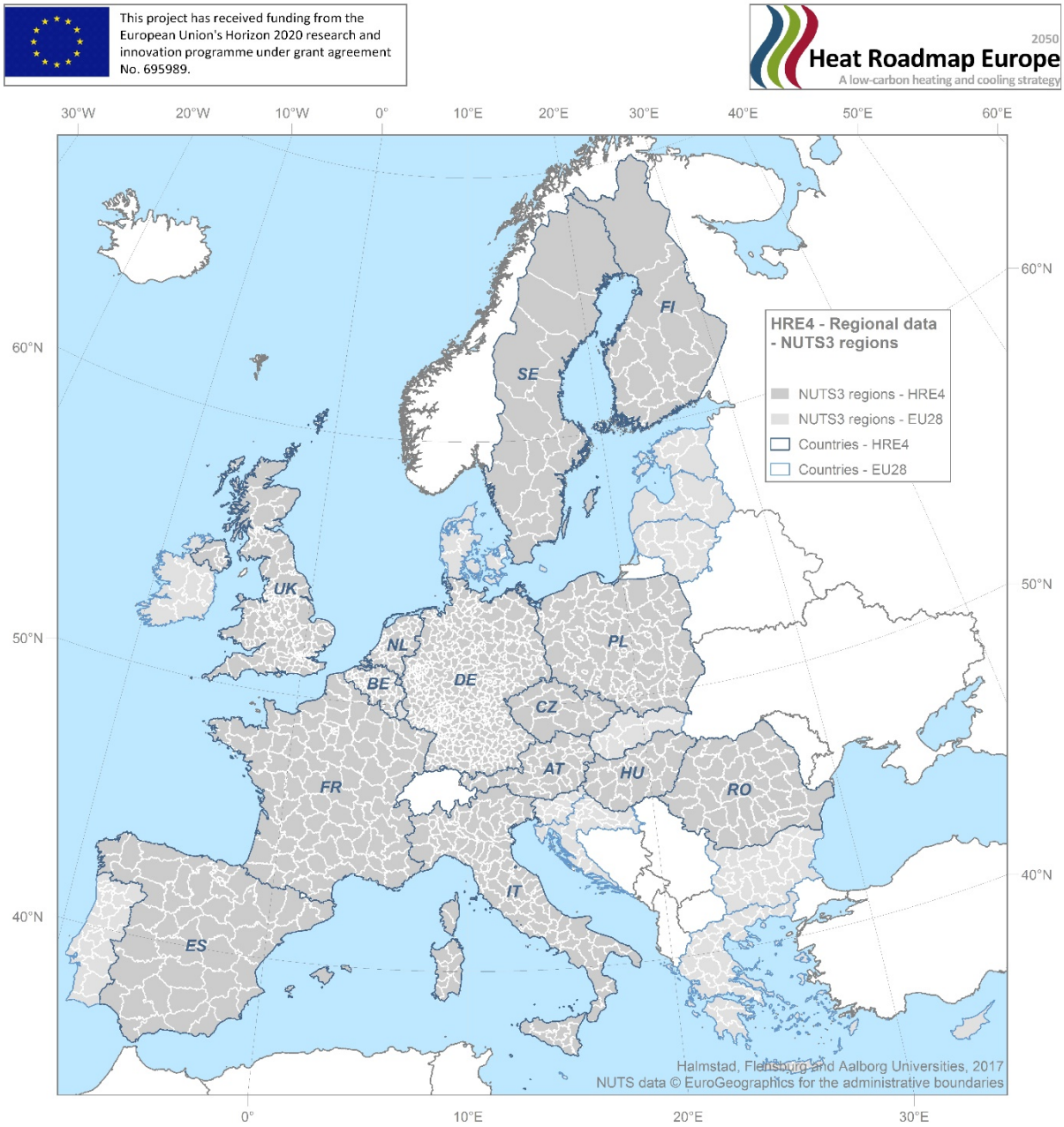

Figure 6.1. Map of the 1140 continental NUTS3 regions present in the 14 MS´s of the EU. Note that seven Atlantic Spanish (ES703 to ES709) and five overseas French NUTS3 regions (FRA10, FRA20, FRA30, FRA40, and FRA50) are excluded in the assessments.

6.2 European Cooling Index

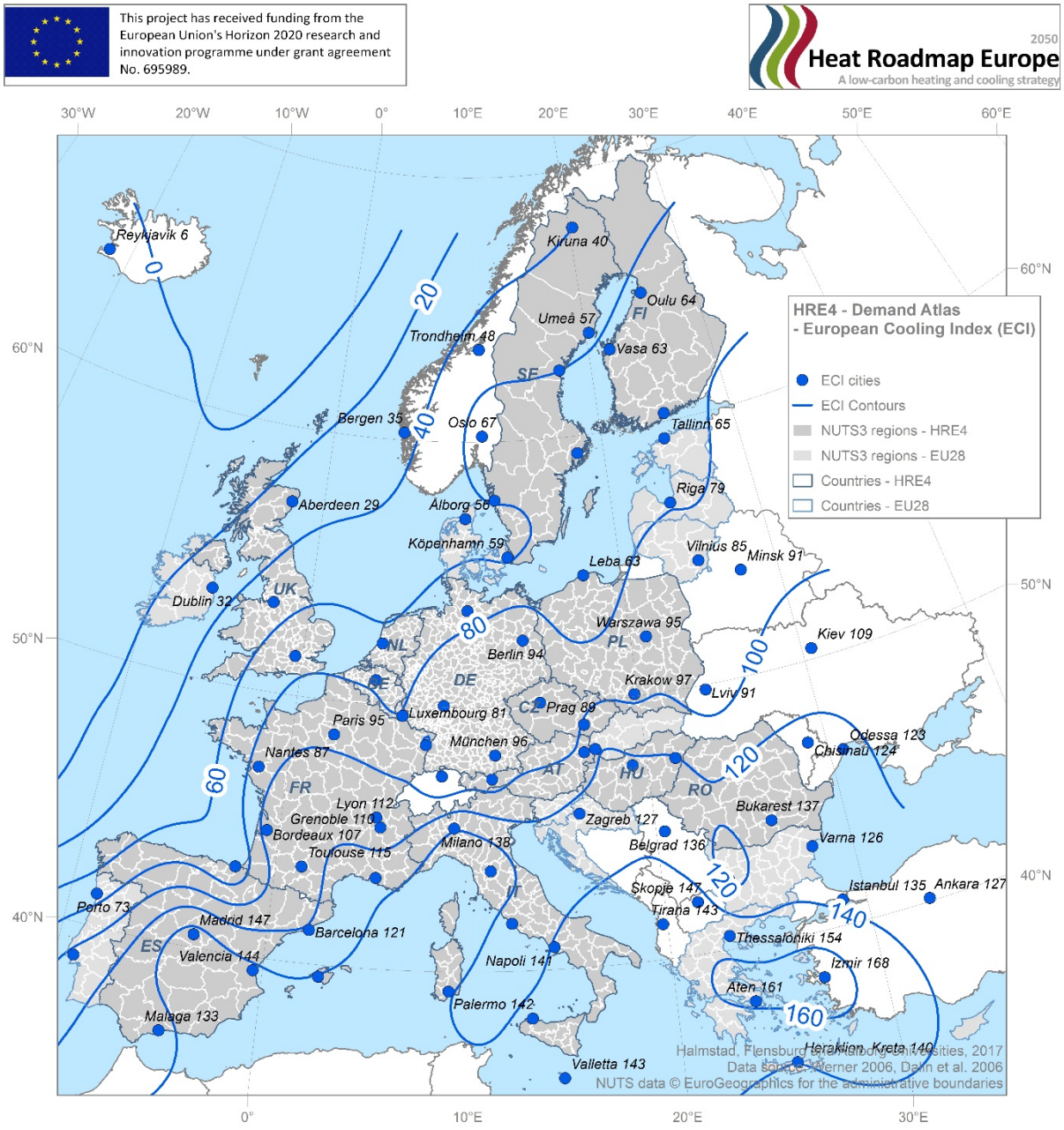

Figure 6.2. European Cooling Index (ECI) values for 80 different locations in Europe and corresponding contour lines established by spatial interpolation. Sources: (Dalin et al., 2005, Werner, 2006b)

6.3 Heat demand density classes

Table 6.1. Heat demand density classification by which to model the choice of heat supply solutions in urban versus rural areas. Sources: concluded from (Energistyrelsen, 2012)

Class	HD [GJ/ha]	HD [TJ/km²]	Meaning
NoData	0 - 200	0 - 20	Rural heat demand
0	200 – 500	20 – 50	Guide for district heating in new buildings
1	500 – 1200	50 – 120	Guide for low temperature district heating in existing buildings
2	1200 - 3000	120 - 300	Guide for conventional district heating in existing buildings
3	3000 - …	300 - …	Guide for obvious potential to develop district heating

6.4 Regional biomass availability maps

This project has received funding from the European Union's Horizon 2020 research and innovation programme under grant agreement No. 695989.

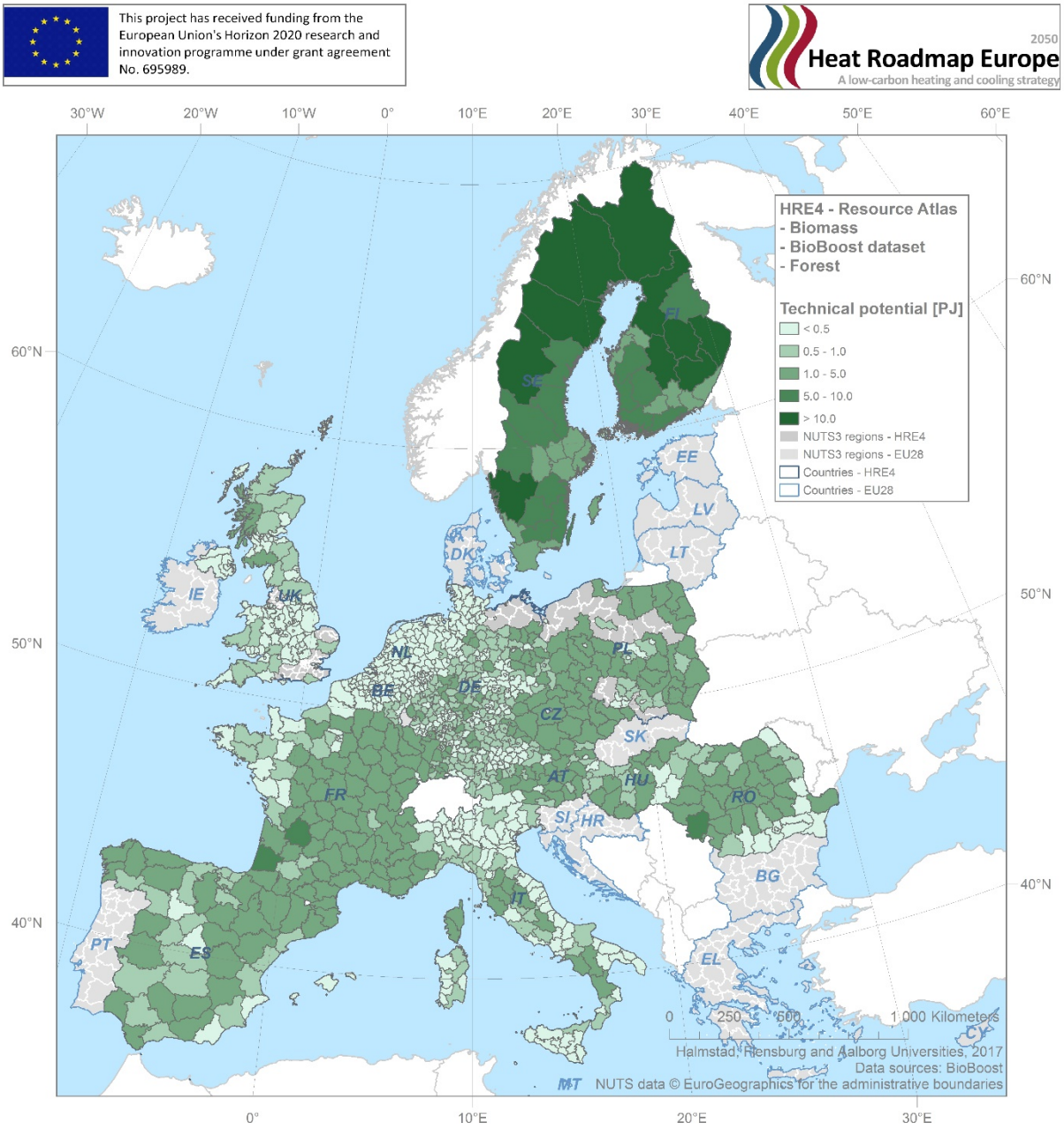

Figure 6.3. BioBoost NUTS3 region data on annual technical potential for forest residues among the 14 MS´s of the EU. Source: (Pudelko et al., 2013).

This project has received funding from the European Union's Horizon 2020 research and innovation programme under grant agreement No. 695989.

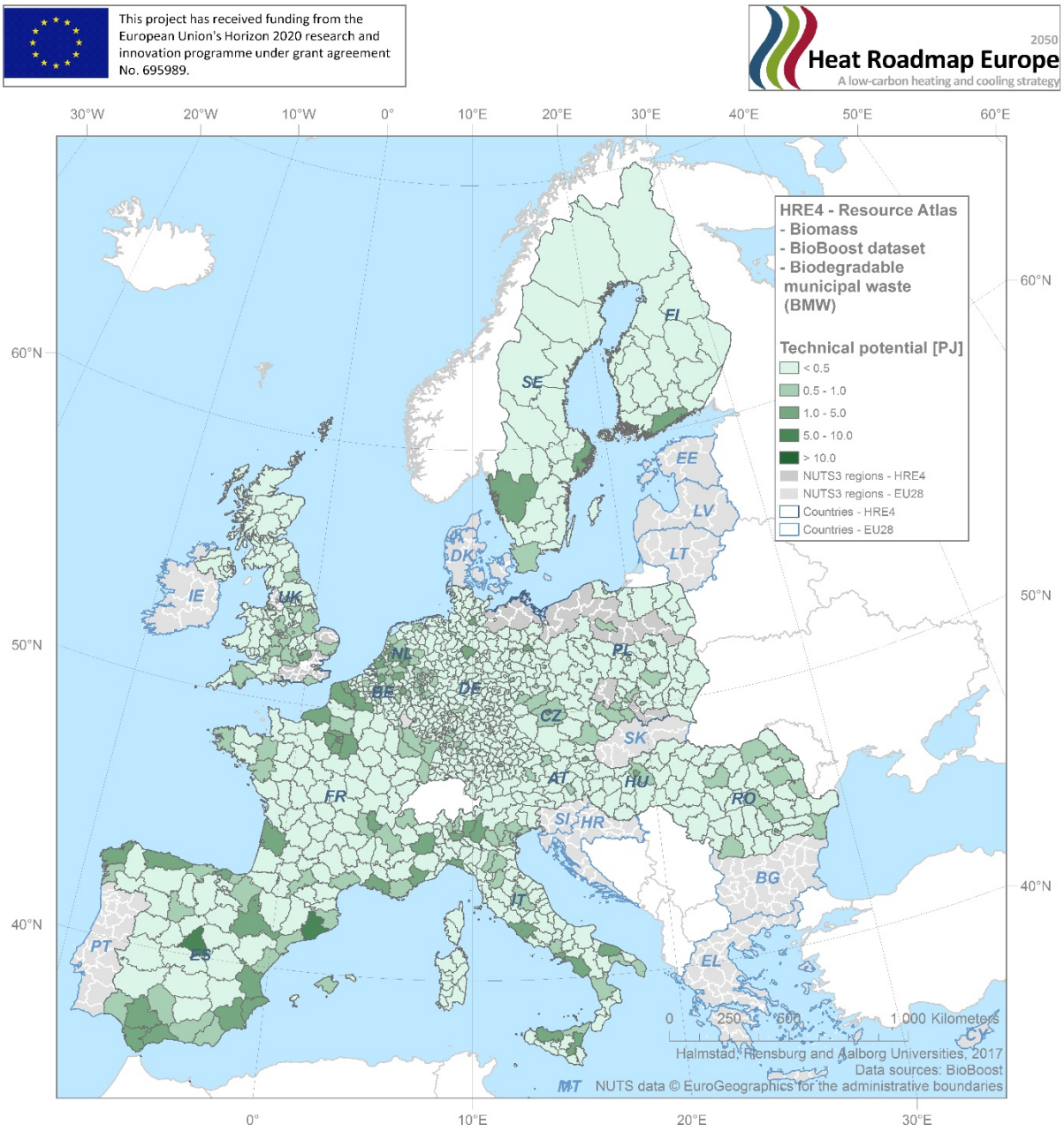

Figure 6.4. BioBoost NUTS3 region data on annual technical potential for biodegradable municipal waste (BMW) among the 14 MS´s of the EU. Source: (Pudelko et al., 2013).

This project has received funding from the European Union's Horizon 2020 research and innovation programme under grant agreement No. 695989.

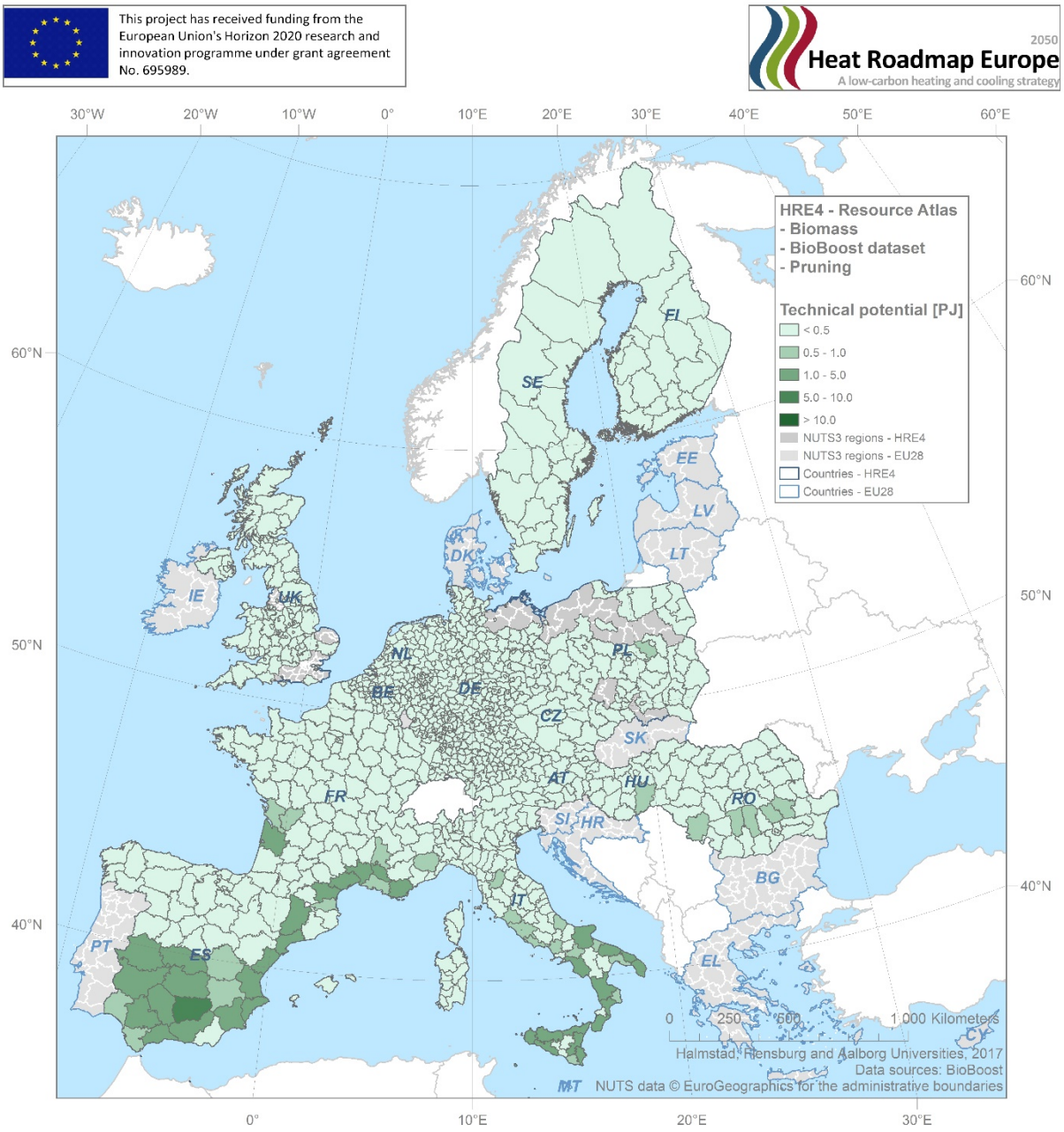

Figure 6.5. BioBoost NUTS3 region data on annual technical potential for pruning among the 14 MS´s of the EU. Source: (Pudelko et al., 2013).

6.5 Heat synergy regions by MS

Table 6.2. Detailed summary of NUTS3 regions (N3R) and total volumes of heat demands (Q_{tot}) and excess heat volumes ($E_{heat,o}$) by priority group for each of the 14 MS´s of the EU

MS / Priority group	N3R	Qtot,N3R [TWh / a]	Eheat,o [TWh / a]
AT	**20**	**48**	**38**
0	4	5	1
1	2	18	16
2	1	3	2
3	3	6	12
4	10	16	8
BE	**31**	**78**	**68**
0	10	19	1
1	4	19	46
2	4	23	5
4	13	17	16
CZ	**14**	**66**	**90**
0	2	6	0
1	4	24	71
2	7	34	11
3	1	2	8
DE	**203**	**425**	**686**
0	56	83	9
1	16	110	301
2	13	61	14
3	28	44	284
4	90	126	77
ES	**46**	**126**	**174**
0	10	9	2
1	7	40	81
2	5	38	7
3	9	15	67
4	15	24	17
FI	**18**	**63**	**58**
1	3	28	27
2	3	12	5
3	6	13	23
4	6	10	4
FR	**79**	**389**	**156**
0	20	52	2
1	11	102	108
2	34	207	35
4	14	27	11
HU	**14**	**47**	**29**
0	3	8	0
1	1	7	4
2	3	18	5
3	1	2	11
4	6	13	8
IT	**91**	**328**	**259**
0	19	55	3
1	6	72	86
2	22	122	30
3	13	25	115
4	31	54	25
NL	**25**	**82**	**155**
0	6	15	1
1	6	36	101
2	3	16	4
3	5	7	43
4	5	8	7
PL	**57**	**150**	**289**
0	11	23	2
1	10	37	193
2	12	39	16
3	7	15	57

4	17	37	21
RO	**27**	**37**	**57**
0	3	2	1
1	1	5	3
3	6	8	36
4	17	22	17
SE	**21**	**82**	**52**
1	4	46	22
2	2	6	3
3	2	5	9
4	13	26	17
UK	**86**	**205**	**314**
0	18	32	3
1	5	18	78
2	17	69	16
3	17	32	191
4	29	53	26
HRE4	**732**	**2125**	**2426**

6.6 DH investment cost maps

This project has received funding from the European Union's Horizon 2020 research and innovation programme under grant agreement No. 695989.

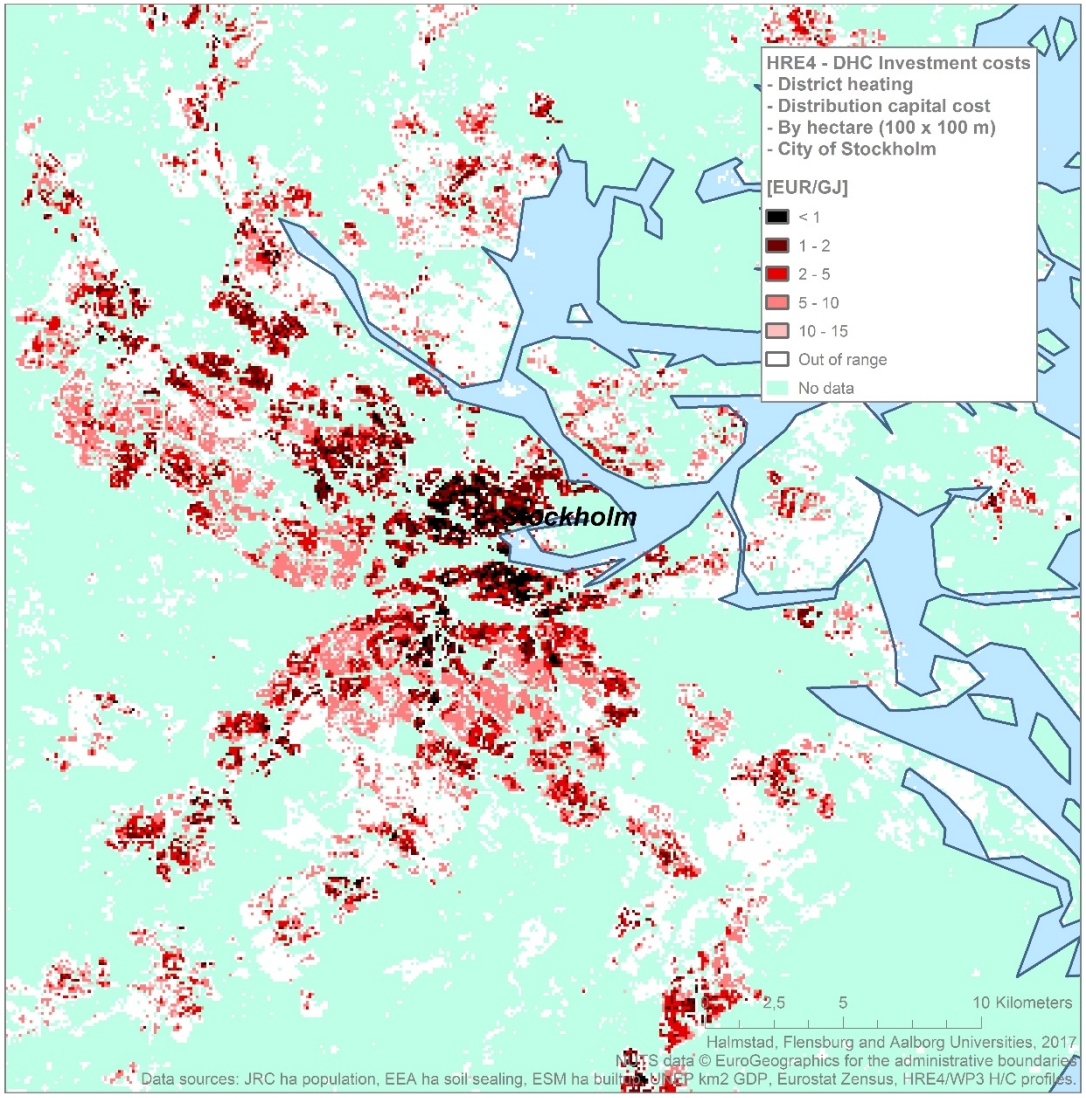

Figure 6.6. Close-up map of marginal distribution capital costs for district heating pipe networks by hectare grid cells; Case study example for the city of Stockholm in Sweden.

This project has received funding from the European Union's Horizon 2020 research and innovation programme under grant agreement No. 695989.

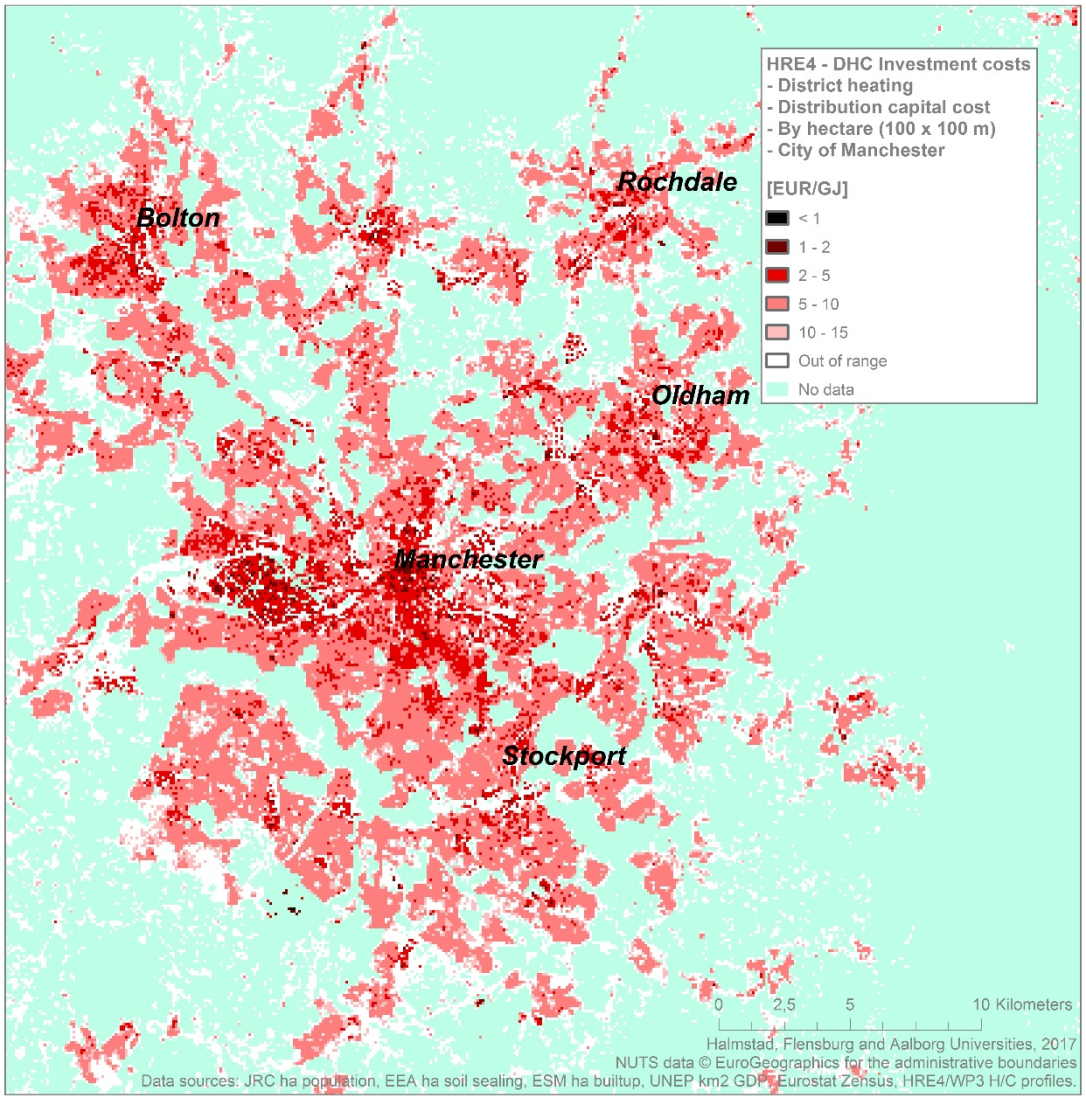

Figure 6.7. Close-up map of marginal distribution capital costs for district heating pipe networks by hectare grid cells; Case study example for the city of Manchester in the United Kingdom.

This project has received funding from the European Union's Horizon 2020 research and innovation programme under grant agreement No. 695989.

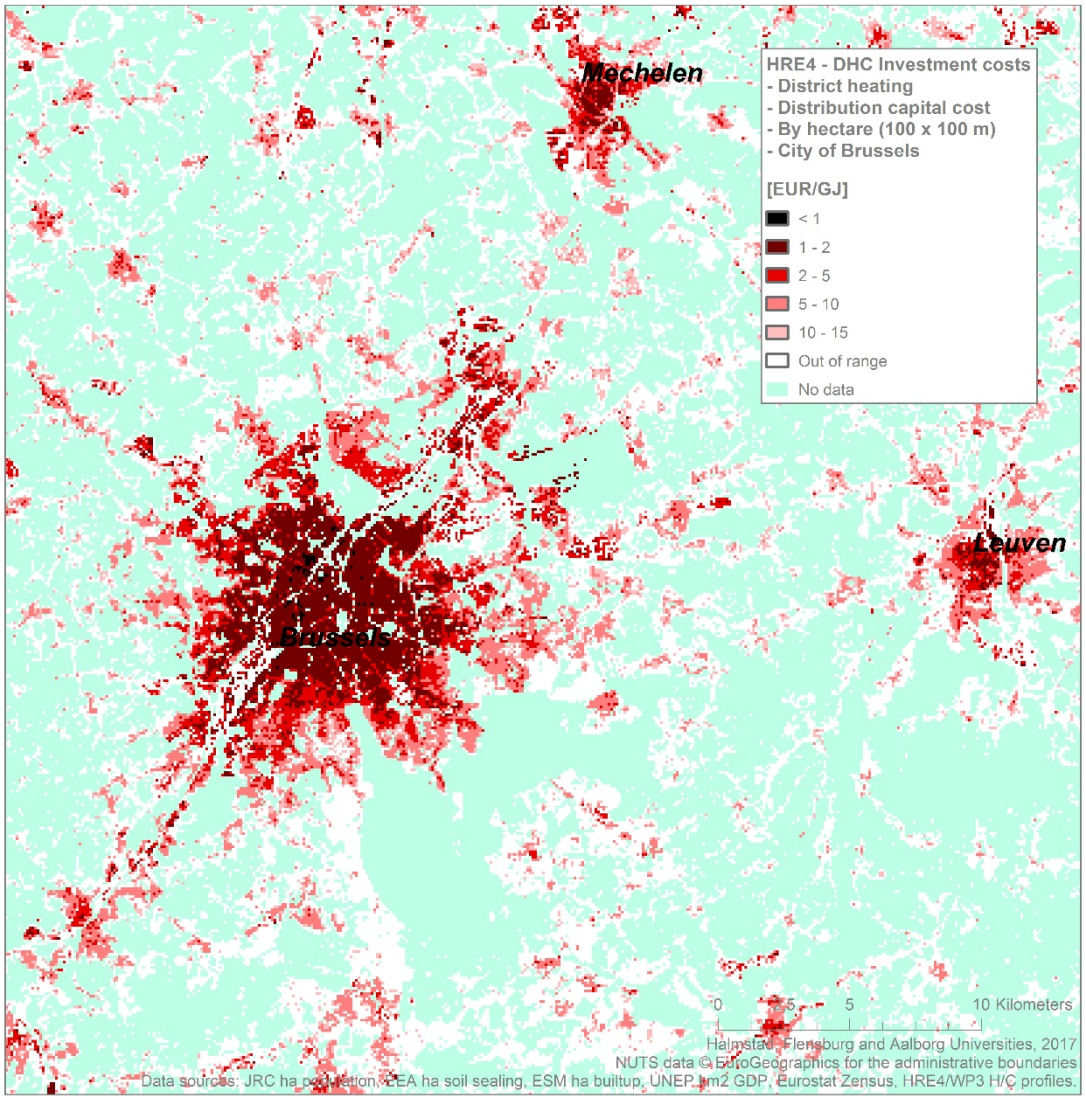

Figure 6.8. Close-up map of marginal distribution capital costs for district heating pipe networks by hectare grid cells; Case study example for the city of Brussels in Belgium.

6.7 DC investment cost maps

This project has received funding from the European Union's Horizon 2020 research and innovation programme under grant agreement No. 695989.

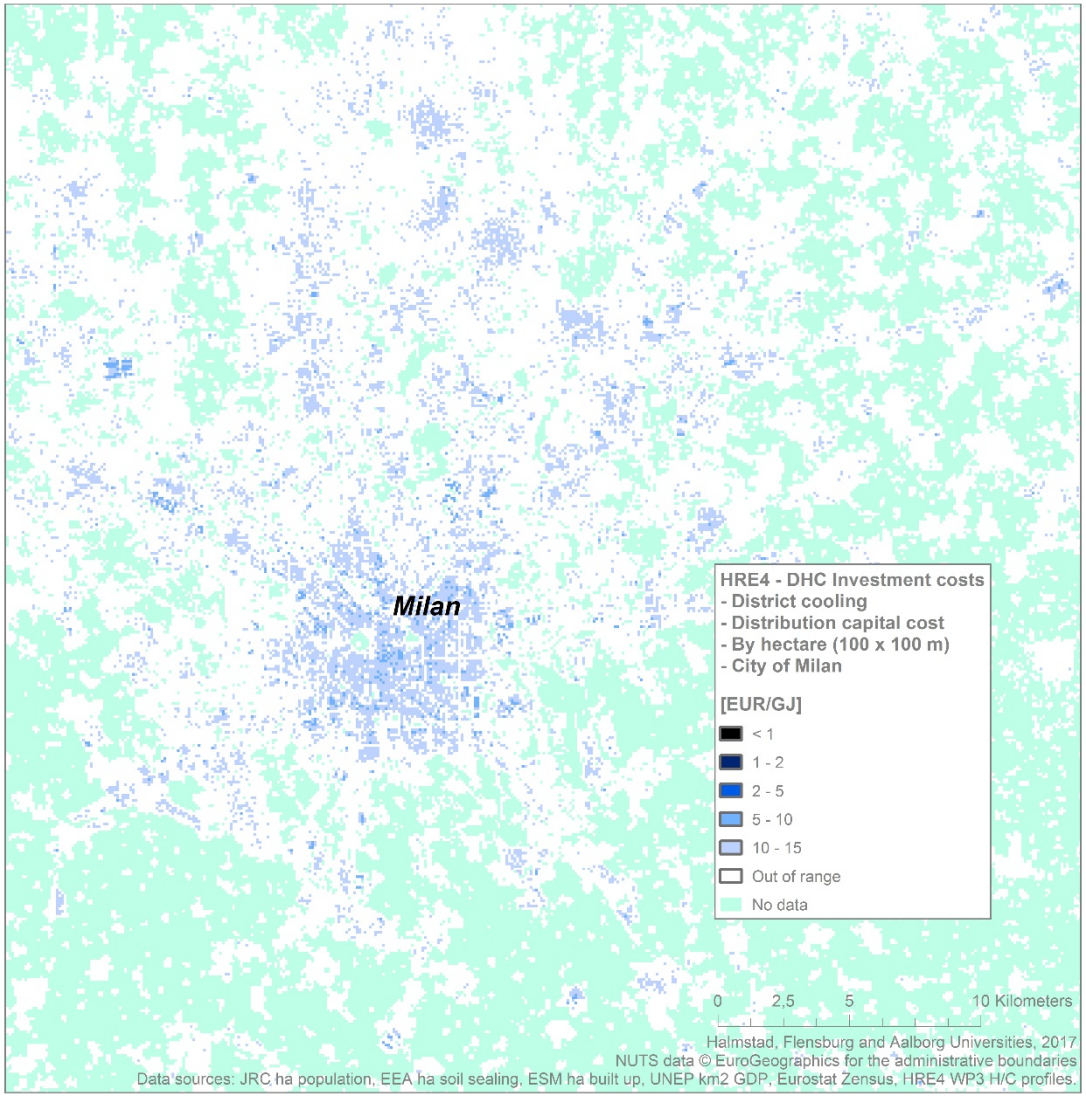

Figure 6.9. Close-up map of marginal distribution capital costs for district cooling pipe networks by hectare grid cells; Case study example for the city of Milan in Italy.

This project has received funding from the European Union's Horizon 2020 research and innovation programme under grant agreement No. 695989.

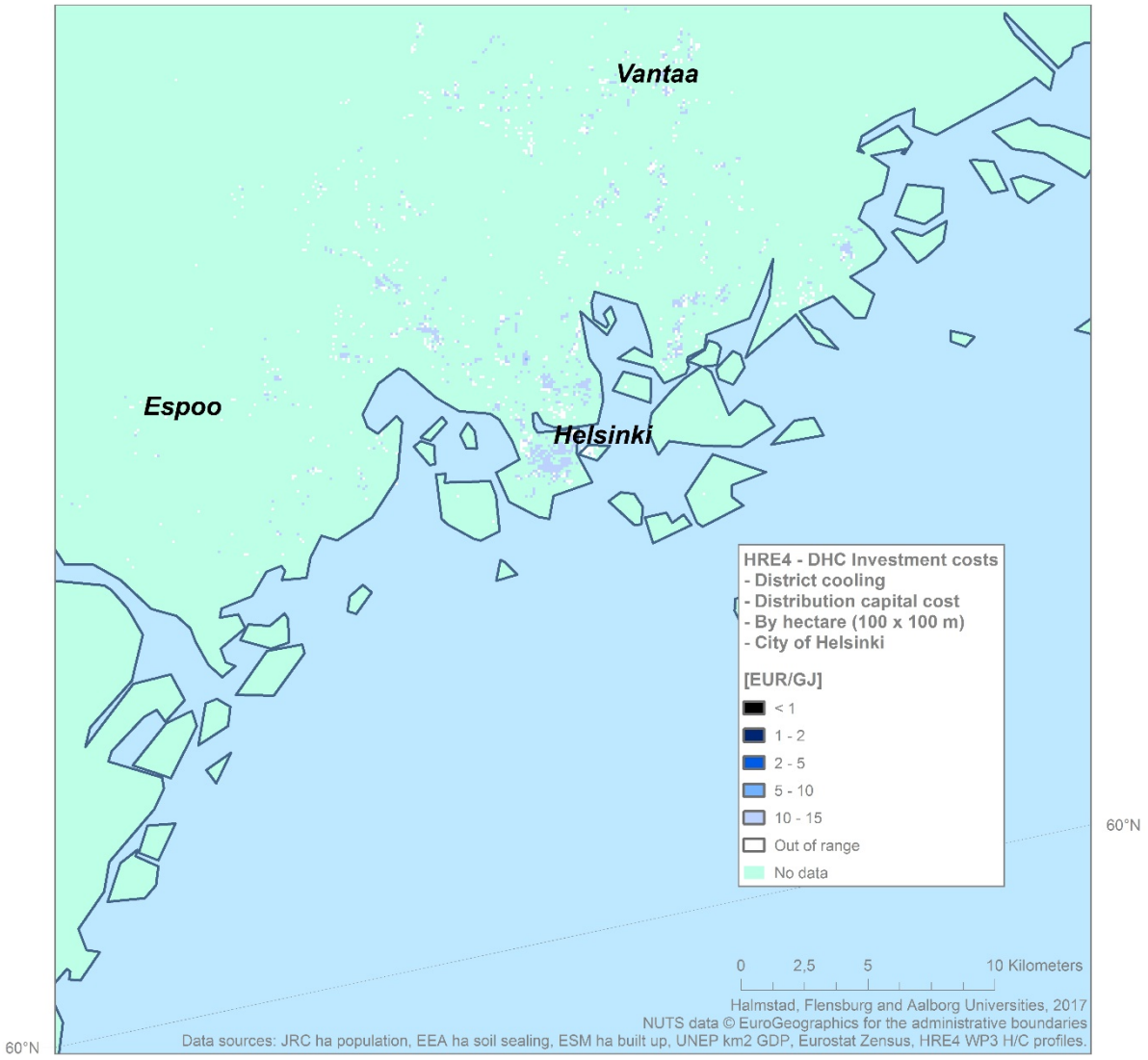

Figure 6.10. Close-up map of marginal distribution capital costs for district cooling pipe networks by hectare grid cells; Case study example for the city of Helsinki in Finland.

This project has received funding from the European Union's Horizon 2020 research and innovation programme under grant agreement No. 695989.

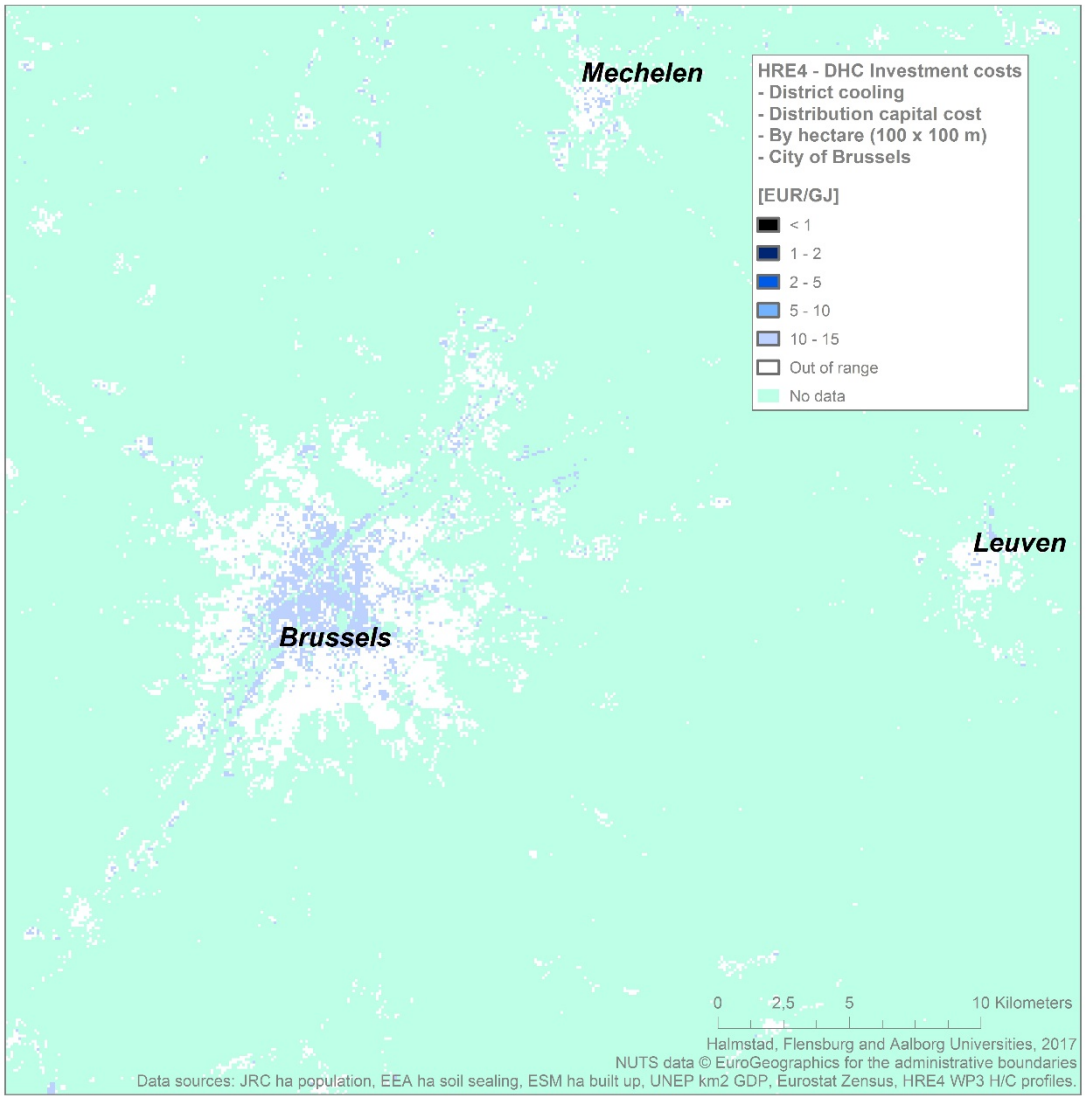

Figure 6.11. Close-up map of marginal distribution capital costs for district cooling pipe networks by hectare grid cells; Case study example for the city of Brussels in Belgium.